Functional and structural joint modelling of age-related changes in the human brain using EEG data and MRI images

Farveh Daneshvarfard

▶ **To cite this version:**

Farveh Daneshvarfard. Functional and structural joint modelling of age-related changes in the human brain using EEG data and MRI images. Neurons and Cognition [q-bio.NC]. Université de Picardie Jules Verne; K. N. Toosi University of Technology (Tehran, Iran), 2020. English. NNT : 2020AMIE0064 . tel-03650508

HAL Id: tel-03650508

https://theses.hal.science/tel-03650508v1

Submitted on 25 Apr 2022

HAL is a multi-disciplinary open access archive for the deposit and dissemination of scientific research documents, whether they are published or not. The documents may come from teaching and research institutions in France or abroad, or from public or private research centers.

L'archive ouverte pluridisciplinaire **HAL**, est destinée au dépôt et à la diffusion de documents scientifiques de niveau recherche, publiés ou non, émanant des établissements d'enseignement et de recherche français ou étrangers, des laboratoires publics ou privés.

Thèse de Doctorat

Mention Biologie Santé
Spécialité Neurosciences – Traitement du signal

présentée à ***l'Ecole Doctorale en Sciences Technologie et Santé (ED 585)*** **de l'Université de Picardie Jules Verne**
et
à Département de génie médical, Faculté de génie électrique et informatique **de l'Université K.N. Toosi**

par

Farveh Daneshvarfard

pour obtenir le grade de Docteur de l'Université de Picardie Jules Verne

Modélisation conjointe fonctionnelle et structurelle des modifications du cerveau humain liées à l'âge à l'aide de données EEG et d'images IRM

Soutenue le 07-01-2020 après avis des rapporteurs, devant le jury d'examen:

M^r Wiro Niessen, Professor, Université Erasmus MC	**Rapporteur**
M^me Gloria Menegaz, Professor, Université de Vérone	**Rapporteur**
M^r Gholamali Hosseinzadeh Dehkordi, Professor, Université de Téhéran	**Président**
M^r Mahdi Mahmoudzadeh, HDR, Université de Picardie Jules Verne	**Examinateur**
M^r Fabrice Wallois: PUPH, Université de Picardie Jules Verne	**Directeur de thèse**
M^r Hamid Abrishami Moghaddam, Professor, Université K.N. Toosi	**Directeur de thèse**

Acknowledgements

Firstly, I would like to express my sincere gratitude to my supervisors, Pr. Hamid Abrishami Moghaddam, and Pr. Fabrice Wallois for their continuous support of my Ph.D study and all the related researches, for their patience, motivation, and immense knowledge. Their guidance helped me in all steps of the research and analyses as well as writing of this thesis. Specifically, I thank Pr. Abrishami Moghaddam for providing the opportunity to work in both MVMIP and GRAMFC labs and Pr. Wallois, as the head of GRMAFC research group, for allowing me to join their team and providing a friendly environment for working.

Besides my advisors, I would express my special and profound gratitude to Dr. Mahdi Mahmoudzadeh. I owe a huge debt of gratitude to him because of all the guidance, supports, ideas, clarifications and collaboration in different steps of the analyses, and to be ready at any moment I need his help. I will never forget his helps, and also his dear wife, Mina Nourhashemi' help and friendship, from the first to the last day of working with them.

Last but not the least, I would like to thank my family: my parents and my brothers and sisters for supporting me spiritually throughout all of these years and I would like to give special thanks and love to my husband who suffered from being far from me for almost 5 years. Without his wonderful and unique characteristic, and his understanding and encouragement, I would not have the necessary calm for doing this thesis. I would also thank all of my Iranian friends in Amiens, Hamed, Pooya, Negar, and in Tehran, Nasrin, Elham, Mehrdad and many other nice and kind friends who supported me as much as a real family and for spending very nice moments together, with great memories remained.

Contents

Glossary

ABR	Auditory Brain-Stem Response
ASSR	Auditory Steady-State Response
CAEP	Cortical Auditory Evoked Potential
DTI	Diffusion Tensor Imaging
EEG	Electroencephalography
ERP	Evoked Response Potential
FA	Fractional Anisotropy
FC	Functional Connectivity
FDR	False Discovery Rate
GFP	Global Field Power
GI	Gyrification Index
GM	Gray Matter
MEG	Magnetoencephalography
MRI	Magnetic Resonance Imaging
mSTG	middle Superior Temporal Gurus
MWF	Myelin Water Fraction
NIRS	Near-Infrared Spectroscopy
PC	Phase Coherence
PCW	Post-conceptual Week
PMA	Post-menstrual Age
pSTG	posterior Superior Temporal Gyrus
RD	Radial Diffusivity
ROI	Region of Interest
SNR	Signal-to-noise Ratio
VEP	Visual Evoked Potential
wGA	week Gestational Age
WM	White Matter

Chapter 1

Introduction

Development of the human brain, as a protracted process, begins prenatally in the third week of fetal life and continues throughout the lifespan. Various factors that contribute to brain development cover a wide range from the molecular events of gene expression to environmental inputs. These different levels of factors and types of processes interact with each other to create a set of events that defines brain development. Actually, brain development is described as a complex set of dynamic and consistent processes that emerge and promote the distinction between new structures and functions in the human brain [1].

Age-related changes in the human brain can be investigated from either structural or functional perspectives. While the first approach concerns the geometrical, dimensional and anatomical changes of the brain with age, alterations in the behaviors, outputs and neurological responses to different endogenous or exogenous stimuli during the development are considered in the functional approach. Understanding both structural and functional brain development throughout the lifespan reveals dimensions of how the brain undergoes changes and provides the necessary information required for therapeutic interventions at various stages of the developmental process.

The most visible part of the structural brain development is a dramatic increase in the total volume of the brain, which begins from the pre-birth period with the highest incidence after birth and resumption until adolescence. A primary assumption for the post-natal increase in the size of the brain is the addition of new neurons. However, this is not the case. The formation of the neurons and their migration to appropriate areas of the brain is almost completed during the prenatal period by around the seventh month of gestation [2]. The main reason for the post-natal increase in the volume is the growth of synapses, dendrites, and fiber bundles. In addition to the formation of dendritic trees and related synapses, the nerve fibers become myelinated during the growth process in the postnatal period. The myelin sheet, which is a multilayer wrapping of insulation around the axons formed by glial cells, is essential for rapid impulse transmission and increases the brain volume [2]. A steady increase

in the synaptic density has been reported in several regions of the human cerebral cortex [3] [4]. While the increase in synapses (synaptogenesis) occurs in all cortical regions, the most rapid bursts of increase and the peak density occur at different ages in different regions. As an instance, rapid growth in the visual cortex is observed between 3 and 4 months and the synaptic density of the visual cortex reaches its maximum between 4 and 12 months. A similar pattern is observed in the primary auditory cortex. However, for some regions of the prefrontal cortex, the synaptogenesis starts at the same time, increases mush more slowly and does not reach its maximum until after the first year [2].

Changes of the human brain continue throughout childhood and adulthood. A toddler's brain is two times more active than an adult's brain with the essential functions established in this critical period of development [5]. Although the infant's brain has most of the necessary cells before birth, the connections are developing all through childhood. The interaction between genetics and the environment has an ongoing influence on the development of the child's brain. Certain skills are attained during the first year of life. The infant learns to distinguish the sounds and recognize the shapes, colors and objects [5]. The ability to use both eyes develops between 3 and 8 months [5]. Language development is an ongoing process in the first 10 years. However, the critical period occurs during the first few years [5]. Motor skills have a critical period of development during the first year of life although there is variability between the infants on the exact time of performing the motor skills such as sitting up, crawling or walking [5].

The brain undergoes changes during adolescence. The human brain reaches its maximum weight by around 10-12 years. However, it will continue a great deal of changes before reaching maturity [5]. A pruning process occurs during adolescence in which almost half of the synaptic connections are eliminated [6]. This refining of synaptic connections is supposed to make space for the formation of mature patterns. Another important brain change in adolescence is that some of the axon pathways become myelinated speeding up the conduction of the information. Decrease of the synaptic connections at the dendrites (gray matter, GM) and increase of the axon myelination, (white matter, WM) results in a higher ratio of WM to GM compared to the time interval before the adolescence [5].

Developmental changes in the adult's brain are less dramatic compared to early development. Normal aging is accompanied by an extensive range of variations with many people functioning intensely well in later stages of their life. However, most of the adults experience a decline in memory and function along with a particular degree of degradation as a normal part of aging. Mental flexibility, speed of the processing, the ability to solve

complex and new problems, memory and learning are the functionalities most degraded by aging. Furthermore, structural features such as the volume and weight of the brain diminish in elderly subjects [5]. The traditional reason used to be referred for this phenomenon was the death of a large number of neurons. However, by applying newer imaging techniques, it has been proved that the number of neurons remains almost constant in normal aging. Actually the main reason for the reduction of the brain size is the shrinking of the cells [7]. Aging-related reduction of the cortical thickness is also a consequence of this shrinking [7].

As mentioned briefly, the human brain undergoes extensive structural and functional changes from infancy to adulthood. Evaluating these changes is essential to closely monitor the normal brain development and investigate the structural and functional pathology of the brain. In the current thesis, magnetic resonance imaging (MRI) and electroencephalography (EEG) signals are applied for modeling structural and functional changes of the brain, respectively. MRI is an appropriate imaging method for the human brain regarding its high contrast for the soft tissues and no ionizing radiations. EEG is also suggested due to its high temporal resolution, less sensitivity to motion artifacts, portability and suitability for the recording of the infants' brain activity.

In the following of Chapter 1, we first represent the basics and the literature behind the analysis of age-related changes of the brain at different periods of life. We review the studies focusing on the functional, structural and joint functional-structural analysis of age-related changes in subsections 1.1, 1.2 and 1.3, respectively. In 1.4 we illustrate the main purpose of the current thesis which is concentrated on both functional and structural development of the premature neonates. Therefore, the rest of the introduction Chapter is dedicated to the developmental aspects of premature infants. More specifically, we describe the dynamics of functional (1.5) and structural (1.6) development in premature neonates, as well as the interaction between the function and structure in the early stages of development (1.7). Furthermore, we review principals and findings regarding the language maturation and asymmetries (1.8); since our analyses are based on investigating the development and asymmetry of the auditory responses of the preterm infants. The last subsection of Chapter 1 is dedicated to the clinical and scientific impacts of the topic and findings.

1.1 Functional analysis of age-related changes

In 1924, Hans Berger revealed the possibility of measuring the electrical activity of the human brain by placing electrodes on the scalp and amplifying the signal (EEG). He observed

that the recorded voltages could be influenced by external stimuli [8]. However, it tended to be very difficult to assess the highly specific neural processes which are the basis of cognitive neuroscience because it was hard to isolate individual neurocognitive processes by using pure EEG. Event-related potentials (ERPs) offered a better approach for extracting more specific sensory, cognitive, and motor events by using simple averaging techniques. In 1935–1936, Pauline and Hallowell Davis recorded the first known ERPs on awake humans. In recent years, ERPs have been used extensively for analyzing event-related EEG signals. The procedure is performed by the repetitive presentation of an event, such as an auditory stimulus through the speakers, and analyzing the small fractions of recorded activity which are evoked by this event. The ERP is then measured by extracting EEG trials time-locked to the stimulus presentation and calculating the average over all the recorded trials. It is assumed that the measured signal is a combination of the ongoing brain activity and an event-related response that is independent of the ongoing activity. Averaging over the trials is necessary since it reveals the time-locked, evoked portion of brain activity and removes activity that is not time-locked to the event. ERPs in response to sensory and cognitive events consist of several positive and negative peaks. Latency, morphology, and topography of these components describe the characteristics of the ERPs and can be associated with the corresponding sensory cortical regions and the cognitive brain functions.

Sensory evoked potentials, the electrical activity measured from the nervous system, are commonly recorded following the presentation of a specific visual, auditory or somatosensory stimulation. In the following, we present functional changes of the human brain corresponding to the visual and auditory modalities.

1.1.1 The visual system

Visual processing is a complex function of the human brain which changes during the life span with the most developmental changes occurred in the infancy [9]. A significant part of the human cerebral cortex is devoted mostly to visual processing [10]. Vision has an outstanding importance in every aspect of our life. It provides the necessary information about our surrounding environment without the need for the adjacency involved in taste, touch and smell [10]. Different brain regions, as well as different perceptual processes, are responsible for specific visual functionalities such as the perception of movement, color, depth, orientation, etc. [10]. Various types of visual stimuli are needed for evaluating different functionalities of the infants' visual system [9].

Visual evoked potentials (VEPs) may be recruited for the loss detection of the visual system caused by optic nerve damage. They can also be applied to assess the emergence and maturation of different functionalities in the infants' visual system [9]. As an instance, the newborns are poor in fixation and discrimination of color and orientation [10]. Therefore, black and white stimuli such as the chess plates and angular designs are preferred for their visual system [10]. A sample of the paradigm for recording VEPs in infants is presented in Fig. 1.1 [11]. The infant is sited in the lap of the caregiver and the visual stimulus is presented continuously on display. Three samples of the presented stimuli are shown in the right figure. The reader may refer to our previous survey [9], presented in Appendix I, for more information regarding the emerging and maturation times of different visual functions and several types of visual stimuli appropriate for cortical function assessment in infants.

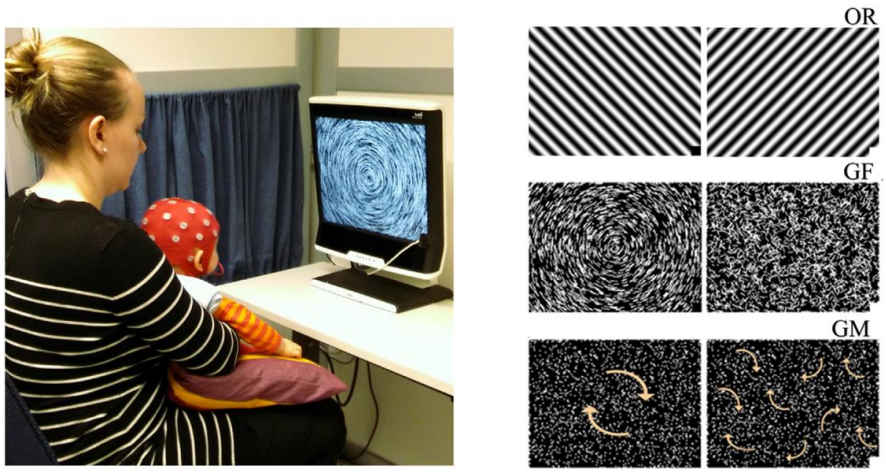

Figure 1.1: In the orientation reversal (OR) stimulus, sine grating switches its orientation continuously between 45° and 135° angles. In the global form (GF) and motion (GM) stimulations, coherent and non-coherent phases are presented alternately. The stimulus consists of short white arc segments in the GF and small white dots in the GM cases [11].

A visual stimulus can be a simple event such as an LED that lights up once and elicits a transient response, recorded as a trial. The stimulus is then presented several times and the trials are averaged to obtain the VEP. This response is appropriate to be analyzed in the time domain following a characteristic pattern which is described as a sequence of positive and negative deflections. On the other hand, a stimulus can be periodically repeated, e.g. LED flickering with a specific frequency and eliciting a response that is suitable to be analyzed in the frequency or time-frequency domain. The ERP consists of the early component (0-10 ms) caused by brainstem activity, middle responses (10-100 ms) which are due to thalamic activity and later components (up to 600 ms) which reflect modifications of the ongoing

cortical activity in response to the stimulus. These ERP components are named according to their polarity and approximate latency (P100, N200, P300, N400 and P600) [12] [13]. The ERP components can be reliable neurophysiological markers for normal brain development useful in early detection of some diseases [14] [15] [16].

Three standard clinical stimulus protocols are commonly used for recording VEPs [17]: pattern-reversal VEP, pattern onset/offset VEP and flash VEP. The pattern reversal VEP is preferred for most purposes due to the relatively low variability of waveform and peak latencies both within a subject and among the normal population [18]. A normal VEP response to a pattern-reversal stimulus is a positive peak which occurs at almost 100 ms. Generally, three separate phases are observed in a typical VEP waveform: an initial negative deflection (N70), a prominent positive deflection (P100), and a later negative deflection (N155). The peak latency and peak to peak amplitudes of these components are often measured in developmental or neuropathological studies [19].

P100 is usually a prominent peak, which shows minimal variation between different subjects and in repeated recordings. However, it is affected by parameters such as the pattern size, contrast, mean illumination, patient's age and poor focus [17]. The latency of the P100 decreases with the maturation of the infants' visual system and reaches about 100 ms in about 4-5 years [20]. While the P100 latency continues to decrease till the middle ages, a significant increase is observed for adults older than 75 years [21] [22]. The P100 has been shown to reflect pre-attentive processes in spatial attention tasks, and to be larger for faces vs. objects during object recognition task [23]. Moreover, there are some evidence that the P100 reflects high-level processes, as it is greater for inverted rather than upright faces [24]. An increase in the latency of the P100 may be a biological marker of various disorders of the visual pathways in the brain. The P100 is generated mainly in the striate cortex as a response to the central region of the visual field. Stimulating one half of the visual field leads to the excitation in the contralateral occipital lobe. Therefore, the P100 might be expected to appear at the electrode contralateral to the half field stimulated. In practice, P100 is usually observed over the lateral electrode ipsilateral to the half field stimulated. This paradoxical topography is attributed to the oblique orientation of the cortex at the occipital pole which includes the central areas of the visual field. [25].

P300, as a large amplitude positive peak, is another important component of the ERPs mostly associated with cognitive information processing (e.g. memory, attention, executive function) [26]. Some regions in the temporal and parietal lobes and the hippocampus are responsible for the generation of the P300 [27]. The amplitude of the P300 component of the

VEP is influenced by the probability that a determined object will appear. Hence it is supposed to be a measure of attention allocation, indicating the difficulty of distinguishing between the target object and the standard stimuli [28] [29] [30] [31]. The N400 component of the VEP is also an ERP supposed to reflect contextual integration. It is often associated with semantic processing under non-congruent or unexpected conditions [32] [33] elicited in a task requiring the processing of irrelevant, but not unexpected, stimuli [34].

Several studies investigated the evolution of the visual system by analyzing the effects of age on the VEPs characteristics [35] [36] [37]. While there is an increase in the peak amplitude and a decrease in the peak latency of the responses at the first years of life, the amplitude declines and the latency increases during the aging [38] [39] [40] [41] [42]. Myelination is the essential maturational process that increases the neural conduction velocity leading to the decrease of the latency of the peak along with development. On the other hand, the observed age-related changes in the amplitude and latency of the evoked potentials are consistent with the biochemical and neurophysiological changes of the brain. Expansion of dendritic arborizations in the cortical neurons to compensate for the synaptic spine deterioration and reduction in the inhibitory neurotransmitters, e.g. gamma-Aminobutyric acid (GABA), had been suggested in normal elderly [43] [44]. The compensation hypothesis (higher brain activity to compensate for diverse neurodegenerative losses) due to plasticity, support the age-related brain activation [45]. Moreover, increasing the latency and decreasing the velocity is observed during the aging which is related to demyelination [46].

Frequency characteristics of the ERPs can also be analyzed for assessing cortical functions at the early stages of development. Power spectra, cross spectra, phase synchrony, local coherence and phase locking were measured as some samples of the frequency features for normal term infants within 2 days of birth responding to a flash stimulus [47]. Significant changes in the frequency-dependent measures were reported in posterior electrodes in the same time window as the VEPs [47]. In addition to the temporal and frequency features, time-frequency domain approaches such as the wavelet transform are appropriate choices for extracting the functional features due to the non-stationary characteristics of the EEG signals [48]. Functional connectivity (FC) measures may also be extracted as age-dependent features for analyzing age-related changes in the brain function [49].

1.1.2 The auditory system

The auditory system is responsible for the analysis of the auditory world so that the listener is able to accomplish the goal of communication and learning. Auditory development involves changes in the peripheral and central nervous system along the auditory pathways which occur both naturally and in response to the stimulation [50]. It implies the fact that perception is influenced by a combination of inherent, genetically programmed changes in anatomy and physiology along with the auditory experiences [50]. The auditory system receives the information from the objects and environment, segregates the sounds, and provides meaning and access to communication tools such as the language. Different features of sound such as the detection threshold, the frequency and the intensity have been studied in a quiet environment and in the presence of noise. The thresholds for detection of the stimuli in a quiet environment improve between the infancy and early school age [51] [52]. While the infants can have thresholds up to 25 dB worse than adults, rapid improvement occurs before the age of 6 months [53]. The difference is then reduced to a 10–15 dB gap when the children reach 5 years of age [50]. It should be noticed that the differences in detecting sounds depend on the frequency. While the sensitivity is near to the adult level by the age of 6 months for high-frequency sounds of around 4000 Hz, it is not the same for the low-frequency sounds around 500 Hz [51] [52]. Frequency discrimination, the ability to perceive a change in the frequency of tonal stimuli, undergoes considerable maturation between 3 and 6 months of age. In 3 months old infants, the discrimination ability is poorer for 4000-Hz tones than 500-Hz. However, at 6 months, the pattern is reversed and the infants are better at discriminating changes imposed on 4000-Hz tones than 500-Hz tones [54]. The adult-like performance of ~1% change in the frequency is observed between 6 and 12 months when the infants can discriminate changes of 2% in the frequency for 4000-Hz tones. Intensity discrimination, the ability to detect a change in the level (in dB) of the sound presentation, is typically measured separately for tones or narrowband stimuli. While the adult listeners can distinguish differences in intensity as small as 1–2 dB [55], the infants between 5 and 7 months need approximately 6 dB difference.

Cortical auditory evoked potentials (CAEPs), measurable from 27 weeks gestational age (wGA) [56], can be used to understand underlying physiological processes and the neural substrates of perception [57]. Wunderlich and Cone-Wesson [58] provided a comprehensive review about the development of the CAEPs in early infancy. They summarized the immaturities of the CAEPs recorded in infants and children compared to those of adults. For

the term newborns and in the early months of life, the typical CAEP waveform recorded in the midline consists of the most prominent features including a broad positive peak, P2, followed by a broad negative trough, N2. Earlier and smaller peaks, P1 and N1, may sometimes be observed in the waveform, but are much less frequently evoked [59] [60] [61]. Latencies of the components decrease from ~300 ms to ~150 ms for the P2, and from ~530 ms to ~300ms for the N2, throughout the first post-natal year [62]. P1 and N1, are barely distinguishable before 4-5 years of age. The latency of the P1 is then decreased from 90 ms (at 4-5 years old) to 50 ms toward adulthood [63]. For the newborn infants, the source of the P2 has been localized to the temporal lobe, in or near the auditory areas [64]. During the first 3 years of life, the latency of the responses decrease and greater prominence of later components is observed [65]. Latencies of the P2 and N2, recorded at the vertex in sleeping infants, have generally been found to decrease with age, specifically over the first months of life [65]. For awake infants, CAEP peak latencies do not necessarily show the same developmental trend. However, the morphology of the waveforms was similar to those of sleeping infants. The latency of the P2 presents less variability with age over the first 4 months of life [66]. Wunderlich et al. [67] recorded CAEPs in response to low (400 Hz) and high (3000 Hz) tones and the word token /bæd/, all presented at 60 dB HL, at a rate of 0.22 Hz. A sample of the CAEP in response to the word token /bæd/ is illustrated in Fig. 1.2 for 2 years and 11 months old infant. Measurements were made for the P1, N1, P2 and N2. The results confirmed that while the CAEPs component latencies were almost stable from birth to 6 years, significantly shorter latencies were observed for the adults compared to the infants and children. Furthermore, components P1 and N2 decreased in the amplitude, while the components N1 and P2 increased in amplitude from birth to adulthood.

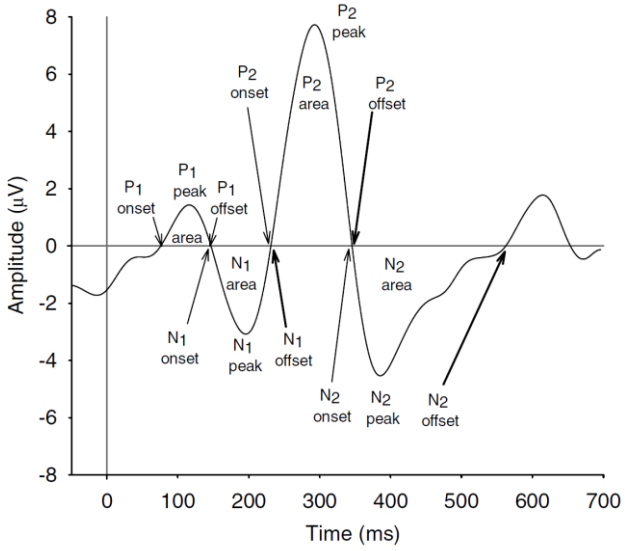

Figure 1.2: CAEP of 2 years and 11 months old infant in response to the word token /bæd/ [67].

The effects of the aging and stimulus presentation rate on the speech CAEPs have also been investigated [68]. The results showed that when presenting the speech stimuli at the medium presentation rate, N1 and P2 latencies were prolonged for the older subjects. However, no age effect was observed when presenting the stimuli at a slower rate. This may be related to the age-related refractory differences in younger and older auditory systems. Refractory issues might influence the synchronized neural activity necessary for the perception of critical time-varying speech cues which may, in turn, explain some of the difficulties of the older people in understanding the speech.

Although most of the studies focused on the temporal characteristics of CAEPs, they may be analyzed in the frequency or time-frequency domain to extract age-dependent variables. Connectivity measures may also be calculated from the CAEPs as the functional features seeking for their age-dependency.

1.2 Structural analysis of age-related changes

Magnetic resonance imaging is extensively used for investigating the structural development of different brain regions due to its high spatial resolution and contrast. Furthermore, MRI has no ionizing radiation which makes it appropriate for imaging the brain structures in fetuses and infants. The structural development of the human brain has been investigated in different periods of life. Knickmeyer et al. [69] revealed a total brain volume increase of 101% in the first year and a 15% increase in the second year of life. The most part of the hemispheric volume development was accounted for by GM, as it increased of 149% in

the first year of life, while the hemispheric WM volume increased by only 11%. Gilmore et al. [70] also reported that brain growth is mainly due to the GM development during the first 2 years. The cortical volume increases much more during the first than during the second year of life. The increase is more remarkable in the frontal and parietal lobes, compared to the primary motor and sensory cortices.

Various studies have extracted structural features such as the cortical volume, surface area, thickness and folding at different ages to investigate developmental changes. As an instance, variations of the cortical volume [69] [71] [72], surface area and folding are illustrated in Fig. 1.3 at different periods of development [73].

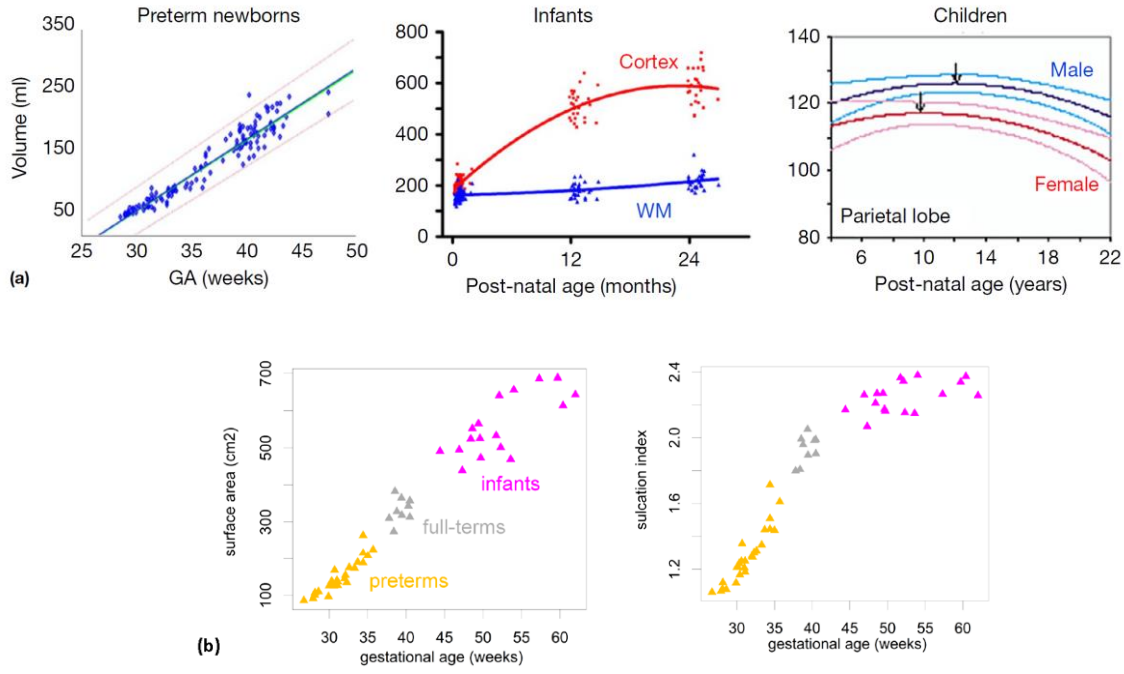

Figure 1.3: (a) Cortical volume development for the preterm newborns, infants and children [69] [71] [72], (b) Developmental changes of the cortical surface area and sulcation index for the preterm and full-term infants [73].

Cortical thickness variation is also studied at different ages. The average cortical thickness is around 1.3mm for the newborns between 27 and 45 wGA [74]. The thickness increases with age so that it ranges from 1.5mm in occipital regions to 5.5mm in the dorsomedial frontal cortex during childhood. The trend undergoes an asynchronous decrease across brain regions during adolescence [75]. Developmental trajectories of the cortical thickness and surface area were reported by Wierenga et al. [76], for the age-range of 7-23.3 years, using a combined cross-sectional and longitudinal design (Fig. 1.4). While a linear decrease was

observed for the cortical thickness with increasing of age, both cortical volume and surface area showed curvilinear trajectories. Changes of the cortical area, thickness and volume in the age range of 23-87 years were presented by Storsve et al. [77] (Fig. 1.5). According to their findings, the mean annual percentage changes of the cortical area, thickness and volume were -0.19, -0.35 and -0.51 in most regions, respectively. Volume changes were mainly due to the changes in the thickness rather than the area. A negative relationship was found between changes in thickness and surface area across several regions.

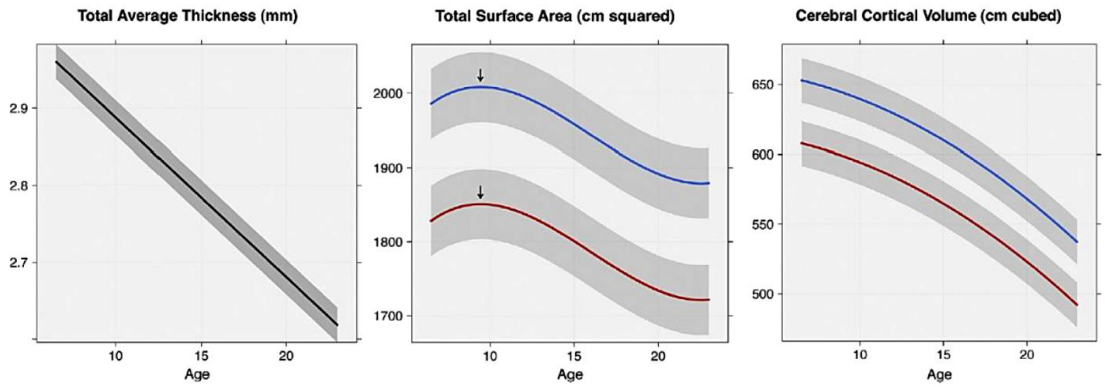

Figure 1.4: The developmental trends of average cortical thickness (mm), total surface area (cm2) and overall cortical volume (cm3). Trends are shown in blue for males and red for females [76].

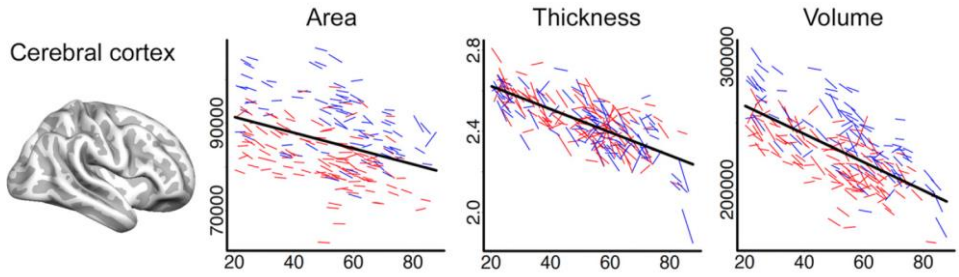

Figure 1.5: Age-related changes of area (mm2), thickness (mm) and volume (mm3) for cerebral cortex. Average values of left and right hemispheres are calculated. Blue and red lines correspond to males and females, respectively [77].

The cortex gets folded during the last trimester of pregnancy with the appearance of primary, secondary and tertiary folds around 20 wGA, 32 wGA and term age, respectively [78]. Gyrification index (GI), a measure corresponding to the degree of folding, is computed as the ratio between the areas (lengths in 2D space) of the pial surface (shown by purple in Fig. 1.6) and outer smoothed surface (shown by blue in Fig. 1.6) [79]. Cortical gyrification is a robust hallmark of the morphological development of the human brain. Gyrification

becomes obvious after 24 wGA [80] and increases significantly during the last weeks before term. The rapid increase continues to reach a transient maximum between weeks 66 and 80 post conception. After this time, the GI declines from a maximal value and reaches the adult level at the age of almost 23 years [81]. The mechanisms behind this developmental behavior are not well understood. However, it is speculated that perinatal programmed cell death and reduction of the cell numbers and connectivity may lead to a reduction in the GI value [82].

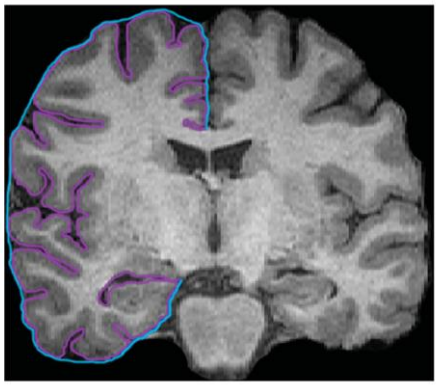

Figure 1.6: The GI is computed by dividing the areas (lengths in 2D space) of the pial surface (shown by the purple line) and outer smoothed surface (shown by the blue line) [79].

1.3 Joint functional and structural analysis of age-related changes

As discussed briefly, various studies investigated the structural and functional age-related changes of the human brain, separately. However, there are only a few studies focusing on the joint structural and functional changes of the brain during the development or aging. MRI-based studies have confirmed that the brain maturation is associated with distinct structural changes in the WM and GM. However, the relation between these changes and the brain function is still poorly understood. The general approach proposed for analyzing the functional and structural correlates of age-related changes of the brain is illustrated in Fig. 1.7. One may extract a functional feature, in the time or frequency domain, from the ERPs. On the other hand, a structural maturation index is calculated from the MR images. Correlations between the extracted functional and structural features with age are evaluated. Furthermore, functional and structural correlates are also examined after removing the effect of age.

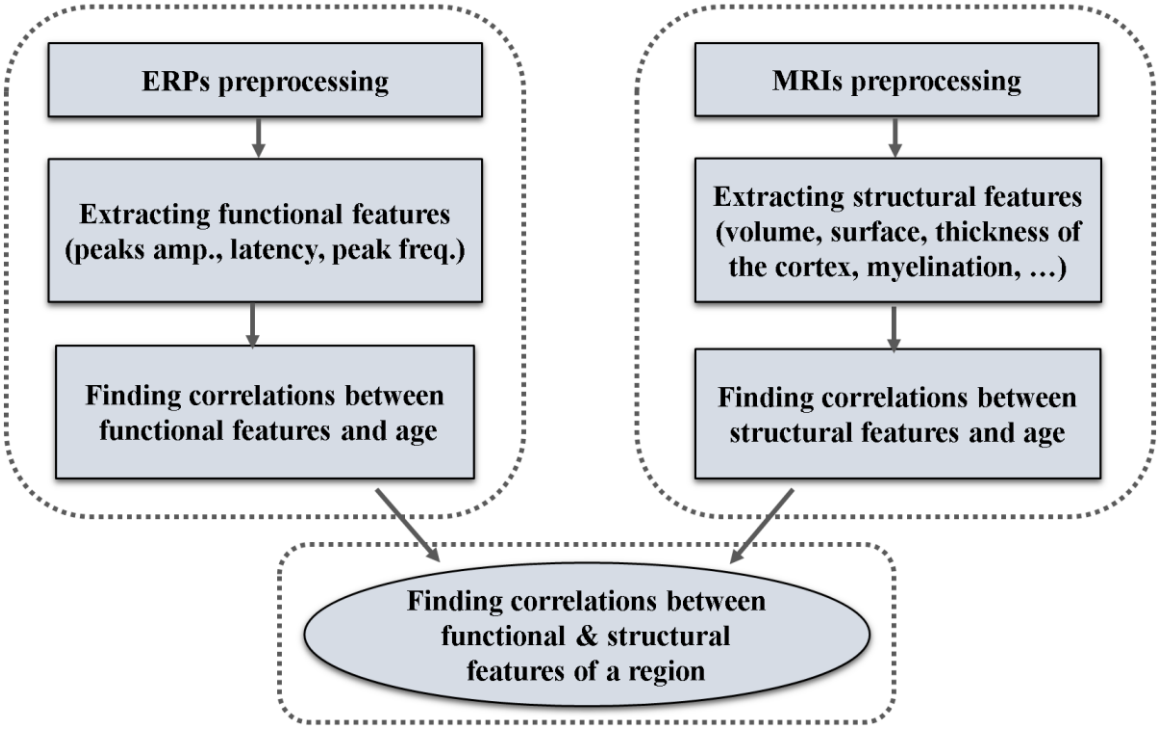

Figure 1.7: General approach proposed for analyzing the functional and structural correlates of age-related changes of the brain.

Structural and functional correlations of the brain were investigated with age, relating the gamma band responses of the primary visual cortex (V1) to age-related structural changes [83]. Significant correlations were observed between the age and the structural features such as the cortical thickness, volume and surface area of pericalcarine and cuneus. Furthermore, a significant negative correlation was observed for gamma-band frequency versus age. Hierarchical regression analyses were performed to examine the unique influence of age and cuneus thickness and volume on gamma peak frequency. Cuneus thickness and volume do not significantly predict gamma peak frequency after accounting for age. Therefore, the age-related decrease observed in gamma peak frequency is not likely the result of the decreased cortical thickness or cortical volume in the visual areas. However, we may conclude that the gamma peak frequency, cuneus thickness, and volume may be related indices of visual cortex maturation. Whitford et al. [84] investigated the relationship between the concurrent structural and functional changes of the brain from adolescence to early adulthood. The GM volume decreased across the age in the frontal and parietal cortices, with the greatest variations occurred in adolescence. On the other hand, the absolute EEG power for the alpha and beta frequency bands showed a curvilinear reduction similar to the GM volume in corresponding

cortical regions. It was suggested that GM reduction reflects the reduction of neuropil, leading to the elimination of the active synapses which is responsible for the observed decrease of the EEG power [84]. In assessment of the initial development for the infants, one may notice that the effect of changes in the skull thickness might also be considered when analyzing changes in the EEG amplitude.

Structure-function relationship was also studied in adults with the main purpose of relating the inter-individual differences in tissue microstructure to the differences in functional responsiveness measures. Horowitz et al. [85] reported that inter-individual variability in conduction speed of interhemispheric transfer of visual and tactile information (assessed with EEG) is related to the inter-individual differences in the axonal diameter of the callosal fibers connecting primary visual and somatosensory cortices (measured by diffusion MRI). For the auditory modality, the relation between the structure and function have been studied from childhood to adolescence [86]. DTI indices (i.e. the anisotropy) in acoustic radiations were correlated with the M100 latency, evaluated through MEG recordings of CAEPs. However, the correlation between the structural and functional measures did not survive after removing the effect of age. For the aging population, the neuroanatomical basis of age-related degradation of neural responses was investigated. Price et al. [87] related the latency of magnetic visual and auditory evoked fields (MEG) to age-related changes in the GM volume and WM microstructure (estimated by diffusion MRI) across the whole brain. Their results confirmed that while the functional properties of the visual responses were related to the microstructural properties of the WM, properties of auditory responses were related to the cortical GM and efficiency of local cortical processing.

1.4 Purpose of the current thesis

Various studies investigated functional and structural changes in the human brain at different periods of life. A key question, although challenging, in studying neurodevelopment, is how these changes affect each other. In other words, how the structural changes in the brain lead to enhancement of the cognitive functions during the development. Several studies focusing on the joint structural and functional changes of the brain during different periods of life were presented in part 1.3. Moreover, further studies on the joint functional and structural analysis of the brain, focusing at the early stages of development will be discussed in 1.7. However, there is a lack of literature on investigating the concurrent analysis of the structural and functional development in preterm infants.

Premature infants may survive when born after 23 wGA, as a result of intensive care [88]. Many structural and functional aspects of the brain are proved to be already matured in the normal healthy preterm infants. The auditory system is already operative at this early age and the CAEPs are recorded as soon as 27 wGA [56]. Although there are several studies focusing on the temporal characteristics of preterm infants' cortical responses, few have been conducted on the frequency domain analysis of these responses. In the current thesis, neurodevelopment of the CAEPs to repetitive syllabic stimuli is studied in preterm neonates based on the frequency domain analysis. To better characterize the lateralization of the preterm brain in the processing of auditory information, we evaluated the lateralization of the responses to the specific repetitive auditory task with phonemes. To investigate the functional and structural correlates of the preterm infant's brain, CAEPs were further analyzed to extract the global field power (GFP), as the functional feature, and MR images were analyzed to extract a maturation index related to myelination as the structural feature. Therefore, the specific approach proposed in the current thesis for joint analysis of the functional and structural brain development in preterm infants can be presented as Fig 1.8.

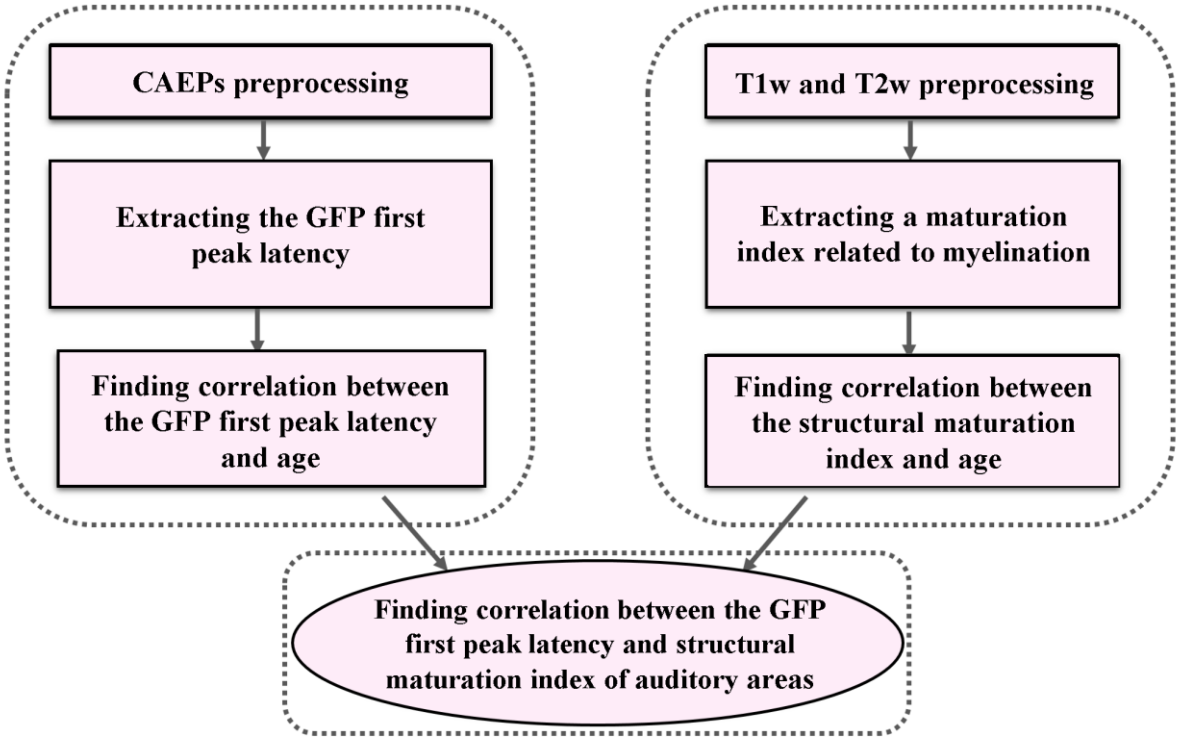

Figure 1.8: Specific approach proposed for analyzing the functional and structural correlates of developmental changes of the preterm infant's brain.

1.5 Dynamic of the functional development in premature neonates

EEG of the premature neonates differs from those of adults regarding the specific structural and functional maturational dynamics which take place at this period of development and should be considered in the interpretation of the signals. Understanding these maturational processes, which explain the dynamic of the EEG at each week GA, is extremely helpful for investigating the physiological and pathological function of the preterm infant's brain according to his/her GA. Synaptic interactions between thalamic afferents (after 28 wGA) being relocated in the cortical plate, the subplate neurons and the pyramidal cells while they are still traveling through the subplate to cortical plate or pyramidal cells that already reached their final destination in the cortical plate produce micro electric fields in the preterm infant's brain, somehow different in the origin and mechanisms to the adult ones. A large set of parallel oriented neurons then synchronizes to develop a macro electric filed which can be measured on the scalp surface. While the brain activity of the adult results from the activity of the complex networks involving the thalamocortical loop or connections [89], the brain activity of the premature infant is due to the local-regional developmental processes. Macroscopic maturation of the preterm brain including the gyration, bone thickness maturation and fontanelles are supposed to impact the amplitude and spatial distribution of the brain activity measured by EEG.

Scalp EEG/MEG recordings of premature neonates provide the most of the knowledge concerning the development of the cortical activity during the last trimester of the fetal period. The earliest recordings have been conducted in the 1950s illustrating the EEG characteristics in preterm infants [90]. These early findings were applied immediately for clinical purposes in characterizing the normal brain activity at each GA, detection of early dysfunctions, monitoring of the brain activity during the treatment in NICU and defining predictive neurodevelopmental outcomes [90].

The neurodevelopment of the EEG characteristics can be divided into two main dynamic processes. The first dynamic is based on identifying the activity of the cortical generators specific to the age of the premature neonate. This generator-based dynamic is constituted by the appearance of generators with activities different in spatio-temporal and frequency characteristics, occurring sequentially during the neurodevelopment. Therefore, we observe the frontal activity between 24 and 28 wGA, theta temporal activities in coalescence with slow waves (TTA_SW) between 26 and 30 wGA, delta brushes between 29 and 36 wGA and finally the frontal transient and slow anterior dysrhythmia between 36 and 42 wGA.

Generally, the first dynamic is the result of interactions between the thalamic afferents, subplate and cortical plate likely to participate in the functionality of cortical neural networks (guidance, synaptogenesis, receptors functionality setup, etc.).

The second dynamic of the EEG during neurodevelopment is network-based. EEG of the newborn is characterized by its discontinuity corresponding to the periods of bursts of activity (UP state) interspersed with quiescent periods of lower activity (DOWN state) called Inter Bursts Intervals (IBI). The bursts are composed of short or long duration complex activities of different frequencies which evolve with age. Theses repetitive bursts experience a gradual increase in the amount of continuous oscillatory activity during development [91]. Their durations increase and their amplitudes decrease with the increment of the GA [90]. This specific pattern has been used in some algorithms for the automatic characterization of the preterm infants' GA [92]. Furthermore, different characteristics of the cortical bursts (e.g. the duration, amplitude, frequency content, shape of the burst, etc.) have significant diagnostic and predictive value for long term neurodevelopmental outcomes [90] [93] [94].

Specific discontinuity observed in the EEG characteristic of the newborn should not be confused with the burst suppression observed in certain pathological situations in the term infants or adults resulting from different pathophysiological processes [95]. This physiological discontinuity diminishes progressively during the maturation leading to the 'trace alternant' at term [90]. At the same time, the amplitude of the EEG decreases and the frequency content increases gradually up to 40 wGA [96]. Generally, the second dynamic, which is the more linear, represents the implementation of the functionality of interactions within cortical neural networks. Furthermore, the gradual introduction of sleep stages from 28 wGA [90] suggests early, progressive interactions between the neural networks of subcortical and cortical structures.

The discontinuous pattern of the early EEG recordings at almost 24 wGA, recognized by sudden high-amplitude bursts of activity, develops to a more continuous pattern toward the term age [97] [96]. CAEPs appear in the early preterm period when thalamic afferents are relocating from the transient subplate zone to the cortical plate [98].

Stimulus-dependent responses have been reported in premature infants from 6 months of GA [56] [60] [99]. Most of the studies investigating functional aspects of the preterm brain have been conducted at 34-35 wGA. At this age, the cochlear functions are almost mature, making the infants capable of distinguishing between various sounds [100] by producing a slow mismatch response to a change of repeated sound in a series. Mahmoudzadeh et al. [101], using functional optical imaging (NIRS), showed the ability of the preterm infants at 30

wGA to discriminate a change of syllable (/ba/ vs. /ga/), while the mismatch response to a novel voice (male vs. female), was observed but limited. They further analyzed EEG recordings in 30-wGA-preterm infants in response to a syllable discrimination task (i.e., a phonetic change: ba vs. ga; and a voice change: male vs. female voice) [88]. The syllables were presented by series of 4 to constitute either standard trials (e.g. /ba/ /ba/ /ba/ /ba/) or deviant trials (e.g. /ba/ /ba/ /ba/ /ga/). Repetition generally induces a decrease in the neural response, repetition suppression (Fig. 1.9), resulting in a mismatch response when deviant and standard trials are subtracted. In adults and post-term infants, this response is observed mainly originating from the posterior superior temporal regions and followed by a later second response (P300 in adults, late slow wave in infants), particularly when subjects are attentive to the trial structure [102] [103] [104].

When analyzing the ERPs of the infants, one must take into account the inherent complexity of the responses. Developmental changes, which are expected to be evident from the morphology of the ERP waveform, are, in many cases, difficult to explain because of the complexity and variability of the responses at this period of life. As an instance, developmental changes in the skull thickness and fontanel, myelination and synaptic density may affect amplitude and latency of the ERPs across different ages. In addition, in premature neonates, much lower frequencies are observed in the ERPs compared to adults, due to less synaptic efficiency. Therefore, premature ERP does not present as many well-defined peaks as in the adult. Generally, large variability (both between and within-subjects) is observed in developmental ERPs challenging the interpretation of the responses. Some parts of the inter-subject variabilities may arise from differences in the number of completed trials, which have been associated with both amplitude and latency differences in certain components [105]. In addition to inter-subject variability, intra-participant variabilities are frequently observed in developmental ERPs. Significant variability has been reported in the infant's brain response to the same stimulus over time [105]. Differences in the topography of the components have been detected for the same participant depending on whether the first half or the second half of the data from a testing session was used for analysis [105]. These variations may be due to the habituation to the stimulus during the session [105]. They may be also because of the changes in the state of the neonate during the recording (e.g., changes in fussiness or sleep state) [105] or even might be related to the lability in the transmission of information through immature circuitries and synapses.

Although several studies investigated the temporal characteristics of the preterm infants' CAEPs, few have been conducted on frequency analysis of these responses. Auditory steady-

state responses (ASSRs) is a frequency-domain approach which measures the ability of the auditory network to fire synchronously with the rhythm of an auditory stimulus [106]. Mahmoudzadeh et al. [88], using a phase coherence analysis in 30 wGA preterm infants, showed the ability of the immature neurons to follow a sequence of 4 syllables separated by 600 ms of silence. Although the auditory stimuli presented in [88] is not exactly a classical ASSR paradigm, regular repetition of the stimuli motivated us to study the ability of the immature auditory network to be entrained by the syllabic rhythmicity. As the frequency of stimulation is known, the same frequency can be studied in neural responses to obtain information on the ability of the immature network to follow the frequency of the auditory stimulation.

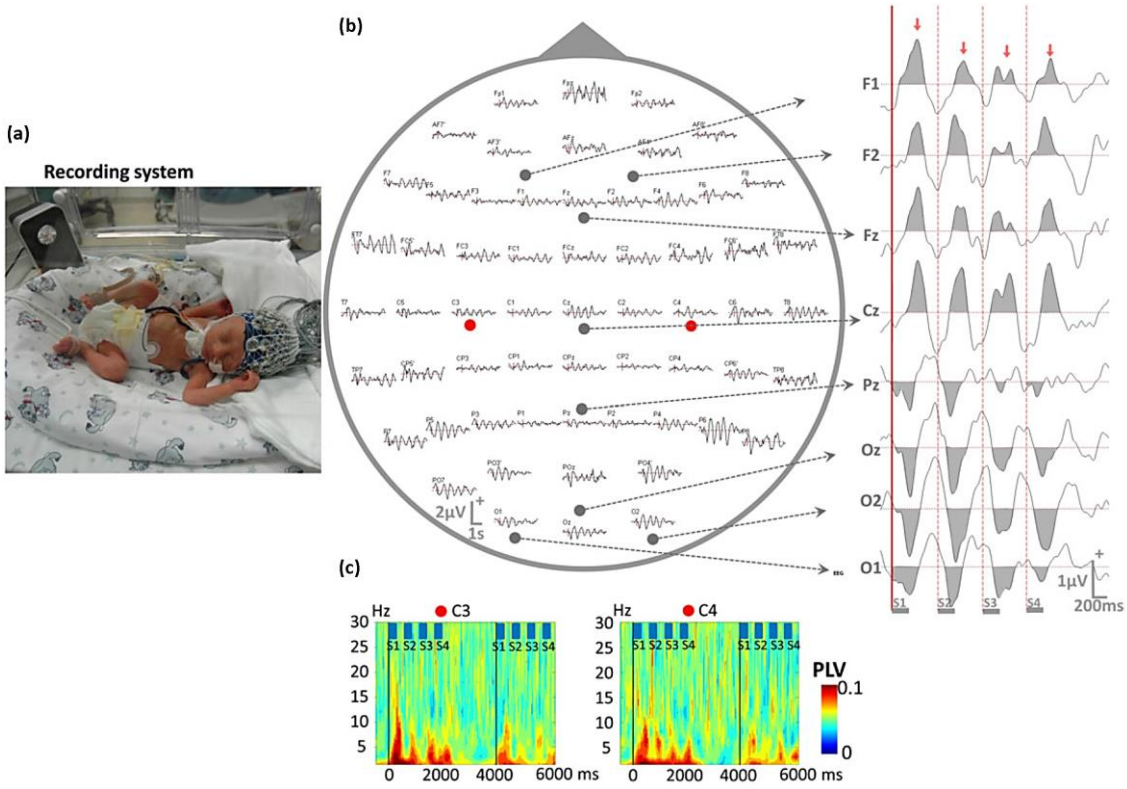

Figure 1.9 (a) Preterm neonate with high-density EEG cap, (b) Grand averages of auditory ERPs (all conditions combined). The amplitude is decreased by repetition of the syllables, (c) Time–frequency representation (phase-locking value) of the grand average over 2 successive trials in C3 and C4 (red dots in the central plot) [88].

1.6 Dynamic of the structural development in premature neonates

Structural brain development relies on several maturational mechanisms that occur asynchronously with different emergence and rates across brain regions. Formation and maturation of the cortical layers and WM connections depend on specific cellular events, driven by biological clocks or entrained by the endogenous and exogenous sensory inputs [107]. These events include the predominance of proliferation and migration during the first trimester of gestation, growth of axons and dendrites during the second and third trimesters, and prolonged postnatal synaptogenesis, myelination and neurochemical maturation (Fig. 1.11) [108].

1.6.1 Development and maturation of the cortex

Neurons and glial cells are preliminarily produced during the embryonic period within two proliferative zones (i.e. the ventricular and sub-ventricular zones). Neurons are then directed toward the brain periphery by the glial cells. They first reach the subplate, a transient layer underneath the cerebral cortex which serves as a waiting compartment for the growing neurons [109]. The subplate is four times thicker than the cortical plate at mid fetal period containing numerous synapses. It is composed of well-differentiated postmigratory neurons as well as migratory neurons, glial cells and ‘waiting’ thalamocortical axons [110]. Areal and laminar position of the migrating neurons are determined by signaling molecules secreted from patterning centers [111] [112] and their respective functional roles are further specified by the expression patterns of several genes [113] [114].

Structural properties of the subplate enable MR imaging of it, providing clinically important information on the development of cortical connectivity in the human fetus. The subplate is a cellular compartment characterized by advanced neuronal differentiation and synaptogenesis [115] and contains a growing front of ‘waiting’ (Fig 1.10.a) thalamocortical afferents [116] [117] [118]. These characteristics make the presence and prominence of the subplate with in vivo MR images as the best indicator of normal development of the cortical connectivity in the human fetus. Several studies confirmed that the human fetus can receive a thalamic input through the transient subplate zone at the end of the mid fetal period [117] [119] [120] [121]. Although the period of development before 28 wGA has been described as non-driven by sensory input [119] [122], there is still the possibility of extrinsic influences during the end of the mid fetal period [110].

Reorganization of the subplate and gradual penetration of thalamocortical afferents into the cortical plate build the framework for a sensory-driven activity in the preterm infant cortex. In the very preterm infants, younger than 24 postconceptional weeks (PCW) (i.e. 26 wGA), thalamocortical afferents accumulate in the superficial subplate (Fig 1.10.b). Between 24 and 26 PCW, thalamocortical afferents invade the cortical plate (Fig 1.10.c) according to their target areas. At this period, the first synapses appear within the cortical plate in a deep-to-superficial fashion. Between 29 and 32 PCW, thalamocortical axons establish synapses with neurons of cortical plate layer IV, leading to the sensory-driven activity in terms of function (Fig 1.10.d). The interhemispheric synchronization is developed between 33 and 35 PCW and the period from 36 PCW to the term maturation is along with the intra-hemispheric (associative) and interhemispheric (callosal) cortico-cortical connectivity [110]. The subplate is the thickest cortical layer showing the maximum value in preterm infants between 22 and 34 wGA [115] [123]. Variations of the subplate zone and its neurons are major events during the perinatal and early postnatal reorganization of the developing cortex, highlighting the importance of monitoring its developmental changes by in vitro and in vivo MR imaging.

Successful MRI visualization of the subplate in preterm neonates indicates that the cortical connections are still in the progress of growth. The intricate roles of the subplate in the relocation of axons to the cortical plate are not limited to thalamocortical afferents. After the relocation of the thalamocortical axons, the cells and the extracellular matrix of the subplate remain involved in the development of long cortico-cortical axons [115] [117] [119]. Protracted postnatal development of the associative cortical circuitry is observed as an essential feature of the human cortex [123]. The observed developmental trends are followed by the disappearance of the subplate, after its transformation and reorganization which represent major perinatal events in the developing cortex [123]. In the primary visual cortex, the subplate disappears during the final weeks of gestation [115]. Numerous subplate neurons are present in the somatosensory cortex of the term newborn [115]. However, it is difficult to delineate the subplate as an architectonic layer [115]. By contrast, the subplate of the prefrontal associative cortex disappears gradually over the 6 postnatal months [123], which is probably related to the protracted growth of short cortico-cortical pathways through the layer VI-WM interface and its role in the postnatal shaping of tertiary gyri [115] [119] [123].

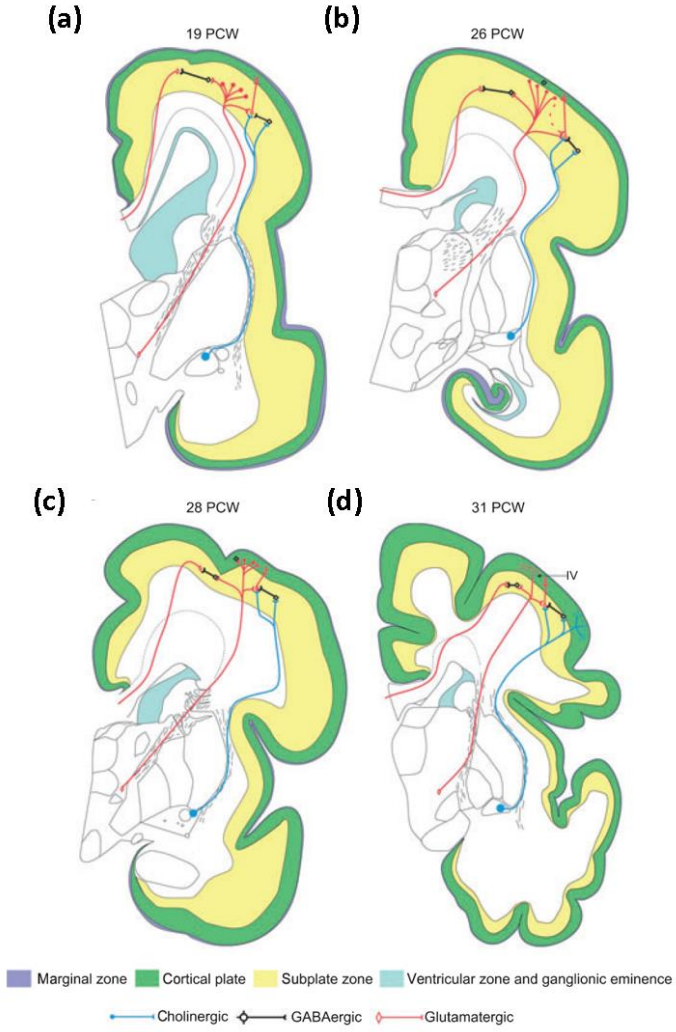

Figure 1.10: (a) Organization of the afferent systems and transient cortical circuitry in human foetuses and preterm infants. The midfoetal 'waiting' period, (b) accumulation of the afferents in the superficial subplate (i.e. below the cortical plate) in very early preterm (22–23 PCW), (c) penetration of the afferents into the cortical plate after 24 PCW, (d) intra-cortical elaboration of thalamocortical fibers after 29 PCW [110].

The human cerebral cortex begins its ontogenetic development around the sixth wGA [124]. It is believed that the development of the cerebral cortex begins with the arrival of primitive corticipetal fibers, followed by the differentiation of horizontal Cajal-Retzius neurons and the establishment of a superficial primary plexiform lamina [124]. Formation of the cerebral cortex occurs in an inside-out manner, i.e. the last migrating neurons are targeted to the more superficial layers of the cortex [112] [125]. In the next step, the neurons are aggregated in the cortical layers to form the cortical neural circuits and regions with specific characteristics [108]. Neural circuits are first developed by overproduction of neuronal axons, dendrites, dendritic spines and synapses and then refined by several processes such as the

elimination of axons, dendritic spines and synapses [126] [127] [128]. After these reorganizations, myelination of the axons occurs in two steps. The first step, the proliferation and settlement of oligodendrocytes around the axons [129], is followed by the second step which is their spiral wrapping [130] and chemical maturation [131] [132]. Developmental periods of occurrence of main neurogenetic events in cortical histogenesis are illustrated in Fig. 1.11 [108]. During the post-term period, cortical maturation continues with the myelination of intra-cortical axons and pruning of axons, dendritic spines and synapses. These developmental changes are reflected in the signal contrasts of MR images, allowing to investigate different maturational stages [107].

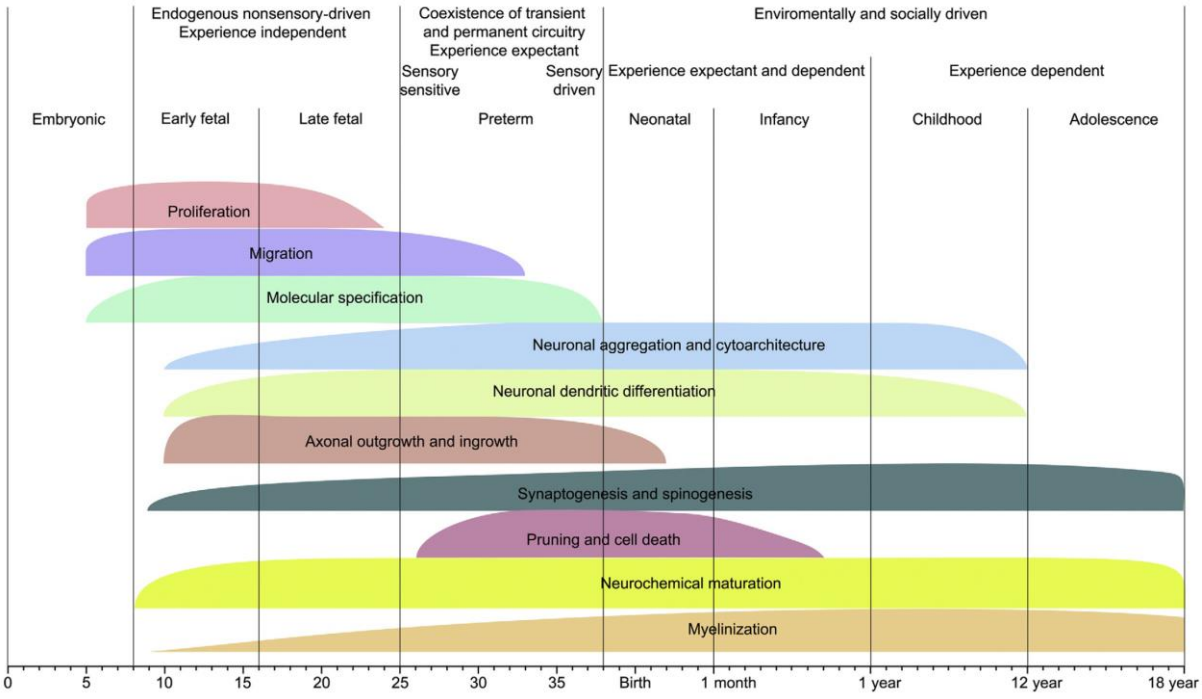

Figure 1.11: Developmental periods of occurrence of main neurogenetic events in cortical histogenesis [108].

1.6.2 Development and maturation of connections

Formation of the connectivity patterns is another developmental process that occurs during the fetal period. The axonal growth produces transient connectivity patterns particularly toward the subplate zone [133]. The transient connectivity patterns start to relocate from the subplate to the cortical plate in the early preterm period. The first connections from thalamus to cortical neurons are established at the beginning of the early preterm period (24 PCW)

[134]. Furthermore, limbic and associative cortico-cortical connections progressively develop before term (17 PCW) [135]. Connectivity development continues after term for short fibers connecting adjacent gyri [136]. Generally, developed connections include overproduced axons that are pruned after birth by interacting with the environmental inputs. The refining of the connectivity occurs in parallel with the reorganization of cortical synaptic patterns [127]. Along with the pruning of the connections, they become functionally more efficient through the myelination of the axons. Myelination accelerates the speed of neural information by establishing the lipid myelin layers around neuronal axons. It is most drastic at the term age and in the first postnatal years. The myelination occurs earlier and faster in sensory than in motor pathways, in projection pathways, connecting subcortical nuclei and cortical regions than in associative ones, in proximal than distal pathways, in central areas rather than the peripheral ones, and in occipital lobe than in parietal, temporal and frontal lobes [137].

1.6.3 Macrostructural development

At the macroscopic level, a remarkable morphological change is observed due to the increase in brain volume. Cortical volume increases from ~10 cm^3 to ~200 cm^3 between the 21–40 wGA [71] [138], and from ~200 cm^3 to ~500 cm^3 during the first two postnatal years [69] [70]. Developmental changes are also evident in the WM volume increasing from ~50 cm^3 to ~150 cm^3 between the 30–40 wGA [71] and from ~150 cm^3 to ~200 cm^3 during the first two postnatal years [69]. Age-related changes continue at a slower rate until adolescence for both the cortical areas and the WM [139] [140]. Increases of the cortical volume occur asynchronously among different brain regions. The increment rates vary at different periods of development. As an instance, the cortical volume increases more in the occipital and parietal regions compared to the frontal areas, during the fetal period (20-28 wGA) [80]. However, it increases more rapidly in the frontal and parietal areas compared to the motor and sensory regions, during the first two years of post-term period [70]. In addition to the growth of the cortical and WM volume, cortical folding also occurs for the central, parietal, temporal, occipital and frontal gyri, respectively, between the 20 wGA and term age [141] [142]. Figure 1.12 presents structural imaging of the developing brain for 3 preterm newborns of different ages and an infant aged 4 weeks post-term age [78]. Momeni et al. [143] presented a 2-week interval for temporal resolvability of age-related atlases to study macroscopic morphological brain development in the early weeks after birth. They constructed two neonatal brain atlases for the age ranges of 39-40 and 41-42 wGA with T1w images [144].

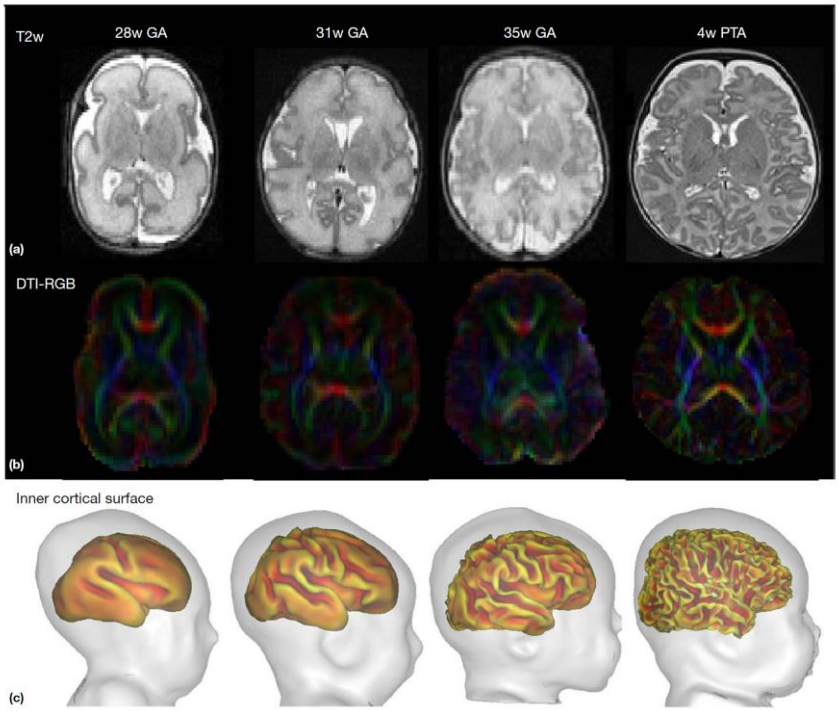

Figure 1.12: (a) T2w images, (b) DTI-RGB directionality maps, (c) Inner cortical surfaces [145] [146] for 3 preterm newborns of different ages and an infant aged 4 weeks post-term age [78].

1.6.4 Measuring structural markers of myelination

Several maturational processes occurring throughout the development of the preterm infant's brain may affect neuronal conduction velocity leading to the reduced latency of the evoked responses. These may include the microstructural organization of the cortical plate and subplate, the evolution of the membranes, connectivity, cortical folding, synaptic bursting, pruning, etc. However, the main factor which contributes to the acceleration of the ERP latencies is the establishment of the myelin layer around the neuronal axons. Few studies have investigated the effect of myelination on the functional output of the infant's brain [147] [148]. As an instance, Dubois et al. [147], related the increase in P1 conduction velocity of the full-term infants' VEPs to the maturation of optic radiations and the transfer time between hemispheres to the maturation of the visual callosal fibers that persist even after having control for the age effect. Structural markers of myelination were extracted by measuring transverse diffusivity in different WM tracts using DTI. In addition to the DTI parameters which present the structural markers of myelination, another MR-extracted feature is proposed which may reflect developmental changes resulted from the myelination. The ratio of T1w and T2w MRI signal intensity is supposed to increases the sensitivity (see Chapter 2)

to measure myelin-related signal intensity changes [149]. This method provides the possibility to measure the myelination for both GM and WM regions; since it does not depend on the axon fiber anatomy compared to DTI. Therefore, it is an appropriate approach for estimating the whole-brain intracortical myelin-related changes which are difficult to be measured directly using existing noninvasive neuroimaging tools [150]. In the current study, we measured the mean value of the T1w/T2w ratio images in each ROI of a neonatal atlas, to relate the latency of the CAEPs to the myelination of different structures for the preterm infants listening to the repetitive syllabic stimuli. Although this measure has been used previously as an estimate of the myelin content in adults [149] [150] [151], children [151] and infants 40-48 wGA [152], we may notice that it may be influenced by other developmental changes in the age-range of our study. Therefore, we may consider it as a structural maturation index measured by combining different sensitivities of the T1w and T2w images to water.

1.7 Functional and structural interaction in the early stages of development

Several studies have highlighted the micro- and macro-structural as well as the functional aspects of the infant's brain maturation which occur asynchronously across different brain regions. However, the link between these structural and functional aspects of brain maturation remains less investigated.

Generally, the brain imaging approaches have replicated and extended the traditional post-mortem studies, make it possible to examine neural development in healthy infants and other groups. Dubois et al. [153] conducted a review survey on the MRI and M/EEG studies of the WM development in human fetuses and infants. In this review, they described how the non-invasive techniques such as MRI and M/EEG have been applied to study the WM maturation. Early architecture and myelination of bundles have been assessed at the structural level with diffusion and relaxometry MRI. On the other hand, the M/EEG have been used to record different visual, somatosensory and auditory evoked responses. As the conduction velocity of the neural impulses increases with the myelination, significant changes are observed in the ERPs' components latency throughout the development. So far only a few studies have related structural and functional markers of WM myelination. However, such multi-modal approaches, although challenging, may help to better understand normal development and characterize early mechanisms of pathologies.

Dubois et al. [154] investigated the WM maturation through an MRI study. As the axons of the WM are progressively ensheathed by myelin, the increasing lipid content and fiber compactness constrain the diffusion of water molecules. These developmental changes can be measured indirectly with DTI, showing some decrease in transverse diffusivity and an increase in fractional anisotropy in most of the tracts during the infancy [155]. At the same time, intense developmental changes are occurring at the functional level which can be measured with MEG/EEG. Latencies of the ERPs are progressively changing, especially during the first post-natal year. For instance, the infant's brain experiences a drastic increase in the speed of visual responses in only a few weeks; P100 (P1) latency is reduced from 300 ms at birth to the adult level (~100-120 ms) around 3 months of age [156]. As the myelination increases the speed of neural conduction, we may expect the MRI indices of WM maturation to be correlated with the neural conduction speed reflected through the latencies of ERP components. The increase in the speed of visual P100, during early infancy, is significantly related to the transverse diffusivity measured in the early visual projection pathways, regardless of the age effect [147].

For the auditory system, the developmental procedure is different from the visual system. Since the womb environment is noisy, the auditory cortex is already subjected to the stimuli before birth. Myelination of the acoustic radiations occurs slowly and the latencies of the auditory responses are also changing more slowly than the latencies of the visual responses. Adibpour et al. [107], studied the relation between microstructural maturation of WM pathways and functional efficiency of evoked responses for two brain networks with different developmental trajectories. In their earlier study of 1 to 4 months old infants [147], they showed that the conduction velocity of visual evoked responses was related more to the optic radiations (projection pathways) maturation than to the infants' age. In [107], they aimed at investigating the same result for projection pathways and extending them to cortico-cortical callosal pathways in the visual network and to similar pathways of the auditory networks. They focused on the WM maturation and correlated structural and functional parameters that have developmental relevance based on the common underlying biological phenomenon of myelination. This type of structure-function relationship is restricted to the WM myelination, which is only one of the several aspects of brain development. However, the myelination is essential in learning and cognitive development, as it increases the speed of neural information transmission and thus the synchrony of impulse conduction between distant cortical regions [157]. Therefore, the concurrent study of the structural and functional maturation of WM, clarify some aspects of the cognitive development. In full-term infants

tested during the first semester, Adibpour et al. [148] found no relation between the conduction speed of the auditory P2 and DTI parameters changes in acoustic radiations, but with the GM maturation in the inferior frontal region.

Considering measures of cortical maturation in addition to WM maturation might be also helpful during the development since it provides a more realistic model for explaining the functional properties of the auditory responses. T1W/T2W ratio image may provide a myelination index which can be used for both the WM and GM, since it does not depend on the axon fiber anatomy compared to DTI. Therefore, it is a useful approach for estimating the whole-brain intracortical myelin-related changes. This measure has been used previously as an estimate of the myelin content in adults [149] [150] [151], children [151] and infants 40-48 wGA [152].

Although several studies investigated functional and structural correlates of age-related changes in the brain for the aging population [87], adults [85], children [86] and full-term infants [147] [148], whether a similar function-structure relation exists for the preterm infants is not understood. In the current study, we investigate how the gradual acceleration of the auditory ERP might be related to the WM and GM maturation in preterm neonates. We analyzed the CAEPs of preterm infants in response to repetitive syllabic stimuli. The latency of the first peak of the GFP was considered the functional feature of interest to be examined for correlation with age and the structural maturation index extracted from brain atlases of the corresponding term age. GFP is calculated for each infant since it provides a global measure from the entire the head less influenced by the variabilities of the individual electrodes which are significant for the preterm infants. Furthermore, we measured the mean value of the T1w/T2w ratio images in each ROI of a neonatal atlas, as a structural maturation index, to relate the latency of the CAEPs to the maturation of different structures. Dividing the T1w signal intensity by T2w corresponding values increases the contrast of the myelin content. The main purpose of this joint structural-functional approach is to highlight the correlations between the functional feature and age, between the structural feature and age and between the functional and structural features before and after removing the effect of age. We also aimed at illustrating the specificity of the observed relation between the function and structure to the auditory involved areas.

1.8 Language maturation and asymmetries

1.8.1 Language network and its lateralization in the adult brain

Language processing in the adult brain is performed through a dedicated network of brain regions extended around the Sylvian fissure (Fig. 1.13). The key point for these regions to function as a network is the information transfer between them which is conducted by dorsal and ventral pathways connecting prefrontal and temporal language relevant regions. These pathways include 1) the dorsal pathway connecting the dorsal premotor (dPMC) with posterior temporal cortex (posterior middle temporal gyrus/ superior temporal gyrus: pMTG/STG), 2) the dorsal pathway connecting Broca's area (BA) 44 with the posterior STG, 3) the ventral pathway connecting the frontal cortex (FC), that is, BA 45 and others, with the temporal (TC), the parietal (PC), and the occipital (OC) cortex and 4) the ventral pathway connecting the anterior inferior FC (aIFC), that is, BA 47 and others, and the frontal operculum (FOP), with the anterior TC (aTC). Functional brain imaging has determined the related function of each of these pathways in language processing. Dorsally, the pathway connecting the TC and premotor cortex supports speech repetition. The other dorsal pathway connecting the TC and posterior Broca's area supports complex syntactic processes. Ventrally, the uncinate fascicle and the inferior fronto-occipital fascicle subserve semantic and basic syntactic processes. Therefore, a neural language network is characterized with at least two dorsal and two ventral pathways [158].

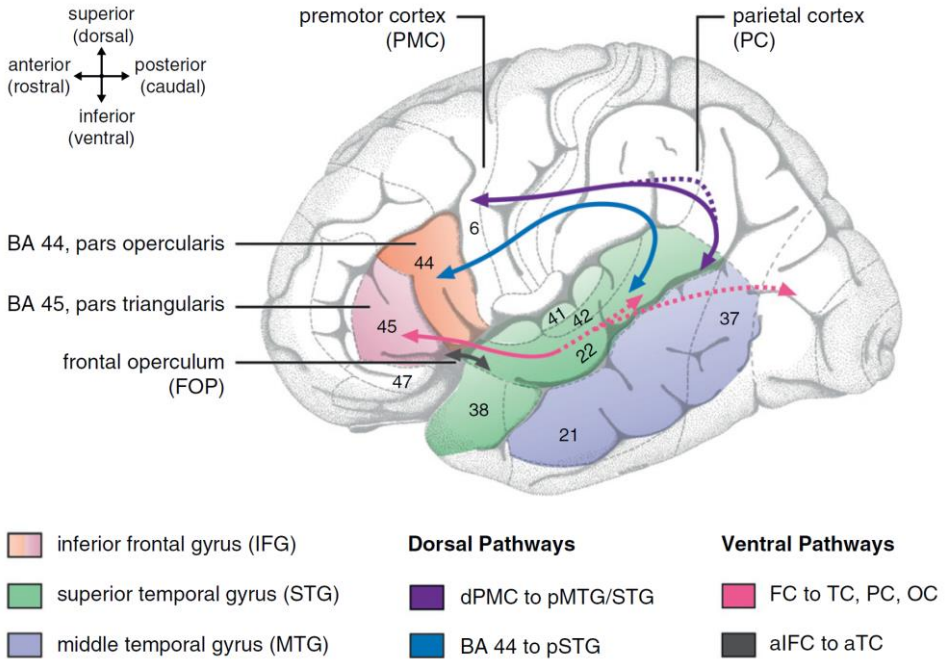

Figure 1.13: Language-relevant brain regions along with the dorsal and ventral pathways [158].

Functional characteristics of the language network can be identified by localizing the brain activity when the subject performs an auditory task such as listening to the sentences and words. As an instance, the brain activity is localized around the perisylvian regions with stronger activity in the left hemisphere while listening to the native language compared to non-native language [159] [160]. However, defining a specific role for each region of the language network is challengeable due to the complex nature of the language including phonology, syntax and semantics. Generally, spectro-temporal features of the speech, notably the fast temporal transitions embedded in the speech stimuli, are better processed by the structural parts of the auditory network in the left hemisphere [161] [162]. Furthermore, there is leftward lateralization for the communicative features of the language which are more pronounced in the familiar (native) versus unfamiliar languages [160].

Regarding the structural characteristics of the language areas, there is an asymmetry between the left and right hemispheres in the perisylvian regions. At the macroscopic level, elongated Sylvian fissure and larger planum temporale are observed in the left hemisphere [163]. Moreover, the WM volume underneath the Heschl's gyrus and primary auditory cortices are larger in the left compared to the right hemisphere [164]. At the microscopic level, the pyramidal neurons of the left auditory cortices are larger [165] and the axons are more myelinated in the WM below the posterior superior temporal cortices of the left hemisphere [166]. Furthermore, the size of the neuronal columns and the distance between them is larger in the left superior temporal lobe [167] and the receptor density profiles of the BA and Wernicke's region are similar in the left but not in the right hemisphere [168]. To investigate whether the observed functional and structural asymmetries are due to the age and exposure of the adult's brain to linguistic stimuli with certain spectro-temporal characteristics, one may study the ontogeny of the lateralization early in life.

1.8.2 Language maturation in infants

The infant's perceptual system is tuned to different aspects of the speech stimuli and the newborns and young infants prefer speech stimuli to other stimuli with similar acoustic characteristics [169] [170]. They are capable of distinguishing between two different languages based on different prosodies [171]. Neonates and even preterm infants of only 6 months gestation discriminate the phonetic contrasts resulted by voice differences (e.g. /ba/

vs. /pa/) or place of articulation (e.g. /ba/ vs. /ga/) [172] [173] [101]. During the first year of life, the infants improve in distinguishing the phonetic contrasts of their native language, while degrade in perceiving similar phonetic contrasts of non-native language [174] [175]. In addition to linguistic abilities, the newborn shows a preference for the mother's voice [176]. Even the preterm infants are able to distinguish the pitch contrasts such as the difference between the male and female voice [101]. Phonetic discrimination abilities have been studied throughout the first postnatal year by comparing the EEG recordings in response to a series of repeated syllables (e.g: /ba/ /ba/ ba/ /ba/) with a series including a deviant syllable (e.g: /ba/ /ba/ ba/ /ga/). The so-called mismatch response, which raised over the fronto-temporal brain areas, demonstrates the responsiveness of the developing network to a change in the synthetic speech stimuli [177] [102] [62] [178]. Furthermore, preterm infants of 6 months of GA, demonstrated mismatch responses for a change in phoneme or voice, distributed over the fronto-temporal regions [88].

Along with the functional linguistic achievements, the neural architecture of the perisylvian regions develops progressively. A gradient in the cortical folding is observed in the preterm period, with the primary auditory cortices preceding the associative ones [179]. For the 1- to 4-month-old infants, a gradient of the maturation is observed, with superior temporal sulcus having the least mature microstructure relative to the inferior frontal region, and further to planum temporale and Heschl's gyrus [180]. Regarding the WM maturation, the dorsal pathways lag behind the ventral pathways [181] [182], but have faster maturation speed between 1 to 6 months of infancy [182].

1.8.3 Language asymmetries in infants

Several studies investigated the functional lateralization of the ERPs to linguistic stimuli and structural asymmetries of the language network in early development. The earliest structural asymmetries are observed during the fetal and preterm periods in the cortical gyri confirming that the Heschl's gyrus, superior frontal and temporal gyrus folding occur 1-2 weeks earlier in the right hemisphere [179] [183]. Asymmetries become more evident in the perisylvian regions during the preterm period and early postnatal months, with thicker Heschl's gyrus, more elongated planum temporale, and stronger growth of the anterior region of the Sylvian fissure in the left, but deeper superior temporal sulcus in the right hemisphere [184] [185] [186] [180]. Regarding the microstructural properties of the left and right perisylvian regions, the inferior frontal sulcus (Broca's area) is more mature on the left,

whereas posterior superior temporal sulcus is more mature on the right hemisphere [180]. Figure 1.14 illustrates the inter-hemispheric asymmetries of maturation for planum temporale, Heschl's gyrus and superior temporal sulcus observed for the 1- to 4-month-old infants [180].

Several EEG studies attempted to investigate the lateralization of early language processing. Phonetic contrasts produced mismatch responses stronger in the left fronto-temporal areas in newborns and 2-3-month-old infants [102] [187]. However, these responses were not found to be left-lateralized in 3-months-olds [177], 8-months-olds [178] and 9- and 12-months old infants [188]. The observed inconsistencies might be related to the poor spatial localization of the EEG signals. Using fNIRS for the preterm infants of 6 months of GA illustrated stronger discrimination responses in the left hemisphere for a change of phoneme but not voice [101]. Investigating fMRI for the 2- and 3-month-old infants showed a more pronounced activation in the left posterior temporal regions (around the planum temporale) for the speech stimuli, whereas a symmetric activation for the music. Similar lateralization was observed for the mother's speech relative to that of a stranger [189].

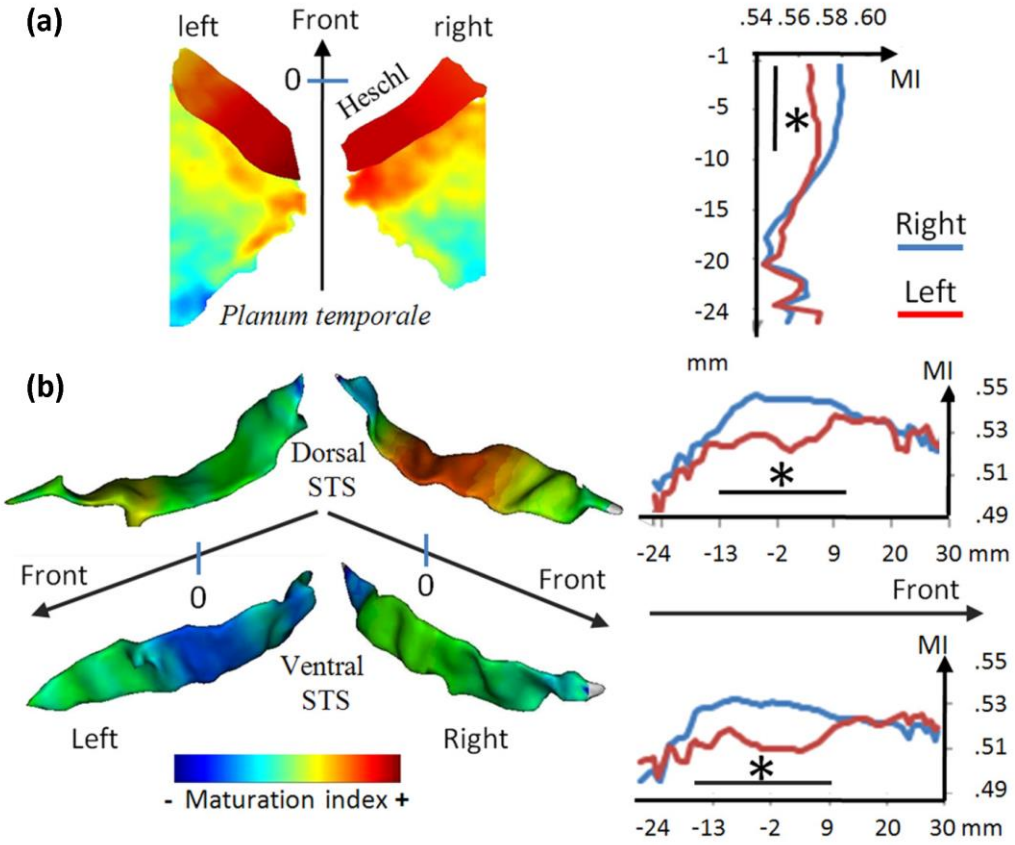

Figure 1.14: Maturation asymmetries in the temporal areas. (a) Two-dimensional projection of the mean value of the maturation index (MI) across infants in Heschl's gyrus and planum temporale. The left planum is larger and there is an anterior–posterior and medial-lateral gradient of maturation in both Heschl's gyrus and the planum. The right column presents the MI measured along the planum anterior–posterior axis. (b) Mean MI of the left and right STS projected on an individual 3-D mesh of the sulcus. The right column presents the MI measured along the anterior–posterior axis of both sulcal banks. Black horizontal lines show the spatial extent of the significant asymmetry measured in each point through permutations. Note also the dorsal–ventral gradient of maturation (planum_dorsal STS_ventral STS) [180].

1.8.4 Lateralization of the auditory responses

ASSRs have been used for evaluating the lateralization of the responses to low modulation rates in adults and children [190] [191] [161] [192] [193]. Generally, the right hemisphere is thought to be sensitive to auditory modulations close to the speech syllabic rate (~1-4 Hz) [161] [192] [193], whereas bilateral [161] [193] or left hemispheric [192] specialization is reported for faster modulations like phonemic rate (~10-50 Hz) [190]. Actually, the temporal/spectral acoustic properties of the auditory stimuli affect the relative hemispheric specialization of their processing [162] [194]. While the broad-band auditory stimuli with rapid changes and temporal complexity are predominantly processed in the left hemisphere, slowly changing narrow-band stimuli and spectral processing of sounds [162] are essentially processed in the right hemisphere [195] [196]. It has been reported that phoneme-rate modulations lateralize to the left hemisphere, while rightward specialization is predominantly involved in low-frequency ASSRs and slower modulation rates such as syllabic-rate modulations [190]. Although the right asymmetry for slow modulations has been previously reported in adults [190], children [197], and newborns [198] [199], it was not clear whether some similar lateralization might exist in preterm infants. Most of the previous works have focused exclusively on lateralization in adults and infants. Only a few studies have investigated the asymmetry in preterm infants. Mahmoudzadeh et al. [101], reported larger BOLD responses over the right frontal and temporal regions, using near-infrared spectroscopy in preterm infants in response to phonemic stimulations. Only the left posterior temporo-parietal region escaped this general pattern and displayed a faster and more sustained response than the right (Fig. 1.15) [101]. Furthermore, they reported left hemisphere lateralization for mismatch responses to a change of phoneme and rightward lateralization for the mismatch responses to a change of voice, using ERPs of the same group of preterm infants [88]. These observations motivated us to investigate the lateralization of low-frequency modulations in our study, which includes the preterm infants at the same ages and processing the same syllabic stimuli as [101].

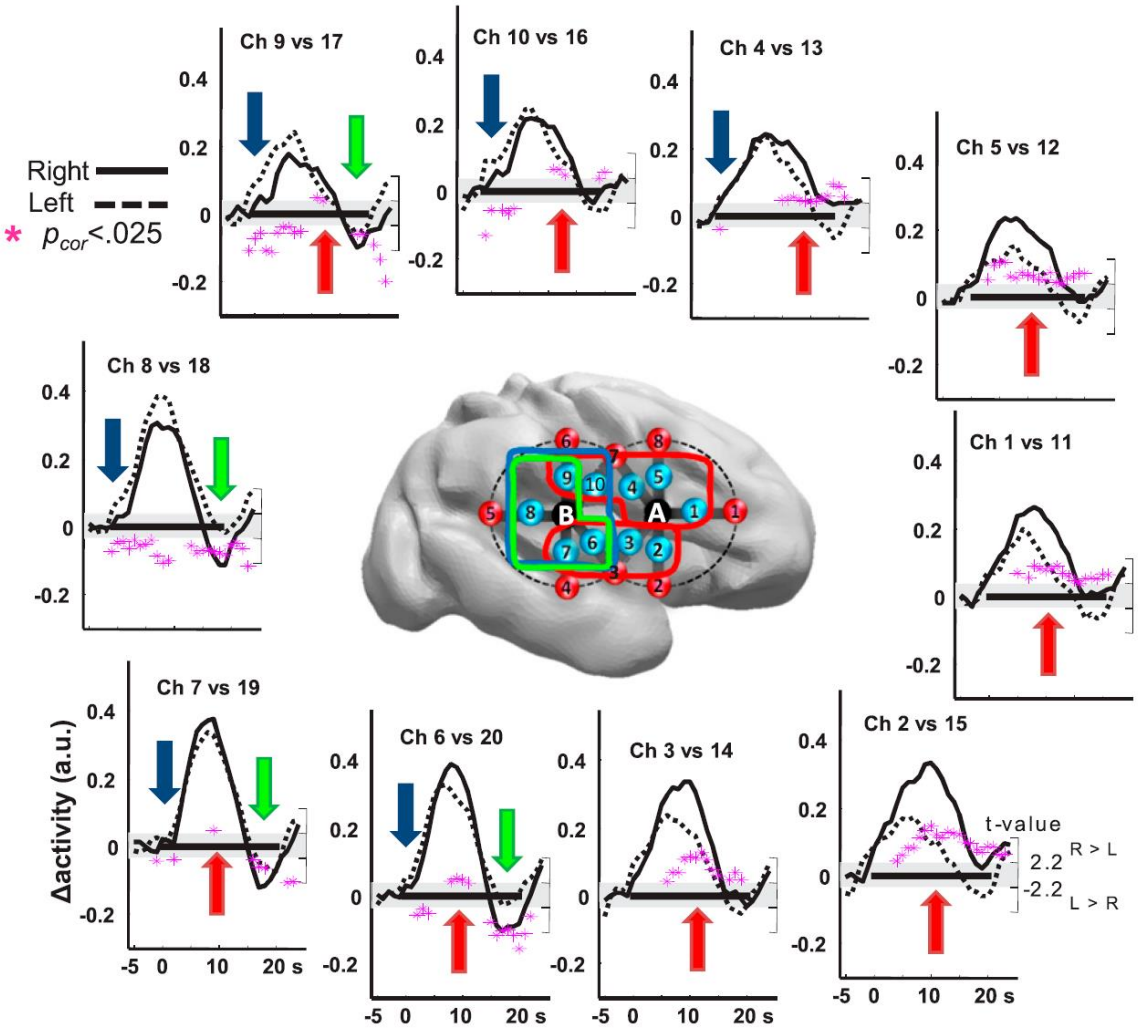

Figure 1.15: Lateralization of the responses to speech syllables in premature infants. The right and left grand average HbO responses to all conditions are plotted for symmetrical channels, whose locations are presented over a right hemisphere view of a preterm brain. Pink stars indicate the t-value of the samples (right scale) included in significant clusters (Pcor < 0.025). Values are positive when right > left and negative for the opposite direction. The four significant temporo-spatial clusters are identified by colored arrows on the plots and lines surrounding the channels on the brain. Responses are larger on the right hemisphere (red clusters) but are faster (blue cluster) and last longer (green cluster) in the posterior left regions [101].

1.9 Clinical and scientific impacts

Premature neonates, even born very early, may survive as a result of intensive care [88]. Longitudinal monitoring of the preterm infants' ERPs, at each wGA, illustrates the emergence, as well as the developmental trend and maturation of different functionalities of their brain. Analyzing the ERPs of the premature newborns provides the reference tool to

non-invasively investigate the normal and pathological functioning of their neural networks. Results of the ERP analysis at each wGA can be used clinically to characterize the normalcy of brain activities according to age, to identify early dysfunctions of brain activity, to set up monitoring during treatment in NICU and to define predictive neurodevelopmental outcomes. In the current thesis, we analyze the ERPs of the preterm infants in response to repetitive syllabic stimuli in the frequency domain. Frequency measures are less sensitive to the inevitable background noise and variability since the analyses are reduced to the specific frequency of stimulation. Furthermore, the variation of the conductivity between the electrode and the scalp which is a result of gel injection do not affect the EEG frequency content, although changing its temporal characteristics [200]. Hence, the frequency analysis is very suitable for studies in preterm and term neonates providing a useful approach to assess certain functional aspects of the capacity of auditory circuits underlying normal neurodevelopment.

On the other hand, analysis of MR images of the preterm infants provides insights on the structural maturation of the brain at each wGA. In our study, we define a maturational index related to the myelination and investigate its developmental changes at each wGA. The range of the variations of different structural features can also be presented as normative data for monitoring the normal development at this critical period of life.

Generally, extracting functional features from the EEG signals and structural features from MR images at each wGA provides normal ranges of variations for each specific feature. In the current thesis, in addition to the information on the ranges of variations for both the functional and structural features, we present the specificity of the interaction between the functional feature extracted from the CAEPs while processing the repetitive syllabic stimuli and structural myelination index of auditory-involved areas extracted from MR images of the infants at the same age. Therefore, a functional-structural relationship characteristic of typically developing preterm neonate is presented by the current findings. To the best of our knowledge, this is the first study focusing on the joint functional and structural development of the auditory-involved area in preterm infants. In the current study, some associations are presented between structural maturation, electrophysiological function and age which support a biophysical model of developmental changes in the preterm infant's auditory system. This work opens an interesting path to detect early deviations related to perinatal disorders or pathologies in which we try to relate structure and function. Since the EEG recording is much easier than MRI in neonatal units, understanding how ERP latencies are related to brain areas and their maturation, or lesion, would be tremendous progress to investigate and follow daily care in neonatal units.

Rest of the dissertation is organized as follows. Chapter 2 introduces the materials and methods applied to conduct the analyses. Chapter 3 presents the study focusing on the neurodevelopment and asymmetry of auditory responses to repetitive syllabic stimuli in preterm infants. Chapter 4 is dedicated to the study aimed at relating developmental changes of the auditory responses to myelin maturation. Finally, Chapter 5 presents the general conclusion of the dissertation and suggested future works.

Chapter 2

Materials and methods

In this chapter, we describe the details of the functional and structural datasets applied in the current thesis. Furthermore, we illustrate the basics and fundamentals behind the methods recruited for analyzing the functional and structural data along with the statistical approaches appropriate for finding the correlations between the structural and functional findings related to the development of the preterm brain.

2.1 Functional dataset

The functional dataset includes the EEG signals of the preterm infants in response to the auditory stimuli, recruited in [201]. Details of the participants, stimuli and recordings are described in the following.

2.1.1 Participants

Nineteen healthy preterm neonates (11 males, 8 females; mean GA at birth: 30.4 ± 1.4 weeks GA) were tested while sleeping at night during their first week of life (mean recording age: 3 days (1–6 days) corresponding to 30.8 ± 1.4 wGA) in Amiens (hôpital Nord), France. All the infants had appropriate birth weight, size, and head circumference for their term age. Furthermore, they had normal auditory and clinical neurological assessments and were considered to be at low risk for brain damage presenting normal ultrasonography and normal EEG for term age. Parents were informed about the study and provided their written informed consent. The study was approved by the Amiens University Hospital local ethics committee (CPP Nord-Ouest II) according to the guidelines of the Declaration of Helsinki of 1975 (ref ID-RCB 2008-A00728-47) [201].

2.1.2 Procedure design and auditory stimulation

The stimuli consisted of four digitized syllables /ba/ and /ga/, naturally produced by a French male (baM, gaM) and a French female speaker (baF, gaF). The syllables were matched for intensity and total duration (285 ms) prevoicing and voiced formant transition duration (40 and 45 ms, respectively). They were presented at a comfortable hearing level of 70 dB (Fig. 2.1) [88].

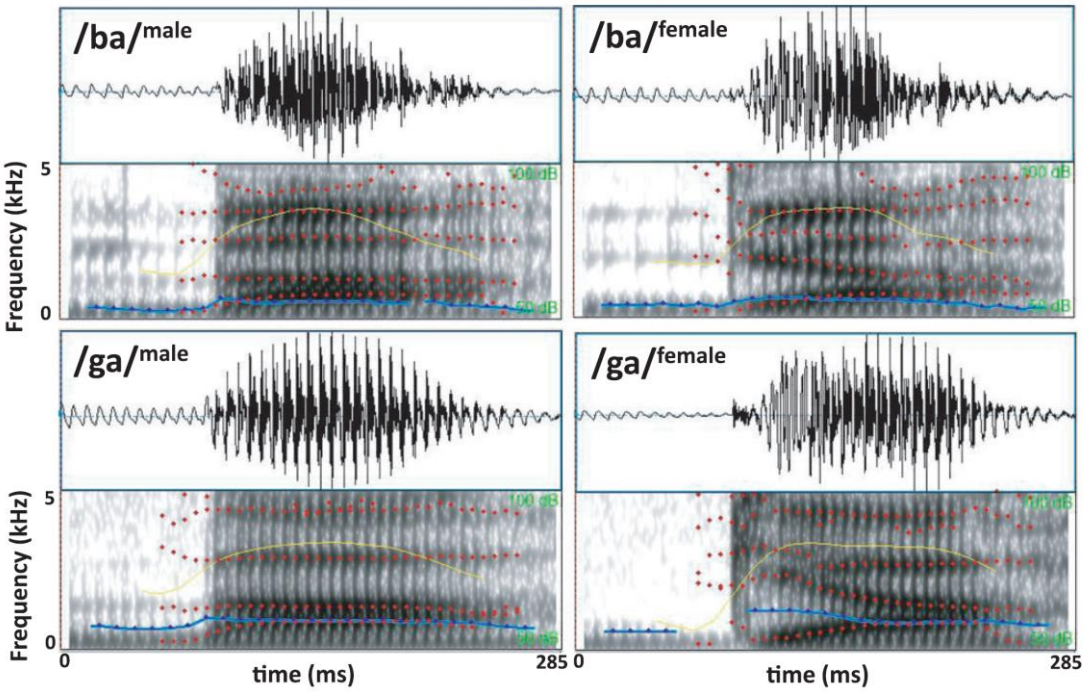

Figure 2.1: The signals and spectrograms containing the syllables /ba/ and /ga/ naturally produced by a French male (baM, gaM) and a French female (baF, gaF) speaker, matched for intensity, total duration (285 ms), prevoicing and voiced formant transition duration (40 and 45 ms, respectively) [88].

The syllables were presented by series of four (separated by an interstimulus interval of 600 ms) to form three types of trials including the standard, deviant voice and deviant phoneme trials. In standard trials, the same syllable was repeated four times (e.g. /baM/ /baM/ /baM/ /baM/). In deviant trials, the last syllable differed with the first three either along the voice dimension (e.g. /baM/ /baM/ /baM/ /baF/), or along the phonetic dimension (e.g. /baM/ /baM/ /baM/ /gaM/). The trials constructed the blocks of five (block duration 20s) separated by an inter-trial interval of 1600ms. There were three types of blocks including one standard block and two deviant blocks. In standard blocks (ST), all trials were standard trials. In deviant blocks (DV and DP) there were three deviant and two standard trials. The reason

behind this design was to avoid infant's expectation of the change on the last syllable of the trial. DV blocks consisted of deviant trials along the voice dimension, and DP blocks consisted of deviant trials along the phonetic dimension. Each deviant block always began with a deviant trial. The following four trials were randomly intermixed in the block. In each block, the repeated syllable was kept constant and was randomly chosen among the four possible syllables (baM, gaM, baF, gaF). Each syllable was presented the same number of times in each condition. The three types of blocks (ST, DV and DP) were randomly presented, separated by 40 s of silence. This particular design (i.e. the silence) allowed the metabolic response to recover its baseline level between blocks. Totally, 108 blocks were presented during the total period of 108 min, including 36 blocks in each condition (ST, DV and DP) [201].

Specific design of this auditory paradigm (i.e. the repetitive characteristic of the stimulation) provides us the opportunity to examine the capability of the preterm brain to follow the rhythmicity of the external ecological stimulations. As the stimulation is repeated with a specific frequency we can observe the same frequency and its harmonics in the recorded response and consider them as age-dependant functional features. In the first part of our analysis, we focus on the repetition of the same syllables, so we just use the standard trials of the current stimuli. In the second part of our analyses, when calculating the GFP of the EEG signals, we use all the standard and deviant trials (after artifact rejection) to have as many trials as possible leading to a more reliable ERP with a higher signal-to-noise ratio (SNR).

2.1.3 EEG cap and recording

The EEG was recorded continuously using 32-61 surface electrodes placed in custom-made tissue caps designed to adapt to the head size of the subjects. The position of the electrodes on the cap was defined according to the standard 10/20 system. The EEG electrodes were Ag/AgCl sintered ring electrodes which were snapped into the electrode adaptors (Fig. 2.2). At first, the infant scalp was slightly abraded with a cleansing solution (NuPrep©) and then the proper cap was placed on the infant's head according to his/her head size. The caps were made from Spandex-like material with electrode holders sewn into it at standard coordinates. Four different sizes of high-resolution EEG cap with 32, 37, 58 and 61 electrode positions are commonly used for the infants. These caps have been proven to be appropriate for infants as young as 28 wGA up to term newborns. By using high-resolution

caps, more electrodes may be positioned on the infant scalp in a relatively small period of time compared to the case of using single disposable electrodes or the low-density clinical recording electrodes. Conductance EEG gel is inserted under each electrode after the placement of the cap using a blunt-tip syringe and the scalp is lightly abraded using cotton swabs. The cap is held by a chin strap which significantly decreases the risk of electrode displacement. Furthermore, a soft net, Surgifix® covered the cap and the electrodes to prevent moving of the cap out of the desired position (Fig. 2.2). The chin strap could be annoying for some of the infants. Therefore, some non-woven swabs (Raffin®; www.raffin-medical.com) were used around the chin [201].

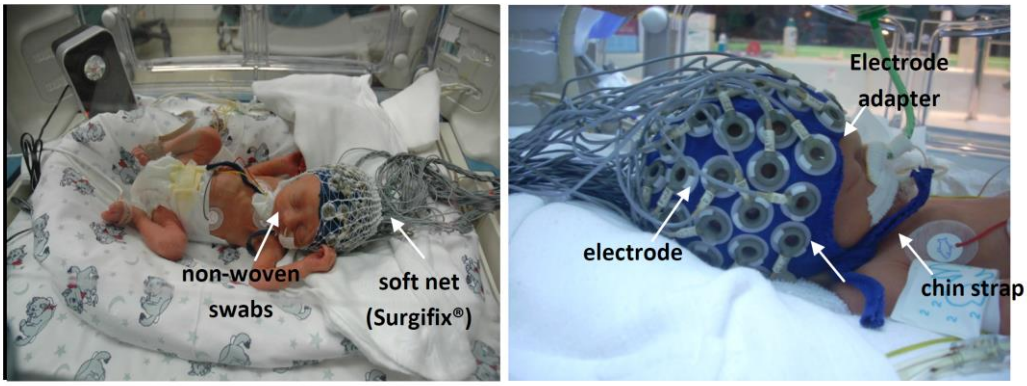

Figure 2.2: Preterm infants wearing a custom-made 32-channel (left) and 37-channel (right) high resolution EEG Cap [201].

In this study, the data are referenced online to an electrode placed on the *Nasion*. The reference electrode should have a low-impedance connection with the scalp. The EEG was amplified by A.N.T® (Enschede, Netherland), DC-50Hz filtered and recorded at a sampling rate of 2048 Hz. The impedance of electrodes was kept below 5 kΩ [201].

2.1.4 Preprocessing

The recordings were visually inspected for the artifacts. The standard approaches used normally in adults cannot be applied to the detection of EEG transients in neonates. The reason is that neonatal EEG recordings present very specific, non-stationary physiological and pathological features. Furthermore, high inter-individual differences are observed in the EEG background activity of the neonates and major intra-individual variations are present in the EEG transients of the infants as a function of their maturation stage. Therefore, an expert visually evaluated each epoch and decided whether to accept it or not [201].

In the current study, the EEG signals were processed offline using MATLAB R16. They were band-pass filtered between 1 and 20 Hz using a low pass zero-phase digital filter followed by a high pass zero-phase digital filter. EEG signals were down-sampled to 512Hz for further analysis. They were segmented into epochs ([−0.5 +2.7 s]) time-locked to the first syllable (S1) of the trial providing 180 standard and 360 deviant trials from each recording electrode for each subject. Trials were then baseline corrected to the 200 ms before beginning of the first syllable. As mentioned earlier, EEG of the preterm infants includes bursts of activity which should be discarded from further analysis. The reason is that the high amplitude of the burst (up to 400 μV) decreases SNR of the single trial and make it necessary to have more than thousand trials for an average SNR of 2 which is the minimum required [201]. Therefore, an automatic artifact-rejection procedure was applied in two steps. In the first step, each trial was rejected if its absolute amplitude exceeded 50 μV. In the second step, each of the remaining trials was discarded if a local amplitude jump between ten successive time-points exceeded 30 μV. Finally, the trials were averaged to obtain the CAEP with an improved SNR compared to the single-trial response.

2.2 EEG signal processing

2.2.1 Frequency characteristic

Although ERPs are usually analyzed in the so-called time domain, additional information on cognitive functions can be assessed when they are analyzed in the frequency domain and considered as event-related oscillations [202]. Steady-state responses are evoked potentials that preserve a stable frequency content over time. Responses to rapidly presented stimuli show a spectrum in the frequency domain with peaks at the rate of stimulation and its harmonics. These steady-state responses are commonly recorded in response to amplitude and/or frequency-modulated stimuli. Therefore, they provide an estimate of how well the brainstem and/or cortex can process small variations in amplitude and/or frequency. Detection of these changes is an essential step in processing speech perception [203]. ASSR is a methodological approach to study auditory development in the frequency domain. ASSR measures the ability of the auditory network to fire synchronously with the rhythm (i.e., modulation rate) of an auditory stimulus. As the brain is stimulated with a specific frequency, we expect the recorded response to show detectable peaks at the target frequency (modulation rate of the stimulation) and its harmonics. Figure 2.3 illustrates a sample of ASSR elicited by a 40Hz sinusoidally modulated 1 kHz tone for young adults [204]. Time waveforms of the

individual subjects' recordings are presented with light traces and the grand average is depicted by a thick dark trace. The stimulus is shown in dark gray (Fig. 2.3.a). The average response spectrum for ASSR recordings is shown in Fig. 2.3.b. ASSRs show dominant energy at the modulation frequency (40 Hz) and integer-related harmonics (i.e., 80, 120 Hz).

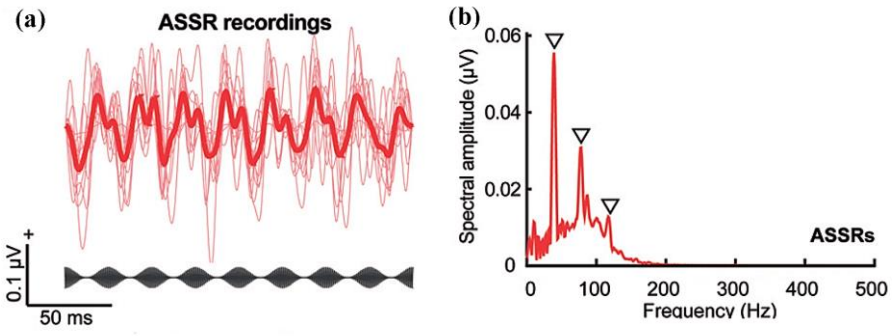

Figure 2.3: ASSR elicited by a 40Hz sinusoidally modulated 1 kHz tone. (a) ASSR time-waveforms for neurobiological recordings. Light traces: overlay of responses from individual subjects; thick dark trace: grand average. The stimulus waveform is shown in dark gray. (b) Average response spectra for ASSR recordings. Dominant energy at the modulation frequency (40 Hz) and integer-related harmonics (i.e., 80, 120 Hz) are distinguishable (adapted from [204]).

As elaborated by the ASSR method, audible tones amplitude-modulated at 40 Hz (more or less) elicit significant scalp potentials in the human brain that follow the modulating frequency. These 40 Hz CAEPs can also be elicited by clicks or tone bursts presented at a rate of about 40/sec, providing a useful approach in clinical audiology for the purpose of threshold estimation. The ASSR approach for estimating the threshold is especially more appropriate for low carrier frequencies, e.g., 500 Hz, where the more commonly used auditory brain-stem responses (ABRs) are less useful. Threshold estimation is based on the determination of the presence or absence of the response at low intensities. In this situation, the CAEP signal may be very small, even after averaging thousands of trials, compared to the background scalp EEG noise. Therefore, objective response detection can be helpful in addition to the visual inspection of the CAEPs [205].

Although the particular auditory stimulation applied in our study, as described in Subsection 2.1.2, does not conform completely to a regular ASSR paradigm, it still provides the repetition of the stimulus with a specific frequency. Since the brain is exposed to a syllable every 600 ms, we expect distinctive peaks around 1.6 Hz and its harmonics. Therefore, temporal responses corresponding to the time interval of the trials with the baseline removed ([0 +2.7 s]), were transformed to the frequency domain using FFT. The number of FFT points was adjusted at the

next power of 2 from the length of the signal. In the next step, the peak amplitudes of the FFT spectrum at the target frequency and its first harmonic were measured as functional features of interest and evaluated for the effect of age on these measurements. The amplitudes of the FFT spectrum at the target frequency and the first harmonic were extracted for each subject and each electrode. The values were then averaged across the 15 channels (Fz, F1, F2, F3, F4, C1, C2, CP1, CP2, Pz, P1, P2, Oz, O1 and O2) for each subject. These 15 channels were the most common channels showing activity between different subjects.

2.2.2 Phase coherence

As mentioned earlier, ASSRs are well suited to be analyzed in the frequency domain. However, the use of phase information in evoked potential analyses has received increasing attention [206] [207] [208]. While a simple inspection of the power spectrum and comparing the peak at target frequency to the adjacent frequencies is helpful, purely objective techniques are also proposed to determine whether or not a genuine response is present. Phase coherence (PC), a statistical measure of phase variance, is the method most commonly used for this purpose [205].

Calculation of PC [205] [208] [209] [210] [211] requires segmentation of the CAEP into multiple subaverages. Subaverages are then transformed into the frequency domain using FFT. For example, a run of 2000 trials could be segmented into 10 subaverages of 200 trials each. In the present study, we applied PC as a complementary frequential feature to study the preterms' response to the auditory stimulation. Sets of 10 trials were averaged, providing several independent subaverages from the total trials available for each electrode of each subject. Each averaged waveform was then submitted to FFT spectral analysis. PC was determined using the following equation:

$$PC = [\left(\frac{1}{n}\sum cos\Phi_i\right)^2 + \left(\frac{1}{n}\sum sin\Phi_i\right)^2]^{1/2} \quad (2.1)$$

where Φ_i is the phase angle of the Fourier component of the *i*th subaverage, and *n* is the number of subaverages.

PC varies from 0 to 1 directly proportional to the variability. It estimates the degree to which the phases of the frequency of interest are dispersed (PC = 0, means phases are evenly dispersed across a 360 ° range among the subaverages) or clustered (PC = 1, means phases are identical in all subaverages) (Fig. 2.4). Recall that both sine and cosine vary from -1 to +1. If the phases for a specific frequency are relatively evenly distributed across 360 °, average sine

and cosine values, and PC, will tend toward zero. However, if all the phases are identical, PC value will equal 1. The closer the value is to 1, the higher the coherence value is, indicating that the amplitude of the response is significant and distinguishable from the amplitude of the background noise.

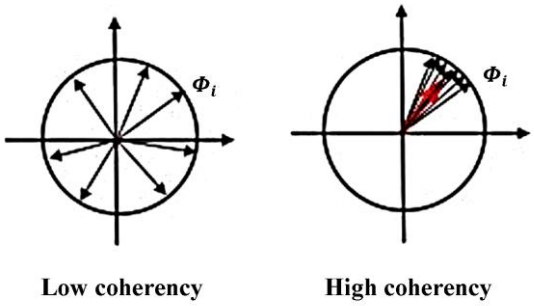

Figure 2.4: Distribution of the phases among subaverages [212].

In the current study, in addition to the amplitude of the frequency response at the target frequency and the first harmonic, the PC value at the target frequency was also tested for its age-dependency. We choose the PC value at the target frequency, since it is the most significant peak in which the response is more closely tuned to the stimuli and at which the coherence is expected to be maximum.

2.2.3 Global field power

The brain electrical activity is conventionally recorded as voltage differences between two electrodes, plotted as a function of time (evoked potential waveform). However, this reflects only a very restricted and biased sample of the electrical field data in the form of the gradient along the line between the two electrodes. Beside the stimulus parameters and the subject's condition, the waveform is affected by the choice of the electrode locations [213]. The brain's electrical response to receiving sensory information constitutes an electrical field, detectable on the entire scalp, with a variable distribution over time. Reconstruction of the distribution of the scalp field does not depend on a specific reference electrode. The brain activity recorded from many scalp locations simultaneously can be displayed as a series of equipotential topographic maps presenting the spatial distribution of the activity at successive time points. In many studies, one may intend to identify the evoked potentials components which correspond to the subsets of the recorded brain activity that are related to specific and discrete steps of information processing following stimulus presentation [214]. Conventional

waveforms of the evoked potentials can be used for extracting the peaks and troughs which are interpreted as the components. However, the waveform analysis, suffers from the inherent ambiguity of the information provided by the time series. Since the electrical activity may only be recorded as potential differences between pairs of electrodes, provided information depends on the activity at both the recording and the reference electrode. Therefore, different electrode locations as well as changing the recording reference will drastically affect the signals recorded as time series [214].

Lehmann and Skrandies [213] described a reference-free method for computing the Global Field Power (GFP). This measure can be used for quantifying the integrated electrical activity of each topographic map by computing a kind of spatial standard deviation. The idea behind this approach is that the scalp fields with few activity presumably contain little information, while the fields displaying much activity reflect the synchronous activation of a large number of intracranial neurons. The latency of an evoked component may reasonably be concurrent with the occurrence time of maximal activity in the potential distributions which is corresponding to the synchronous activation of a maximal number of neurons [214]. GFP is computed as the root of the mean of the squared potential differences (u_i - u_j) between all possible electrode pairs within the field (n indicates the number of the electrodes) (Eq. 2.2).

$$GFP = \sqrt{\left(\frac{1}{2n}\right) * \sum_{i=1}^{n} \sum_{j=1}^{n} (u_i - u_j)^2} \quad (2.2)$$

Using the GFP for determining the latency of the ERP components is based on the features of the scalp field by considering all the recording points in a given potential field distribution, simultaneously. Therefore, it is unambiguous and identifies components topographically independent of the reference location [214]. Figure 2.5 shows a sample of the GFP, the ERP waveforms and topographic maps presenting the components in response to the auditory stimuli containing the speech and non-speech stimulations in standard and deviant conditions [215].

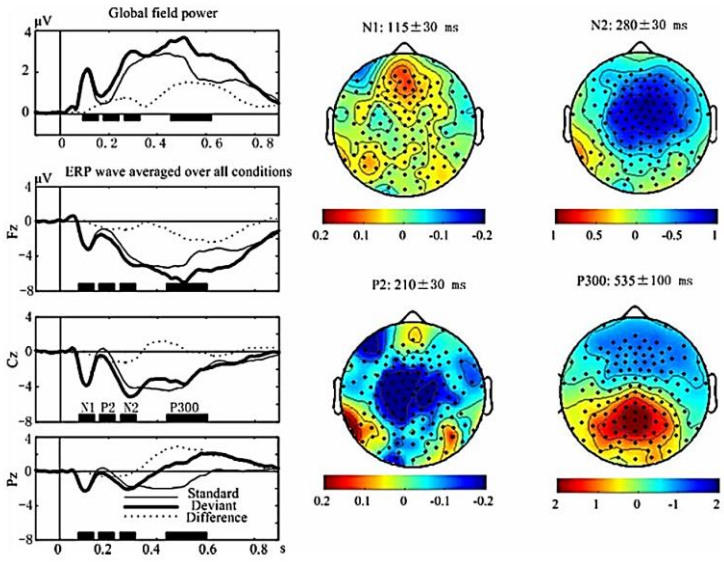

Figure 2.5: Global field power, ERP waveform averaged over all experimental conditions, and topographic distribution maps for the N1, P2, N2, and P300 components [215].

GFP presents a global measure of the brain activity which does not rely on the individual electrode's waveforms, making it robust against the low evoked response to noise ratio. Therefore, the occurrence times of GFP maxima are appropriate choices for the ERP studies of preterm infants, when decision making on peak detection in the time domain is challenging or impossible. In our study, the first-peak latency of the GFP signal is considered as the functional feature of interest for the study of age and structure-related dependencies. The same fifteen channels, used in the previous analysis of the CAEPs in the frequency domain, were applied for calculating the GFP signal of each subject. The GFP first-peak latency was investigated for age-related correlation in the period of the current study. It was also assessed for some correlations with the myelin-related structural maturation index extracted from MR images of almost the same age infants. Details of the MRI dataset, image processing and extracting the structural maturation index are described in the following.

2.3 Structural dataset: Imperial College London neonatal structural atlas

To perform conjoint modeling of functional and structural brain development in preterm infants, we required the MR images of the preterm neonates of almost the same age as our functional dataset. We used MR images from the Imperial College London repository. T1w and T2w templates of each wGA are provided by the detailed spatio-temporal neonatal structural atlas [216] with 87 labeled structures of the developing brain (Fig. 2.6). The atlas construction is described in detail in [217].

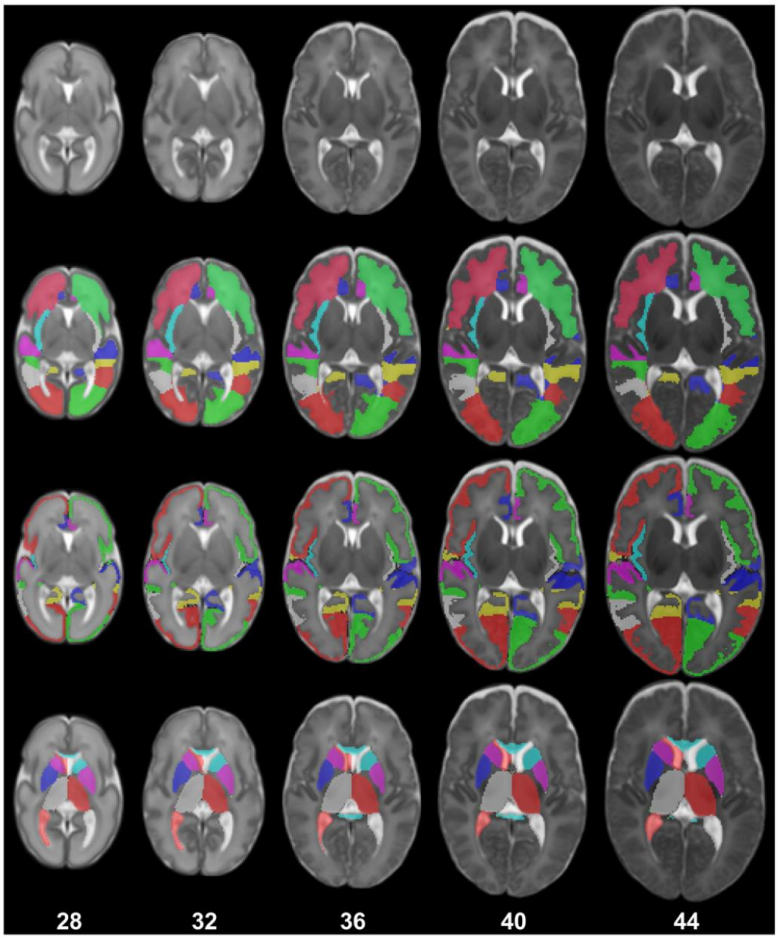

Figure 2.6: The maximum probability structural atlas shown at different ages. The structures of the atlas (second row: WM structures, third row: CGM structures, fourth row: subcortical GM structures and ventricles) are defined in the coordinate space of the spatio-temporal template of Serag et al. [218] (first row) [217].

2.3.1 Subjects

A cohort of 380 infants recruited from the Neonatal Intensive Care Unit at Queen Charlotte's and Hammersmith Hospitals was studied for the purpose of the atlas reconstruction [217]. The criteria for excluding the infants were focal abnormalities on MR imaging as determined by an expert perinatal neuro-radiologist. From the total 380 infants (467 images), 14 infants (19 images) were excluded due to abnormality. 4 infants were reported to have cystic periventricular leukomalacia (PVL) (7 images), 5 presented Hemorrhagic Parenchymal Infarction (HPI) (6 images), 2 with pseudocysts (3 images), 1 with cerebellar hemorrhage, 1 with multiple WM infractions and 1 with multiple cystic lesions following meningitis. Furthermore, 28 images were excluded due to motion artifacts. The remaining 338 infants (298 preterm infants and 40 healthy term-born infants) who were born

at a median (range) GA of 30 (23^{+2}–42) weeks were studied. Some of the preterm infants had chronic lung disease (CLD), patent ductus arteriosus (PDA) and culture-positive sepsis. Several preterm infants were scanned on 2 or 3 occasions, resulting in 420 MR imaging datasets. The time interval between the scans ranges from 6 days to 16 weeks, with a median of 8^{+1} weeks. The term born infants were scanned only once. The median post-menstrual age (PMA) at imaging was 39^{+1} (27^{+1}–44^{+6}) weeks and postnatal age at scan was 5^{+3} (0–19^{+5}) weeks. Details of the characteristics of the term-born and preterm infants are presented in Table 2.1.

Table 2.1: Details of the characteristics of the term-born and preterm infants recruited in the neonatal structural atlas reconstruction [217].

	Preterm infants	Term controls
Number of infants/images:		
Total number	298/380	40/40
Chronic lung disease (CLD)	49/54	–
Patent ductus arteriosus (PDA)	32/38	–
Culture positive sepsis	23/28	–
Age at birth (weeks)	29^{+3} (23^{+2}–36)	39^{+2} (36^{+1}–42)
Age at scan (weeks)	37^{+6} (27^{+1}–44^{+6})	40^{+6} (37–44^{+4})
Postnatal age at scan (weeks)	6^{+5} (0^{+1}–19^{+5})	0^{+6} (0–5^{+5})
Weight at birth (kg)	1.17 (0.54–3.71)	3.42 (1.93–4.34)
Weight at scan (kg)	2.19 (0.64–5.5)	3.48 (1.93–4.71)
Head circumference at birth (cm)	27 (20–38.5)	34.3 (30.2–38.7)
Head circumference at scan (cm)	31.6 (22–39.6)	35.4 (30.2–38)

2.3.2 MR imaging acquisition

Permission for MR imaging was granted by Queen Charlotte's and Hammersmith Hospitals Research Ethics Committee (09/H0707/98, 07/H0704/99 & 07/H0707/101). Written parental consent was also obtained prior to imaging. The images were acquired by a 3T Philips Intera system with the following parameters: (1) T1w 3D MPRAGE: TR=17 ms, TE=4.6 ms, inversion delay=1500 ms, flip angle=13◦, acquisition plane=sagittal, voxel size = 0.82×1.03×1.6 mm, FOV=210×167 mm and acquisition matrix=256×163; (2) T2w fast spin-echo (FSE): TR=8700 ms, TE=160 ms, flip angle=90◦, acquisition plane=axial, voxel size=1.15×1.18×2 mm, FOV=220 mm and acquisition matrix=192×186. All the examinations were supervised by a pediatrician experienced in MR imaging procedures. Preterm infants at term age were sedated with oral chloral hydrate (25–50 mg/kg) prior to scanning. The pulse oximetry, temperature and electrocardiography were monitored. Ear protection was used, comprising earplugs moulded from a silicone-based putty (President Putty, Coltene

Whaledent, Mahwah, NJ, USA) placed in the external auditory meatus and neonatal earmuffs (MiniMuffs, Natus Medical Inc., San Carlos, CA, USA).

2.3.3 Segmentation method

An accurate and robust automatic segmentation pipeline presented by Makropoulos et al. [219] was used for parcellating the neonatal brain into multiple cortical and subcortical regions. Significant changes in the brain shape and appearance related to the development, along with the lower SNR and partial volume effects in the neonatal brain make the automatic segmentation of the neonatal MR images challenging. Makropoulos et al. [219] proposed a framework for accurate intensity-based segmentation of the developing neonatal brain, from the early preterm period to term-equivalent age, into 50 brain regions. The algorithm is based on an expectation-maximization (EM) scheme similar to that of Van Leemput et al. [220], with a spatial prior term and intensity model of the image. The spatial priors of the structures were obtained by averaging the warped labels from the 20 manually segmented atlases of Gousias et al. [221] and the image intensities were modeled using a Gaussian Mixture Model (GMM). Extensive validation verified the robustness of the algorithm at different ages of the developing neonatal brain. The readers are referred to [219] for more details on the pipeline. Table 2.2 presents the automatically parcellated regions. The segmentation method was further extended to detect cortical sulci and provide detailed delineation of the cortical ribbon [217]. Examples of the proposed segmentation technique applied to early preterm and term-equivalent brain can be seen in Fig. 2.7 and 2.8, respectively.

Table 2.2: Regional structures of the brain segmented using the automatic method in Makropoulos et al. [219].

WM, CGM structures	Subcortical regions
Frontal lobe (left/right)	Hippocampus (left/right)
Parietal lobe (left/right)	Amygdala (left/right)
Occipital lobe (left/right)	Cerebellum (left/right)
Anterior temporal lobe, medial part (left/right)	Brainstem
Anterior temporal lobe, lateral part (left/right)	Caudate nucleus (left/right)
Gyri parahippocampalis et ambiens, anterior part (left/right)	Thalamus (left/right)
Gyri parahippocampalis et ambiens, posterior part (left/right)	Sub-thalamic nucleus (left/right)
Superior temporal gyrus, middle part (left/right)	Lentiform nucleus (left/right)
Superior temporal gyrus, posterior part (left/right)	Corpus callosum
Medial and inferior temporal gyrus, anterior part (left/right)	Lateral ventricles (left/right)
Medial and inferior temporal gyrus, posterior part (left/right)	
Fusiform gyrus, anterior part (left/right)	
Fusiform gyrus, posterior part (left/right)	
Insula (left/right)	
Cingulate gyrus, anterior part (left/right)	
Cingulate gyrus, posterior part (left/right)	

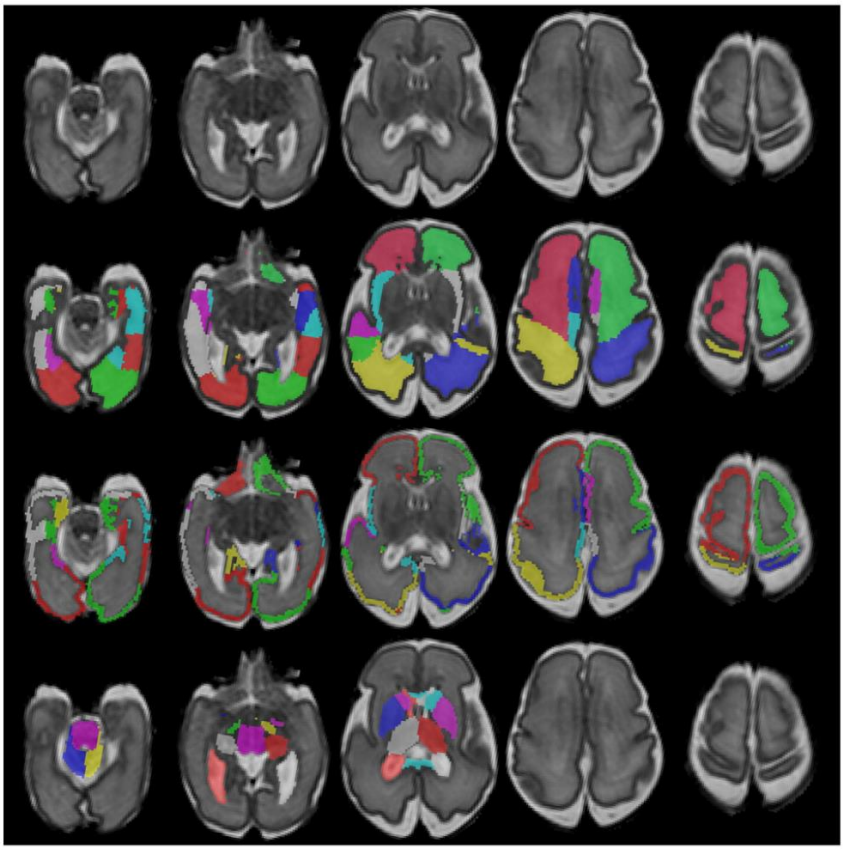

Figure 2.7: Segmentation results of a neonatal MRI acquired at 28 weeks PMA at scan with the 82 labels overlaid (second row: WM labels, third row: CGM labels, fourth row: subcortical GM labels and ventricles) [217].

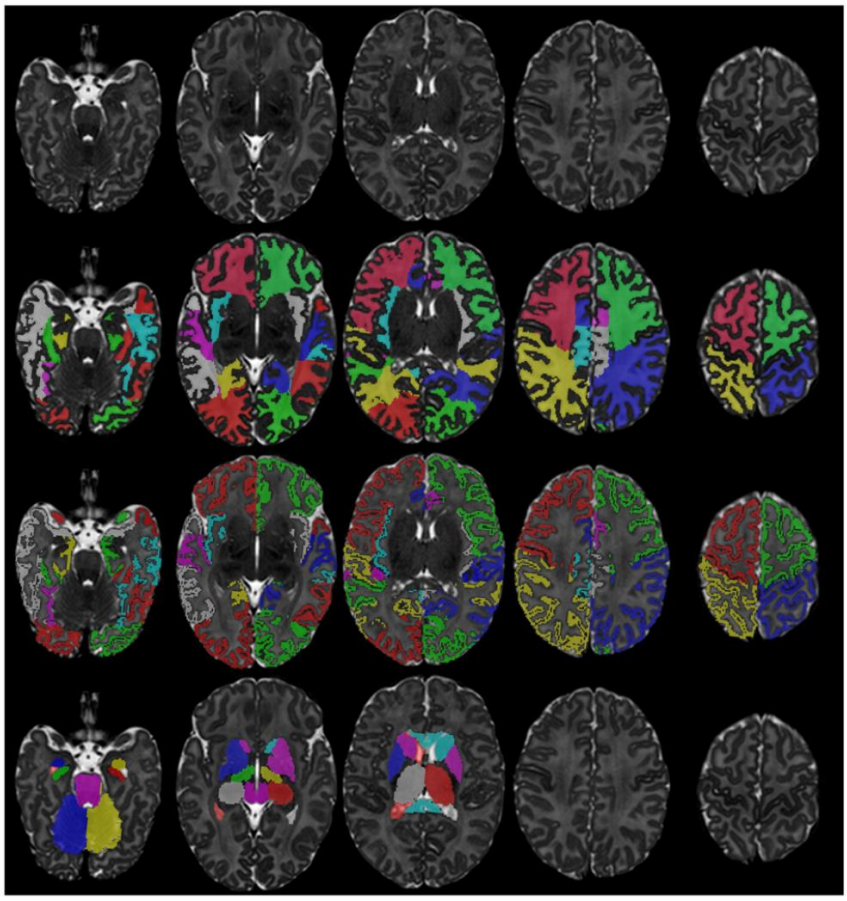

Figure 2.8: Segmentation results of a neonatal MRI acquired at 44 weeks PMA at scan with the 82 labels overlaid (second row: WM labels, third row: CGM labels, fourth row: subcortical GM labels and ventricles) [217].

2.4 Myelination index

The developing brain undergoes significant changes from a mostly non-myelinated state for the cerebral WM to a nearly fully mature WM myelination within the first few years of life. Quantification of the myelination process in the WM is the purpose of many brain development studies, especially with application to distinguish neurodevelopmental disabilities. DTI has been widely used as one of the major approaches to analyze the myelination, mainly by applying the DTI property maps fractional anisotropy (FA) and radial diffusivity (RD). Although these measures are sensitive to myelination, one should notice that they are also sensitive to other brain maturation or pathologic processes, such as fiber organization/wiring, axonal size, fiber packing/density, changes in brain water content, synaptogenesis, axonal pruning and neuronal death [152]. Therefore, care should be taken when attributing the observed changes in diffusion measure to a specific microstructural

feature such as myelination. A more specified measure of the myelin maturation can be obtained via multi-component analysis of T1 and T2 relaxation, also called multi-component relaxometry [222]. The so-called myelin water fraction (MWF), may be obtained by quantifying the myelin-bound water signal within myelin folds. This myelin biomarker is proved to be correlated with the histological assessments [223]. However, a limitation of the traditional MWF imaging is the acquisition time of the MR protocol, which is not appropriate for the applications in neonatal studies which require fast scan acquisitions [152].

Another simpler, alternative way to quantify the myelination process is presented by Glasser et al. [149]. The use of high-resolution T1w and T2w MR images, commonly acquired in many neuroimaging studies, is proposed to provide an estimate of myelin content via the ratio of these two images. Although other sources also contribute to the signal in the T1w/T2w ratio values, specifically in the first stages of development, the major contribution within the cerebrum originates from the local myelin content [152]. Glasser et al. [149] showed how the ratio images could be employed to illustrate the variations in myelin between cortical GM areas. Therefore, this approach provides the opportunity to measure the myelination in both WM and GM and proposes a quantitative estimate of myelin content that can be compared across the subjects at different ages. This method does not depend on the axon fiber anatomy, in contrast to DTI. Therefore, it can be used for estimating whole-brain intracortical myelin-related changes, which are difficult to measure directly using existing noninvasive neuroimaging tools [150].

Dividing the T1w image by the aligned T2w image mathematically removes the signal intensity bias related to the sensitivity profile of the radio frequency receiver coils, which is similar in both images. It also increases the contrast related to the myelin content. Both of these effects are illustrated by a simple approximation (Eq. 2.3) [149]. If the myelin contrast is shown by x in the T1w image and 1/x in the T2w image, and the receive bias field is represented by b in both images, the T1w/T2w ratio image equals x^2, i.e., enhanced myelin contrast, with no bias field contribution. Since the noise in the T1w and T2w images is uncorrelated, there is increased myelin contrast relative to the noise [149].

$$\frac{T1w}{T2w} \approx \frac{x*b}{\left(\frac{1}{x}\right)*b} = x^2 \tag{2.3}$$

The T1w/T2w ratio image may be used to investigate age-related changes in signal intensity in both adults and infants [151] [152]. Although this measure has been extracted as an estimate of myelin content in adults [149] [150] [151] children [151], and infants [152], we should notice that it may be influenced by other developmental changes in the age range of

our study. Therefore, we consider it as a structural maturation index measured by combining various sensitivities of the T1w and T2w images relative to water.

In our analysis, a ratio image was created for each wGA from 28 to 32, corresponding to the age range of our functional data. The values of the ratio image intensities in each region of interest (ROI) were averaged to give a maturation index for that specific brain region. The index was measured for both the total GM and the total WM, as two potential global measures of the structural development in the preterm infants' brain. Furthermore, it was calculated for all the brain regions provided by the neonatal atlas (GM+WM), including the superior temporal gyrus in the middle (mSTG) and posterior (pSTG) part, which are assumed to be more involved in the auditory task. All the regions were investigated for structure and function relations, seeking for those presenting the most correlation coefficient.

2.5 Modeling (Regressions)

2.5.1 Hierarchical regression

Hierarchical regression is a statistical approach of investigating the relationships among, and testing hypotheses about, a dependent variable and several independent variables [224]. It is a way to show if the variables of your interest explain a statistically significant amount of variance in your dependent variable after accounting for all other variables [225]. The term "Hierarchical" refers to the fact that the independent variables are not entered into the regression simultaneously but in steps. In fact, the hierarchical regression is a framework for model comparison rather than a statistical method. In this framework, several regression models are built by adding variables to a previous model at each step; later models always include smaller models in previous steps. In many cases, our main goal is to determine whether newly added variables show a significant improvement in R^2 (the proportion of explained variance in the dependent variable by the model) [225]. It is common to report coefficients of all variables in each model and differences in R^2 between models as the additional variance explained by the later variable added to the model.

Hierarchical regression deals with how predictor (independent) variables are entered into the model. Specifically, it refers to the process of adding or removing predictor variables from the regression model in different steps. For instance, if you want to predict the college achievement (your dependent variable) based on high school GPA (your independent variable), while controlling for demographic factors, you might enter the demographic factors into the model in the first step, and then enter high school GPA into the model in the second

step. This would let you observe the predictive power that high school GPA adds to your model above and beyond the demographic factors.

In our study, hierarchical regression analysis was conducted to examine the unique influence of age and maturation index of each ROI (as independent variables) on the GFP first-peak latency (as dependent variable). Therefore, the age and structural maturation index of each region were entered to the model in different steps to examine the unique variance in GFP first-peak latency, accounted for by the maturation index or age, after removing the variance in GFP first-peak latency accounted for by the other variable. The hierarchical regressions were carried out using IBM SPSS Statistics 24.

2.5.2 Partial correlation

Partial correlation is a method of measuring the strength and direction of a linear relationship between two continuous variables while controlling for the effect of one or more other continuous variables (i.e. 'covariates' or 'control' variables). Although partial correlation does not distinguish between the independent and dependent variables, the two variables are often considered in such a manner. Therefore, we may have one continuous dependent variable and one continuous independent variable, as well as one or more continuous control variables. When we are interested in measuring the strength of the numerical relationship between two variables of interest, using their correlation coefficient will give misleading results if there is another, confounding, variable that is numerically related to both variables of interest. This misleading information can be avoided by controlling for the confounding variable, which is performed by computing the partial correlation coefficient.

A simple method to calculate the sample partial correlation between two variables is to conduct the two linear regressions between each of them and the control variable, get the residuals, and calculate the correlation between the residuals. Let X and Y be the random variables taking real values, and let Z be the n-dimensional vector-valued random variable (n-dimensional control variable). We write x_i, y_i and z_i to denote the *i*th of N observations from some joint probability distribution over real random variables X, Y and Z, with z_i having been augmented with a 1 to allow for a constant term in the regression. Solving the linear regression problem reduces to finding (n+1)-dimensional regression coefficient vectors W_X^* and W_Y^* such that:

$$W_X^* = argmin_W\{\sum_{i=1}^{N}(x_i - \langle w, z_i\rangle)^2\} \quad (2.4)$$

$$W_Y^* = argmin_W\{\sum_{i=1}^{N}(y_i - \langle w, z_i\rangle)^2\} \quad (2.5)$$

with N representing the number of observations and $\langle \boldsymbol{w}, \boldsymbol{v} \rangle$ showing the scalar product between the vectors $\boldsymbol{w}$ and $\boldsymbol{v}$. The residuals are then:

$$e_{X,i} = x_i - \langle W_X^*, z_i \rangle \tag{2.6}$$

$$e_{Y,i} = y_i - \langle W_Y^*, z_i \rangle \tag{2.7}$$

The sample partial correlation is then obtained by the usual formula for sample correlation, but between these new derived values:

$$\hat{\rho}_{XY.Z} = \frac{N\sum_{i=1}^{N} e_{X,i}e_{Y,i} - \sum_{i=1}^{N} e_{X,i}\sum_{i=1}^{N} e_{Y,i}}{\sqrt{N\sum_{i=1}^{N} e_{X,i}^2 - (\sum_{i=1}^{N} e_{X,i})^2}\sqrt{N\sum_{i=1}^{N} e_{Y,i}^2 - (\sum_{i=1}^{N} e_{Y,i})^2}} = \frac{N\sum_{i=1}^{N} e_{X,i}e_{Y,i}}{\sqrt{N\sum_{i=1}^{N} e_{X,i}^2}\sqrt{N\sum_{i=1}^{N} e_{Y,i}^2}} \tag{2.8}$$

In our analysis, the two variables looking for their partial correlation were the GFP first-peak latency (as the dependent variable) and the structural maturation index of each ROI (as the independent variable). Age was considered as the control variable. Therefore, we first conducted the linear regressions between the GFP first-peak latency and age, as well as between the structural index of each ROI and age, to obtain the residuals and after that performed linear regression between the residuals to provide the partial correlation coefficient with the effect of age removed. The partial correlations were carried out using IBM SPSS Statistics 24.

2.5.3 Statistical analysis

A t-test is a type of inferential statistic used to determine if there is a significant difference between the means of two groups, which may be related to each other in certain features. It is used as a hypothesis testing tool, which allows testing of an assumption applicable to a population. Essentially, a t-test provides the opportunity to compare the average values of the two datasets and determine if they come from the same population. Mathematically, the t-test takes a sample from each of the two datasets and establishes the problem statement by assuming a null hypothesis that the two means are equal. Based on the applicable formulas, a t-value is calculated (proportional to the differences between the two means) and compared against the standard values (t-distribution values), and the assumed null hypothesis is accepted or rejected, accordingly. This comparison helps to determine whether the difference between the groups represents a true difference in the study or it is likely a meaningless statistical difference. If the null hypothesis qualifies to be rejected, it indicates that the mean difference is strong enough, not occurred by chance, and the data sets really have intrinsic differences.

In our study, we used t-test to investigate the lateralization of the functional or structural features. In fact, the t-test was used to investigate if the observed differences between the calculated values of the features in the right and left hemispheres are statistically significant. For the functional feature (peak amplitude at the target frequency), we performed one-tailed t-test to assess the alternative hypothesis that the population mean of the values of the right hemisphere is greater than the left hemisphere. However, as we performed the t-test for each pair of the available electrodes (i.e. multiple comparisons), we needed to correct the p-values by a method to control for the multiple comparisons error. Multiple-hypothesis testing involves much more complicated errors than single-hypothesis testing. While we typically control the type I error rate (rejection of a true null hypothesis, also known as a 'false positive) for a single-hypothesis test, a compound error rate should be controlled for multiple-hypothesis tests. The false discovery rate (FDR) is a method of conceptualizing the rate of type I errors in null hypothesis testing when conducting multiple comparisons. FDR-controlling algorithms are designed to control the expected proportion of "discoveries" (rejected null hypotheses) that are false (incorrect rejections) [226]. In our study, we used 'mafdr' command of MATLAB R16 to perform the FDR correction. The reader may refer to [227] for details of the procedure introduced by Storey (2002) implemented in the 'mafdr' command.

2.5.4 Conclusion

In this chapter, we described the details of the functional and structural datasets used in different analyses of the current thesis. Information regarding the participants, design and stimuli, recordings and preprocessing of the EEG were provided and the functional features considered for evaluating developmental changes of the preterm infants' brain were introduced. In the next chapter, all the procedures and analyses along with the results and discussion are presented regarding the neurodevelopment and asymmetry of the CAEPs of the preterm neonates to the repetitive syllabic stimuli.

In the current chapter, we further introduced the structural dataset and the structural maturation index as well as the functional feature which is used for the joint structural and functional study. All the details of the analyses along with the results and discussion regarding the functional and structural correlates of the preterm infants' brain, are presented in Chapter 4. Some basics and fundamentals of the statistical methods, recruited in the following two chapters, for analyzing the correlations between the structural and functional

findings and studying the lateralization of the functional and structural features, were elaborated with more details in the current chapter.

Chapter 3

Neurodevelopment and asymmetry of auditory-related-responses to repetitive syllabic stimuli in preterm neonates based on frequency-domain analysis

Sensory development of the human brain begins prenatally, allowing cortical auditory responses to be recorded at an early age in preterm infants. Despite several studies focusing on the temporal characteristics of preterm infants' cortical responses, few have been conducted on frequency analysis of these responses. In this study, we performed frequency and coherence analysis of preterm infants' auditory responses to series of syllables and also investigated the functional brain asymmetry of preterm infants for the detection of the regularity of auditory stimuli. Cortical auditory evoked potentials (CAEPs) were recorded in 16 preterm infants with a mean recording age of 31.48 weeks gestational age (29.57-34.14 wGA) in response to a repetitive syllabic stimulus. Peak amplitudes of the frequency response at the target frequency and the first harmonic, as well as the phase coherence (PC) at the target frequency were extracted as age-dependent variables. A functional asymmetry coefficient was defined as a lateralization index for the amplitude of the target frequency at each electrode site. While the findings revealed a significant positive correlation between the mean amplitude at the target frequency vs. age (R^2=0.263, p=0.042), no significant correlation was observed for age-related changes of the mean amplitude at the first harmonic. A significant correlation was also observed between the mean PC and age (R^2=0.318, p= 0.023). A right hemisphere lateralization over many channels was also generally observed. The results demonstrate that rightward lateralization for slow rate modulation, previously observed in adults, children and newborns, appears to be in place at a very young age, even in preterm infants.

3.1 Introduction

Development of the auditory system is an intricate process beginning early in gestation (Hall 2000). Major structures of the ear, including the cochlea, develop between 23 and 25 weeks gestational age (wGA) (Cheour-Luhtanen et al. 1996; Eldredge and Salamy 1996; Hall 2000) and the capacity of the foetus to perceive and react to auditory inputs, related to brainstem network activation, emerges around 26 weeks of foetal life (Ruben 1992). After 28 wGA, the thalamocortical auditory system is sufficiently mature to perceive complex sounds and discriminate between different speech phonemes (Draganova et al. 2007; Renaud et al. 2008; Mahmoudzadeh et al. 2013; Mahmoudzadeh et al. 2017; Mahmoudzadeh et al. 2018), corresponding to the beginning of language and speech development (Mehler et al. 1988). A critical period for neurosensory development of the auditory system starts around 25 wGA. During this period, the hair cells of the cochlea, the axons of the auditory nerve and the neurons of the temporal lobe in the auditory cortex are tuned to receive signals of specific frequencies and intensities (Graven and Browne 2008).

Cortical brain development can also be studied in preterm infants, who, as a result of intensive care, can survive when born after 28 wGA, and even 23 wGA (Mahmoudzadeh et al. 2017). Arousal behaviour confirms that the auditory system is already operative at this early age (Copriviza and Lima 1984) and threshold auditory sensitivity has been evaluated using auditory brainstem responses (ABRs) () (Schulman-Galambos and Galambos 1975; Despland and Galambos 1980; Lary et al. 1985; Ribeiro and Carvallo 2008). Hearing function rapidly improves from about 28 wGA to reach adult threshold sensitivity at term (Galambos et al. 1982). Cortical auditory evoked potentials (CAEPs) are recorded from 27 wGA (Rotteveel et al. 1987), with differences in wave amplitude and latency as a function of age (Weitzman and Graziani 1968; Rotteveel et al. 1987). Sound discrimination capacities, associated with mismatch responses, have been observed in response to changes of syllables and voices in healthy neonates tested ten weeks before term (28–32 wGA) (Mahmoudzadeh et al. 2013; Mahmoudzadeh et al. 2017; Mahmoudzadeh et al. 2018).

Auditory steady-state responses (ASSRs) is another methodological approach to study auditory development. ASSR measures the ability of the auditory network to fire synchronously with the rhythm (i.e., modulation rate) of an auditory stimulus (Picton et al. 2003). ASSRs evoked by brief recurrent tones over a wide range of stimulus repetition rates have been assessed at different ages (Tlumak et al. 2012). At high repetition rates, the magnitude of the responses at the trained frequencies was considerably lower in children than

in adults. In infants aged 3-10 months, ASSRs in response to repetitive speech syllables revealed a systematic increase in the amplitude of the harmonics (Anderson et al. 2015). Recently in (Mahmoudzadeh et al. 2017), phase coherence analysis in 30 wGA preterm infants showed that immature neurons were able to follow a sequence of 4 syllables separated by 600 ms of silence, with reproducible topographies. Because of habituation, the amplitude of the evoked response decreased with repetition, with a weak, although significant phase-locking value across trials.

Although the auditory stimuli presented in (Mahmoudzadeh et al. 2017) does not correspond to a classical ASSR paradigm, regular repetition of the stimuli motivated us to study the ability of the immature auditory network to be entrained by the syllabic rhythmicity. As the frequency of stimulation is known, the same frequency can be studied in neural responses in order to obtain information on the ability of the immature network to follow the frequency of the auditory stimulation. This measure is less sensitive to background noise and analyses are reduced to the specific frequency of stimulation (Tlumak et al. 2012). Variations of conductivity between the electrode and the scalp due to gel injection also do not affect the EEG frequency content, in contrast with its amplitude (Kappenman and Luck 2010). Furthermore, because the left and right hemispheres have different structural and functional maturational profiles (Dehaene-Lambertz and Spelke 2015), and because a certain degree of hemispheric asymmetry of auditory responses has been described in adults (Poelmans et al. 2012) that may affect the functional responses, we also analyzed the lateralization of the responses.

3.2 Methods

3.2.1 Participants

EEG signals of 16 preterm infants with mean recording age of 31.48 wGA (29.57-34.14 weeks), recruited in our previous study (Mahmoudzadeh et al. 2017), were reanalyzed for the purposes of the present study. All infants had appropriate birth weight, size, and head circumference for their term age. The electroencephalogram was considered to be normal for gestational age. The infants were considered to be at low risk for brain damage on the basis of normal auditory and clinical neurological assessments. Written informed consent was provided by the infants' parents and the study was approved by the Amiens University Hospital local ethics committee (CPP Nord-Ouest II) according to the guidelines of the Declaration of Helsinki of 1975 (ref ID-RCB 2008-A00728-47).

3.2.2 Procedure design and stimulation

The stimuli consisted of four syllables (/ba/ and /ga/, produced by male and female speakers) presented at a comfortable hearing level (≈70 dB) via speakers placed at the infant's feet (Mahmoudzadeh et al. 2013; Mahmoudzadeh et al. 2017). Syllables were matched for intonation, intensity, total duration (285 ms), prevoicing and voiced formant transition duration (40/45 ms). They were presented in series of 4 separated by 600 ms intervals. Five series separated by 1600 ms of silence constituted a block. Each block lasted 20 s and was followed by 40 s of silence. In each block, the repeated syllable was randomly chosen from among the 4 possible syllables. This presentation was applied in our previous study to evaluate syllabic discrimination in early preterm infants (Mahmoudzadeh et al. 2013; Mahmoudzadeh et al. 2017). While in the standard trials, the same syllable was repeated four times, in deviant trials, the last syllable differed from the first three in voice or phonetic dimension. Although different from the classical ASSR paradigm, this regular presentation allowed to study the ability of the preterm brain to follow external ecological stimulations. Therefore, only the recorded responses corresponding to the standard trials, were used in this study for further analysis. Our previous results have shown that infants of this age are able to discriminate the two phonemes (/ba/ vs. /ga/) and the two voices (male vs. female) with distinct neural networks (Mahmoudzadeh et al. 2013; Mahmoudzadeh et al. 2017).

3.2.3 EEG recordings and preprocessing

The EEG signals were recorded using Ag/AgCl surface electrodes and a nasion reference. The sampling rate was 2048 Hz and the signals were amplified by A.N.Ts (Enschede, The Netherlands) and filtered at DC-50 Hz. The impedance of the electrodes was kept below 5 kΩ and the number of the electrodes (31-61) was determined according to the infant's head circumference. A minimum of 31 electrodes were placed on the 10–20 points for all infants and additional electrodes were placed on intermediate positions according to the infant's head circumference.

The recorded signals were band-pass filtered between 1 and 20 Hz and down-sampled to 512 Hz. They were segmented into epochs ([−0.5 +2.7 s]) time-locked to the first syllable (S1) of the trial, providing 180 standard trials from each recording electrode for each subject. Trials were then baseline corrected to the 200 ms before the S1 onset. An automatic artifact-rejection procedure was applied as follows. Each trial was rejected if its absolute amplitude exceeded 50 µV or when a local amplitude jump between ten successive time-points exceeded

30 µV. The average number of 156 trials was remained for each infant and each electrode after the artifact exclusion.

3.2.4 Frequency analysis

As the brain was exposed to a syllable every 600 ms, we expected a distinctive peak around 1.6 Hz and its harmonics. Temporal response corresponding to the time interval of the trials with the baseline removed ([0 +2.7 s]), was transformed to the frequency domain using FFT. We, then, measured the peak amplitudes of the FFT spectrum at the target frequency and its first harmonic and tested the effect of age on this measurement. The amplitudes of the FFT spectrum at the target frequency and the first harmonic were extracted for each subject and each electrode and averaged across the 15 channels (Fz, F1, F2, F3, F4, C1, C2, CP1, CP2, Pz, P1, P2, Oz, O1 and O2) for all the subjects. These 15 channels are the most common channels showing activity between different subjects. Data analysis was performed by means of MATLAB R16 and the number of FFT points was adjusted at next power of 2 from length of signal.

3.2.5 Phase coherence analysis

We applied phase coherence (PC) as a complementary frequential feature to study the preterms' response to the auditory stimulation. Calculation of phase coherence (Jerger et al. 1986; Stapells et al. 1987; Picton et al. 1987; Dobie and Wilson 1989; Ali and Jerger 1992; Dobie and Wilson 1994; Leigh-Paffenroth and Fowler 2006; Thatcher 2012) requires segmentation of the CAEP into multiple subaverages. Subaverages are then transformed into the frequency domain using FFT. In the present study, sets of 10 trials were averaged, providing several independent subaverages from the total trials available for each electrode of each subject. Each averaged waveform was submitted to FFT spectral analysis. PC was determined by means of the following equation:

$$PC = [\left(\frac{1}{n}\sum cos\Phi_i\right)^2 + \left(\frac{1}{n}\sum sin\Phi_i\right)^2]^{1/2} \quad (3.1)$$

where Φ_i is the phase angle of the Fourier component of the *i*th subaverage, and *n* is the number of subaverages. PC ranges between 0 and 1, which is directly proportional to variability. It estimates the degree to which the phases at each frequency are dispersed or clustered. The more identical the average phases are, the more the PC value tends towards

one. The PC value at the target frequency of the auditory response was tested for its age-dependency. We choose the PC value at the target frequency, as it constitutes the most significant peak in which the response is more closely tuned to the stimuli and at which the coherence is expected to be maximal.

3.2.6 Lateralization index

A functional asymmetry coefficient was defined as a lateralization index, LI=(Right-Left)/(Right+Left), for the most prominent feature, the amplitude of the target syllabic frequency, at each electrode site and submitted to a *t*-test. The normalized value, Right/(Right+Left) or Left/(Right+Left), is less influenced by the intersubject variability related to the individual level of auditory maturation. Therefore, it provides a more sensitive measure than the original indices (Left or Right) for statistical comparison of right and left hemisphere activities. The number of repeated measures was corrected with False Discovery Rate (FDR) correction.

3.3 Results

Grand averages of the responses are depicted in Fig. 3.1.a for several electrodes. Fourier amplitudes of the grand averages are presented in Fig. 3.1.b. In the previous study (Mahmoudzadeh et al. 2017), using the same stimuli and Global Field Power (GFP) analysis, the evoked responses to each syllable induced peaks with complex topography in the time domain. While the maximum positivity in the ERP is observed in frontal area, the maximum negativity is observed in posterior area, as described in (Mahmoudzadeh et al. 2017), suggesting two simultaneous dipoles located in the bilateral temporal areas. The temporal responses as well as the FFT and phase coherence spectra at one right (F4) and one left (F3) electrode are illustrated in Fig. 3.2 for an individual neonate (30 weeks and 4 days GA). As expected, distinctive peaks were observed at the target frequency and the first harmonic.

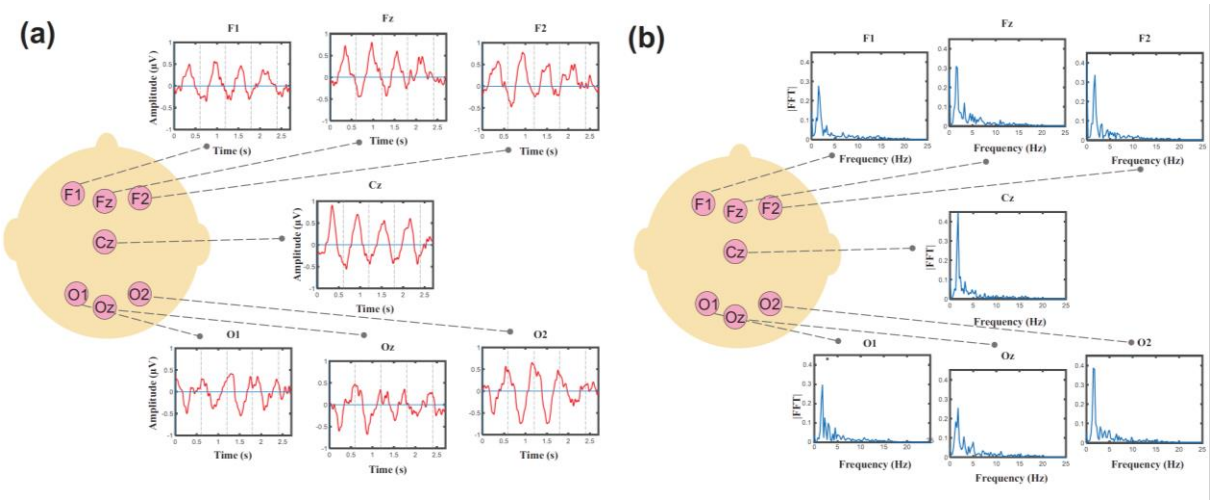

Figure 3.1: (a) Grand averages of the responses for several electrodes, (b) Fourier transforms of the grand averages. High frequencies are not illustrated as they contain values near to zero.

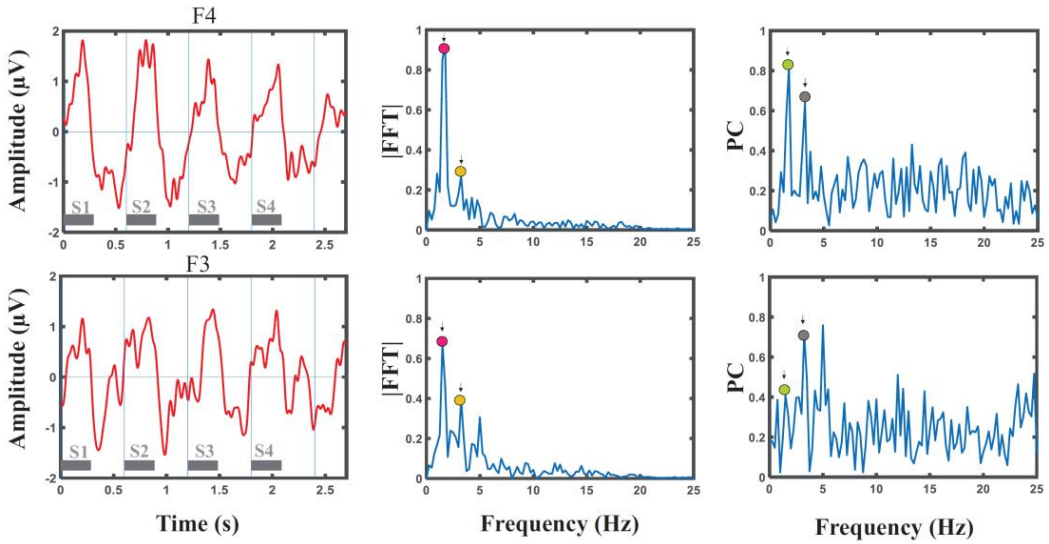

Figure 3.2: Temporal responses, FFT and PC spectra for an individual neonate (30 weeks and 4 days GA) at one right (F4, top row) and one left (F3, bottom row) electrode. The peak amplitudes corresponding to the target frequency and the first harmonic are marked in the FFT and PC spectra.

A global increase of the amplitudes of the FFT spectrum at the target frequency and its harmonic was observed with increasing age (Fig. 3.3.a, Fig. 3.3.b), captured by a positive correlation between amplitude and age, significant at the target frequency (R^2=0.263, p=0.042), but not at the first harmonic (R^2=0.156, p=0.13). An age effect (R^2=0.318, p= 0.023, Fig. 3.c) was also observed for the phase coherence averaged across the 15 channels in each infant.

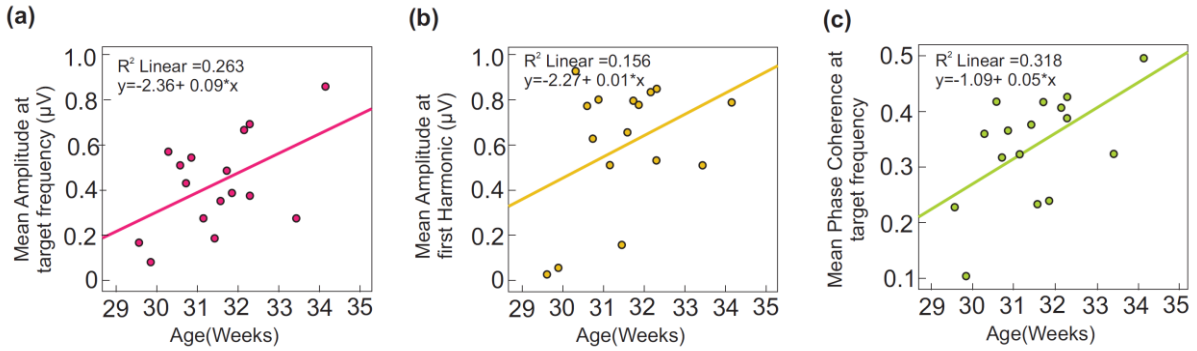

Figure 3.3: (a) Significant positive correlation between the mean amplitude at the target frequency across 15 channels and age, (b) Positive trend between the mean amplitude at the first harmonic across 15 channels and age, (c) Significant positive correlation between the mean PC at the target frequency across 15 channels and age.

Topographic maps presenting the peak amplitude of the responses at the target frequency, the first harmonic and the PC at the target frequency are illustrated for two neonates, at 31 weeks and 3 days GA (Fig. 3.4.a) and 34 weeks and 1 day GA (Fig. 3.4.b). These topographic maps were created to provide the distribution of the extracted features all over the head. They exhibited an asymmetric pattern which motivated us to investigate asymmetry in more details. They also illustrated developmental changes between two subjects with different ages. However, developmental changes and asymmetry are more evident on the maps corresponding to the first frequency feature (first column).

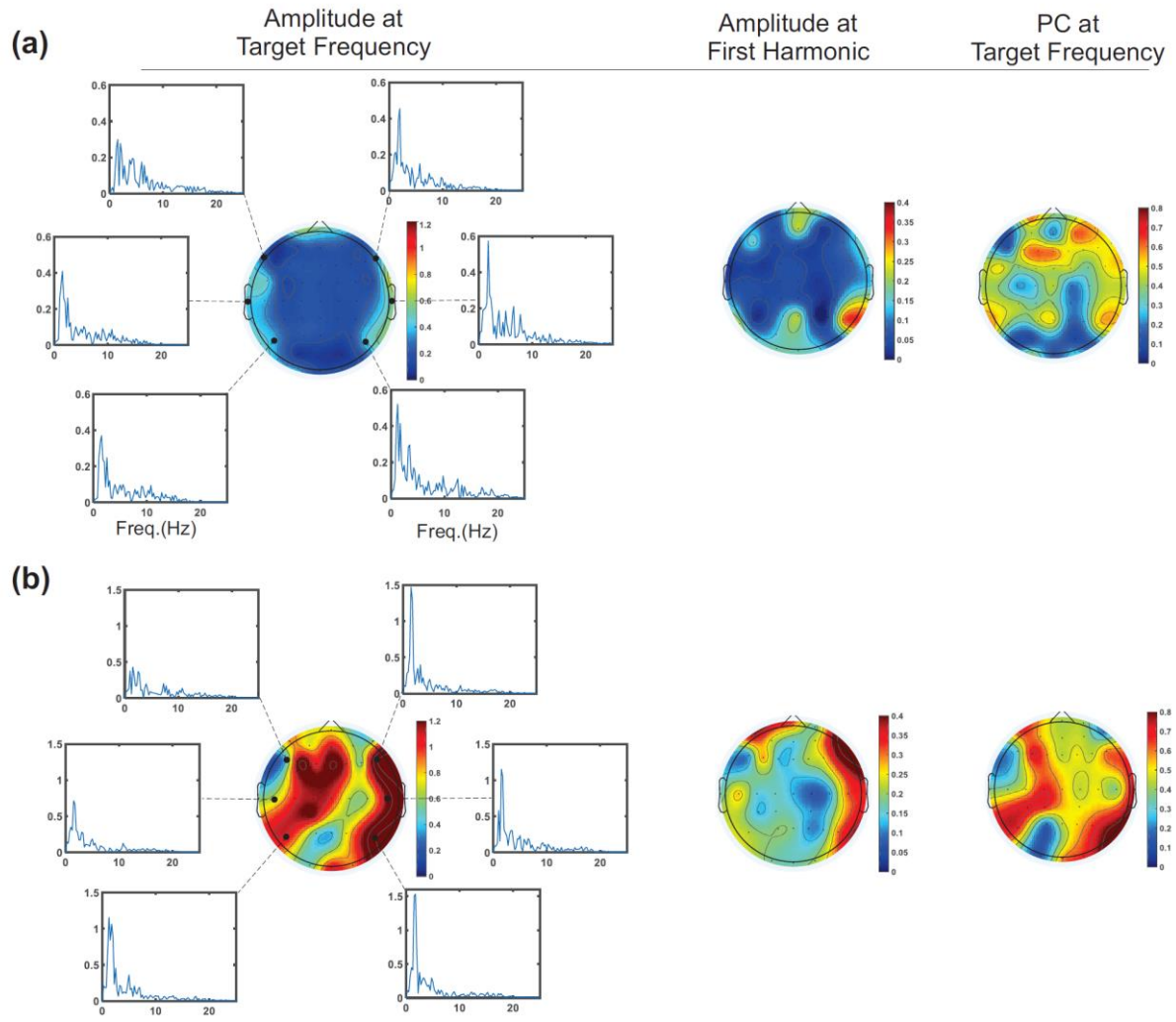

Figure 3.4: Topographic maps presenting the peak amplitude of the auditory responses at the target frequency, the first harmonic, and the PC at the target frequency for two neonates, at 31 weeks and 3 days GA (a) and 34 weeks and 1 day GA (b).

Asymmetry coefficients were calculated for each pair of available electrodes by averaging the LI values across subjects (Fig. 3.5.a). To obtain a fine-grained lateralization map, we considered all the possible pairs of electrodes (more than 15 common channels used for previous analysis) and performed one-tailed *t*-test analysis at each site as several studies have reported a rightward lateralization at early ages (Chiron et al. 1997; Mahmoudzadeh et al. 2013; Roche-Labarbe et al. 2012). A robust rightward bias was observed for some of the auditory-involved areas marked in Fig. 3.5.a and 3.5.b by red circles (Corrected p-values: P6-P5: $p<0.001$, C6-C5: $p=0.029$, C4-C3: $p=0.045$, F6-F5: $p=0.043$, Fc2-Fc1: $p=0.043$). The effect size of the differences between the means of paired channels was also calculated as the Cohen's d (P6-P5: d= 2.080, C6-C5: 1.343, C4-C3: 0.779, F6-F5: 0.859, Fc2-Fc1: 0.836).

Furthermore, we checked for the laterality in the opposite direction. Although Af4-Af3 (d=-1.012) and Cp4-Cp3 (d=-0.828) presented p-values less than 0.05, they showed no significant leftward lateralization after FDR correction. Finally, we did not observed variations of the lateralization index with age in the age-range considered in the present study.

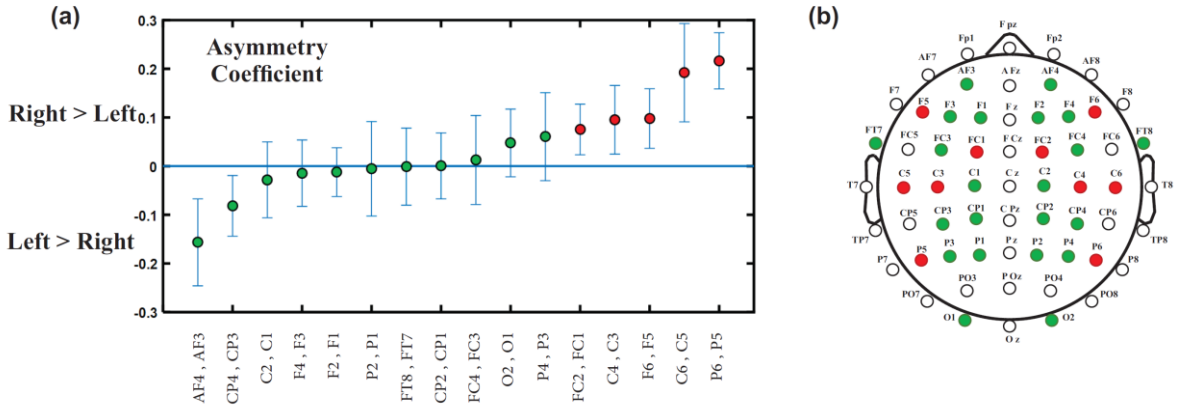

Figure 3.5: (a) Asymmetry coefficients calculated as the average of the LI values across the subjects for each pair of the available electrodes. The error bars indicate the standard error, (b) Locations of the available pairs of electrodes over the head. Electrodes with rightward biases are marked by red circles in both figures. The green circles show the channel pairs with no rightward bias. The white circles correspond to the channel pairs not investigated due to insufficiency of the available data.

3.4 Discussion

Frequency and coherence analyses of CAEPs were performed in very-early preterm infants in order to investigate the temporal accuracy of the immature auditory network. This type of analysis, focused on a precise frequency band, is more robust to the background noise. ASSRs have been previously used to evaluate responses to low modulation rates, as present in speech (Alaerts et al. 2009; Poelmans et al. 2012; Vanvooren et al. 2014) and their hemispheric asymmetries (Boemio et al. 2005; Abrams et al. 2008; Ha¨ma¨la¨inen et al. 2012; Poelmans et al. 2012; Vanvooren et al. 2014). The right hemisphere is thought to be sensitive to auditory modulations close to the speech syllabic rate (Boemio et al. 2005; Abrams et al. 2008; Ha¨ma¨la¨inen et al. 2012), whereas bilateral (Boemio et al. 2005; Ha¨ma¨la¨inen et al. 2012) or left hemispheric (Abrams et al. 2008) specialization is reported for faster modulations. Although right asymmetry for slow modulations has been previously reported in adults (Poelmans et al. 2012), children (Abrams et al. 2009), and newborns (Telkemeyer et al. 2009; Telkemeyer et al. 2011), it was unclear whether some lateralization might already be observed

in preterm infants. Our results suggest that a rightward bias is already in place in preterm infants.

3.4.1 Age-related changes in auditory cortical responses

The human infant undergoes critical development of the auditory system during the period between 25 wGA to 5 or 6 months of age (Graven and Browne 2008). In the age range considered in our study (29.57 to 34.14 wGA), neurons are reaching their target locations and generate many connections within the cortical plate (Zatorre and Belin 2001). This neural synaptogenesis provides the basis for increased synchronization within a larger population of neurons, resulting in more clearly defined evoked potentials relatively to the background noise. This mechanism provides the structural background for the significant positive correlations, observed between age and the amplitude and PC value at the target frequency. The increase in phase coherence reveals that the neuronal response is more and more in line with the stimulus whereas the increase in amplitude might be related to the number of neurons and to the strength of their firing. Both features uncover the functional auditory improvement during the third trimester of pregnancy.

3.4.2 Asymmetry analysis

In adults, the temporal/spectral acoustic properties of the auditory stimuli determine the relative hemispheric lateralization of their processing (Zatorre and Belin 2001; Schonwiesner et al. 2005). In general, broad-band auditory stimuli with rapid changes and temporal complexity are predominantly processed in the left hemisphere, while slowly changing narrow-band stimuli and spectral processing of sounds (Zatorre and Belin 2001) are essentially processed in the right hemisphere (Zatorre et al. 2002; Tervaniemi and Hugdahl 2003). It has been hypothesized that each hemisphere is dominant for analysing modulations at different timescales and that phoneme-rate modulations lateralize to the left hemisphere, while rightward specialization is predominantly involved in low-frequency ASSRs and slower modulation rates such as syllabic-rate modulations (Poelmans et al. 2012).

While previous works have focused exclusively on lateralization in adults and infants, only a few studies have investigated the asymmetry in preterm infants. Using near-infrared spectroscopy at the same preterm age as the current study, larger BOLD responses were recorded over the right frontal and temporal regions when preterms were processing the same syllables as here. Only the left posterior temporo-parietal region escaped this general pattern

and displayed a faster and more sustained response than the right (Mahmoudzadeh et al. 2013). The infants included in the current study were selected from those recorded in (Mahmoudzadeh et al. 2017). The selection was based on the signal to noise ratio (SNR) in the frequency domain of the evoked auditory responses to syllable presentation. Three neonates were excluded from the analysis due to the low SNR.

Several other structural and functional studies reported a rightward asymmetry in preterm neonates' development. The right Superior Temporal Sulcus (STS) is larger than the left one in preterm infants (Dubois et al. 2008) as in adults (Bonte et al. 2013; Leroy et al. 2015; Bodin at al. 2018) and some right sulci appear earlier than their left counterparts (Chi et al. 1977). Resting state cerebral blood flow is larger (Lin et al. 2013) and EEG power is higher in the right hemisphere relative to the left in premature neonates (Myers et al. 2012). Syllables elicited larger right than left responses in premature infants and the discrimination responses to both a change of voice, and of phoneme induced a response in the right Inferior Frontal Gyrus (Mahmoudzadeh et al. 2013). The present study further shows that at a low-frequency rate, a rightward asymmetry both in terms of amplitude and of phase coherence is noticeable in many EEG channels, consistent with the results in adults (Poelmans et al. 2012), children (Abrams et al. 2008), and newborns (Abrams et al. 2009; Ha¨ma¨la¨inen et al. 2012). Thus, hemispheric asymmetries are a property of the developing human brain, already present at multiple structural and functional levels during gestation.

The asymmetry index did not change with age during the preterm period contrary to what has been reported after term for fast auditory modulations. Although at term, bilateral processing of fast auditory modulation has been reported in newborns (Telkemeyer et al. 2009; Telkemeyer et al. 2011), hemispheric biases are changing with age and rate of modulation in a complex pattern (Shaw et al. 2009; Bishop 2013), probably influenced by maturation and experience (Minagawa-Kawai et al. 2011). Using a monaural stimulus at 4Hz, Vanvooren et al. (2014) showed that right hemispheric specialization for processing syllable rate modulations appears to be mature in prereading children, at a very young age (Vanvooren et al. 2014).

Current findings, together with previous observations (Mahmoudzadeh et al. 2013; Mahmoudzadeh et al. 2017), could have important implications for monitoring the emergence and normal development of specific brain functionalities in preterm infants. More specifically, frequency analysis is very suitable for studies in preterm and term neonates and can provide a useful approach to assess certain functional aspects of the capacity of auditory circuits underlying normal neurodevelopment.

3.5 Conclusion

This study, using a frequency approach, demonstrates the ability of the preterm infant's auditory network to process slow modulation with a rightward hemispheric lateralization. This ability is observed at a time when thalamocortical fibres invade the cortical plate, suggesting a strong temporal and spatial genetic fingerprint for auditory processing. The positive correlation between the extracted functional features and age suggests that this ability matures during the third trimester.

Acknowledgement

This work was supported by the Picardie regional council (Hemisphere Nord), by EGIDE France and CISSC Iran under the grant number 961/93-9-2 (Jundi Shapour scientific collaboration program) and by the Co-tutelle program of the French Embassy in Tehran for PhD students.

3.6 References

Abrams DA, Nicol T, Zecker S, Kraus N. (2008). Right-hemisphere auditory cortex is dominant for coding syllable patterns in speech. *J Neurosci, 28*, 3958 –65.

Abrams DA, Nicol T, Zecker S, Kraus N. (2009). Abnormal cortical processing of the syllable rate of speech in poor readers. *J Neurosci, 29*, 7686 –93.

Alaerts J, Luts H, Hofmann M, Wouters J. (2009). Cortical auditory steady-state responses to low modulation rates. *Int J Audiol, 48*, 582-93.

Ali AA, Jerger J. (1992). Phase coherence of the middle-latency response in the elderly. *Scand Audiol, 21*, 187-94.

Anderson S, Parbery-Clark A, White-Schwoch T, Kraus N. (2015). Development of subcortical speech representation in human infants. *J Acoust Soc Am, 137*, 3346-55.

Bishop DV. (2013). Cerebral asymmetry and language development: cause, correlate, or consequence? *Science, 340*, 1230531.

Bodin C, Takerkart S, Belin P, Coulon O. (2018). Anatomo-functional correspondence in the superior temporal sulcus. *Brain Struct Funct, 223*, 221-32.

Boemio A, Fromm S, Braun A, Poeppel D. (2005). Hierarchical and asymmetric temporal sensitivity in human auditory cortices. *Nat Neurosci, 8*, 389 –95.

Bonte M, Frost MA, Rutten S, Ley A, Formisano E, Goebel R. (2013). Development from childhood to adulthood increases morphological and functional inter-individual variability in the right superior temporal cortex. *Neuroimage, 83*, 739-50.

Cheour-Luhtanen M, et al. (1996). The ontogenetically earliest discriminative response of the human brain. *Psychophysiology, 33*, 478-81.

Chi JG, Dooling EC, Gilles FH. (1977). Gyral development of the human brain. *Ann Neurol, 1*, 86-93.

Chiron C, et al. (1997). The right brain hemisphere is dominant in human infants. *Brain, 120*, 1057-65.

Copriviza KL, Lima CG. (1984). Auditory arousal in preterm infants. *NSSLHA, 11*, 3-9.

Dehaene-Lambertz G, Spelke ES. (2015). The Infancy of the Human Brain. *Neuron, 88*, 93-109.

Dehaene-Lambertz Gh, et al. (2010). Language or music, mother or Mozart? Structural and environmental influences on infants' language networks. *Brain Lang, 114*, 53-65.

Despland PA, Galambos R. (1980). The auditory brainstem response (ABR) is a useful diognostic tool in the intensive care nursery. *Pediatr Res, 14*, 154-8.

Dobie RA, Wilson MJ. (1989). Analysis of auditory evoked potentials by magnitude-squared coherence. *Ear Hear, 10*, 2-13.

Dobie RA, Wilson MJ. (1994). Objective detection of 40 Hz auditory evoked potentials: phase coherence vs. magnitude-squared coherence. *Electroencephalogr Clin Neurophysiol, 92*, 405-13.

Draganova R, Eswaran H, Murphy P, Lowery C, Preissl H. (2007). Serial magnetoencephalographic study of fetal and newborn auditory discriminative evoked responses. *Early Hum Dev, 83*, 199-207.

Draganova R, Ross B, Wollbrink A, Pantev C. (2008). Cortical steady-state responses to central and peripheral auditory beats. *Cereb Cortex, 18*, 1193-200.

Dubois J, Benders M, Cachia A, Lazeyras F, Ha-Vinh Leuchter R, Sizonenko SV, Borradori-Tolsa C, Mangin JF, Hüppi PS. (2008). Mapping the early cortical folding process in the preterm newborn brain. *Cereb Cortex, 18*, 1444-54.

Eldredge L, Salamy A. (1996). Functional auditory development in preterm and full term infants. *Early Hum Dev, 45*, 215-28.

Galambos R, Hicks G, Wilson MJ. (1982). Hearing loss in graduates of a tertiary intensive care nursery. *Ear Hear, 3*, 87-90.

Graven SN, Browne J. (2008). Auditory development in the fetus and infant. *Newborn Infant Nurs Rev, 8*, 187-93.

Ha¨ma¨la¨inen JA, Rupp A, Solte´sz F, Szu¨cs D, Goswami U. (2012). Reduced phase locking to slow amplitude modulation in adults with dyslexia: an MEG study. *Neuroimage, 59*, 2952–61.

Hall JW. (2000). Development of the ear and hearing. *J Perinatol, 20*, s812-s820.

Herdman AT, Lins O, Van Roon P, Stapells DR, Scherg M, Picton TW . (2002). Intracerebral sources of human auditory steady-state responses. *Brain Topogr, 15*, 69-86.

Jerger J, Chmiel R, Frost JD, Coker N. (1986). Effect of sleep on the auditory steady state evoked potential. *Ear Hear, 7*, 240-5.

Kappenman ES, Luck SJ. (2010). The effects of electrode impedance on data quality and statistical significance in ERP recordings. *Psychophysiology, 47*, 888-904.

Kostovic I, Judas M, Petanjek Z, Simic G. (1995). Ontogenesis of goal-directed behavior: anatomo-functional considerations. *Int J Psychophysiol, 19*, 85-102.

Lary S, et al. (1985). Hearing threshold in preterm and term infantsby auditory brainstem response. *J Pediatr, 107*, 593-9.

Lehongre K, Ramus F, Villiermet N, Schwartz D, Giraud AL. (2011). Altered low-gamma sampling in auditory cortex accounts for the three main facets of dyslexia. *Neuron, 72*, 1080-90.

Leigh-Paffenroth ED, Fowler CG. (2006). Amplitude-modulated auditory steady-state responses in younger and older listeners. *J Am Acad Audiol, 17*, 582-97.

Leroy F, et al. (2015). New human-specific brain landmark: the depth asymmetry of superior temporal sulcus. *Proc Natl Acad Sci U S A, 112*, 1208-13.

Liégeois-Chauvel C, Lorenzi C, Trébuchon A, Régis J, Chauvel P. (2004). Temporal envelope processing in the human left and right auditory cortices. *Cereb Cortex, 14*, 731-40.

Lin PY, Roche-Labarbe N, Dehaes M, Fenoglio A, Grant PE, Franceschini MA. (2013). Regional and hemispheric asymmetries of cerebral hemodynamic and oxygen metabolism in newborns. *Cereb Cortex, 23*, 339-48.

Mahmoudzadeh M, Dehaene-Lambertzc Gh, Kongolod G, Fourniera M, Goudjild S, Wallois F. (2018). Consequence of intraventricular hemorrhage on neurovascular coupling evoked by speech syllables in preterm neonates. *Dev Cogn Neurosci, 30*, 60-9.

Mahmoudzadeh M, et al. (2013). Syllabic discrimination in premature human infants prior to complete formation of cortical layers. *PNAS, 110*, 4846-51.

Mahmoudzadeh M, Wallois F, Kongolo G, Goudjil S, Dehaene-Lambertz Gh. (2017). Functional maps at the onset of auditory inputs in very early preterm human neonates. *Cereb Cortex, 27*, 2500-12.

Mehler J, et al. (1988). A precursor of language acquisition in young infants. *Cognition, 29*, 143-78.

Millman RE, Prendergast G, Kitterick PT, Woods WP, Green GGR. (2010). Spatiotemporal reconstruction of the auditory steady-state response to frequency modulation using magnetoencephalography. *NeuroImage, 49*, 745–58.

Minagawa-Kawai Y, Cristia` A, Dupoux E. (2011). Cerebral lateralization and early speech acquisition: a developmental scenario. *Dev Cogn Neurosci, 1*, 217-32.

Moore JK, Perazzo LM, Braun A. (1995). Time course of axonal myelination in the human brainstem auditory pathway. *Hear Res, 87*, 21-31.

Myers MM, Grieve PG, Izraelit A, Fifer WP, Isler JR, Darnall RA, Stark RI. (2012). Developmental profiles of infant EEG: overlap with transient cortical circuits. *Clin Neurophysiol, 123*, 1502-11.

Obrig H, Rossi S, Telkemeyer S, Wartenburger I. (2010). From acoustic segmentation to language processing: evidence from optical imaging. *Front Neuroenergetics, 2*, 13.

Picton TW, John MS, Dimitrijevic A, Purcell D. (2003). Human auditory steady-state responses. *Int J Audiol, 42*, 177–219.

Picton TW, Vajsar J, Rodriguez R, Campbell KB. (1987). Reliability estimates for steady-state evoked potentials. *Electroencephalogr Clin Neurophysiol, 68*, 119-31.

Poelmans H, Luts H, Vandermosten M, Ghesquiere P, Wouters J. (2012). Hemispheric Asymmetry of Auditory Steady-State Responses to Monaural and Diotic Stimulation. *J Assoc Res Otolaryngol, 13*, 867-76.

Power AJ, Mead N, Barnes L, Goswami U. (2012). Neural Entrainment to Rhythmically Presented Auditory, Visual, and Audio-Visual Speech in Children. *Front Psychol, 3*, 216.

Renaud Jardri, et al. (2008). Fetal cortical activation to sound at 33 weeks of gestation: A functional MRI study. *Neuroimage, 42*, 10-8.

Ribeiro FM, Carvallo RM. (2008). Tone-evoked ABR in full-term and preterm neonates with normal hearing. *Int J Audiol, 47*, 21-9.

Roche-Labarbe N, et al. (2012). Near-infrared spectroscopy assessment of cerebral oxygen metabolism in the developing premature brain. *J Cereb Blood Flow Metab, 32*, 481-8.

Ross B, Herdman AT, Pantev C. (2005). Right hemispheric laterality of human 40 Hz auditory steady-state responses. *Cereb Cortex, 15*, 2029-39.

Rotteveel JJ, de Graaf R, Stegeman DF, Colon EJ, Visco YM. (1987). The maturation of the central auditory conduction in preterm infants until three months post term. V. The auditory cortical response (ACR). *Hear Res, 27*, 95-110.

Ruben RJ. (1992). The ontogeny of human hearing. *Acta Otolaryngol, 112*, 192-6.

Sano M, Kaga K, Kuan CC, Ino K, Mima K. (2007). Early myelination patterns in the brainstem auditory nuclei and pathway: MRI evaluation study. *Int J Pediatr Otorhinolaryngol, 71*, 1105–15.

Schonwiesner M, Rubsamen R, von Cramon DY. (2005). Hemispheric asymmetry for spectral and temporal processing in the human antero-lateral auditory belt cortex. *Eur J Neurosci, 22*, 1521-8.

Schulman-Galambos C, Galambos R. (1975). Brainstem auditory evoked responses in premature infants. *J Speech Hear Res, 18*, 456-65.

Shaw P, et al. (2009). Development of cortical asymmetry in typically developing children and its disruption in attention-deficit/hyperactivity disorder. *Arch Gen Psychiatry, 66*, 888–96.

Sininger YS, Bhatara A. (2012). Laterality of basic auditory perception. *NIH, 17*, 129-49.

Stapells DR, Makeig S, Galambos R. (1987). Auditory steady-state responses: threshold prediction using phase coherence. *Electroencephalogr Clin Neurophysiol, 67*, 260-70.

Telkemeyer S, Rossi S, Koch SP, Nierhaus T, Steinbrink J, Poeppel D, Obrig H, Wartenburger I. (2009). Sensitivity of newborn auditory cortex to the temporal structure of sounds. *J Neurosci, 29*, 14726 –33.

Telkemeyer S, Rossi S, Nierhaus T, Steinbrink J, Obrig H, Wartenburger I. (2011). Acoustic processing of temporally modulated sounds in infants: evidence from a combined near-infrared spectroscopy and EEG study. *Front Psychol, 2*, 1-14.

Tervaniemi M, Hugdahl K. (2003). Lateralization of auditory-cortex functions. *Brain Res Brain Res Rev, 43*, 231-46.

Tervaniemi M, Hugdahl K. (2003). Lateralization of auditory-cortex functions. *Brain Res Rev, 43*, 231-46.

Thatcher RW. (2012). Coherence, phase differences, phase shift, and phase lock in EEG/ERP analyses. *Dev Neuropsychol, 37*, 476-96.

Tlumak AI, Durrant JD, DelgadoRE, Boston JR. (2012). Steady-state analysis of auditory evoked potentials over a wide range of stimulus repetition rates: Profi le in children vs. adults. *Int J Audiol, 51*, 480-90.

Toffanin P, de Jong R, Johnson A, Martens S. (2009). Using frequency tagging to quantify attentional deployment in a visual divided attention task. *Int J Psychophysiol, 72*, 289-98.

Vanvooren S, Poelmans H, Hofmann M, Ghesquie`re P, Wouters J. (2014). Hemispheric Asymmetry in Auditory Processing of Speech Envelope Modulations in Prereading Children. *J Neurosci, 34*, 1523-9.

Weitzman WD, Graziani LJ. (1968). Maturation and topography of the auditory evoked response of the prematurely born infant. *Psychobiol, 1*, 79-89.

Wernicke C. (1874). *Der aphasische Symptomencomplex; eine psychologische Studie auf anatomischer Basis.* Breslau: Cohn and Weigert.

Yamasaki T, Goto Y, Taniwaki T, Kinukawa N, Kira J, Tobimatsu S. (2005). Left hemisphere specialization for rapid temporal processing: a study with auditory 40 Hz steady-state responses. *Clin Neurophysiol, 116*, 393-400.

Zatorre RJ, Belin P. (2001). Spectral and temporal processing in human auditory cortex. *Cereb Cortex, 11*, 946-53.

Zatorre RJ, Belin P, Penhune VB. (2002). Structure and function of auditory cortex: music and speech. *Trends Cogn Sci, 6*, 37-46.

Chapter 4

Functional and structural correlates of the preterm infant's brain: Relating developmental changes of auditory evoked responses to myelin maturation

Functional responses recorded during the last trimester of gestation reveal that human sensory activity begins before birth, allowing the brain to process the external environment. Along with the maturation of brain, new cognitive skills emerge in the human infant's brain. The development of non-invasive techniques provides the opportunity to study the relationship between the brain structural maturation and cognitive development *in vivo*. Here, we aimed to relate developmental changes of the latency of cortical auditory evoked potentials (CAEPs) to a structural maturation index, presumed to be representative of myelination. CAEPs to syllables were recorded in 17 preterm neonates with a mean recording age of 30.5 weeks gestational age (28.4-32.2 wGA). The latency of the first peak of the global field power (GFP) was considered the functional feature of interest to be examined for correlation with age and the structural maturation index extracted from brain atlases of the corresponding term age. GFP latency significantly decreased with age ($R^2 = 0.311$, $p = 0.02$). Structural maturation indices, calculated as the mean values of T1w/T2w image intensities, were extracted for various brain regions. We observed significant correlations between the maturation indices of the auditory-involved areas and the latency of the GFP first-peak, as well as age. In hierarchical models, neither the structural maturation index nor age contributed to significant additional variance in the GFP first-peak latency after accounting for the variance associated with the other parameter.

4.1 Introduction

With age, numerous factors (the development of membranes, myelin, connectivity, etc.) modify the brain while, in parallel, the infant gradually achieves new cognitive skills. However, the intricate relationship between structural maturation and new cognitive and behavioral skills is still poorly understood. Recent development of non-invasive techniques, such as magnetic resonance imaging (MRI) and magneto- and electroencephalography (M/EEG), has provided the opportunity to study the relationships between brain maturation and cognitive development *in vivo* (Dubois et al. 2008, 2016; Adibpour et al. 2018). Such a joint structural and functional approach, despite being challenging, is important for characterizing normal brain development and understanding the early mechanisms of disease.

Event-related potentials (ERPs) are an easy approach to measure how the brain responds to stimulation. Cortical auditory evoked potentials (CAEPs) are recorded in premature infants from 27 wGA (Rotteveel et al. 1987), showing developmental changes with respect to the components amplitudes and latencies (Weitzman and Graziani 1968; Graziani et al. 1974; Rotteveel et al. 1987). Sound discrimination abilities, revealed by slow mismatch responses, are also observed before term. Most studies have been conducted at 34-35 wGA, at an age, the cochlear functions are almost mature (Bisiacchi et al. 2009) but similar results are also reported at an earlier age using EEG (Alho et al. 1990; Cheour et al. 2002; Cheour-Luhtanen et al. 1996; Kushnerenko et al. 2001; Novitski et al. 2007) and MEG in fetuses (Draganova et al. 2007), as early as 27 wGA (Holst et al. 2005). Using near-infra-red spectroscopy (NIRS) in healthy neonates tested ten weeks before term (28–32 wGA), Mahmoudzadeh et al (2013), observed that different peri-sylvian networks comprising superior temporal but also inferior frontal areas were involved in syllable and voice discrimination.

In a previous study (Mahmoudzadeh et al. 2017), we showed that it is possible to record auditory ERPs to syllable sequences already at six months gestation after preterm birth, with reproducible topographies. Furthermore, mismatch responses, denoting sound discrimination capacities, were observed in response to unexpected changes of syllables and voices. In another study (Daneshvarfard et al. 2019), using a frequency-domain approach, we demonstrated that the same repetitive syllabic stimuli were processed with a rightward lateralization in the same group of preterm infants. These results suggest that preterm neonates perceive and process the environment. The question remains as to how these responses are related to brain structure and how they develop. To date, only a few studies have related structural to functional markers of maturation. Dubois et al. (2008) measured

visual ERPs to faces and transverse diffusivity in various white matter (WM) tracts using diffusion tensor imaging (DTI) data in healthy full-term infants during the first semester. The authors related the increase in P1 conduction velocity of visual evoked potentials (VEPs) to the myelinization of optic radiations. Adibpour et al. (2018) confirmed this relation and further showed that the transfer time between hemispheres was related to the maturation of the visual callosal fibers. These relations persisted after controlling for the effect of age. Dockstader et al. (2012) reported that P1 latency from visual evoked responses recorded in 6- to 12-year-old children were inversely related to the fractional anisotropy (FA), measured by DTI, in visual and motor association regions. Similar structure-function relationships have also been demonstrated in adults, with an inverse relationship between the latency of the visual P1 and the microstructure (FA) of bilateral parietal and right lateral frontal WM (Stufflebeam et al. 2008).

Few studies have examined the auditory modality (Dubois et al. 2016). The observed decrease in latency of the left and right superior temporal gyrus (STG) auditory responses, measured by MEG, is related to the maturation of acoustic radiation, based on DTI anisotropy, in children and adolescents (Roberts et al. 2009). In contrast, Adibpour et al. (2019) found no association between the conduction speed of the auditory P2 and changes in DTI parameters in acoustic radiations in full-term infants tested during the first semester, except for gray matter (GM) maturation in the inferior frontal region. In an aging population, cumulative delays in auditory evoked responses were not related to auditory tract properties but rather to the GM volume of the superior temporal regions (Price et al. 2017). The lack of correlations between component latencies and myelination parameters in auditory tracts can be explained by the short length of acoustic radiations relative to optic radiations, which can mask a difference in velocity between individuals and also by the fact that relatively late components were considered in these studies.

Several mechanisms may contribute to the acceleration of electrical components throughout development, particularly during the preterm period. These may include microstructural organization of the cortical plate and subplate, the development of intracortical connectivity, cortical folding, synaptic bursting, pruning, etc. (Dubois et al. 2016). However, myelination, the establishment of lipid myelin around neuronal axons, is considered to be the main factor that contributes to the acceleration of ERP latencies. Its main role is to facilitate the synchronized neuronal communication responsible for higher-order cognitive functions (Dockstader et al. 2012).

Here, we investigated how the gradual acceleration of the auditory ERP may be related to WM and GM maturation in preterm neonates. The auditory system is already functional *in utero*, but its development is protracted during infancy and toddlerhood (Dubois et al. 2016). We restudied the data of infants from our already published study (Mahmoudzadeh et al. 2017). Since MRI data could not be obtained for these newborns, we used public atlases of T1-weighted (T1w) and T2-weighted (T2w) images for each given gestational week. It has been proposed that the ratio of T1w and T2w MRI signal intensity increases the sensitivity of measuring myelin-related signal intensity changes (Glasser and Van Essen 2011). This method has been proposed to measure myelination for both GM and WM regions and does not depend on axon fiber anatomy, unlike DTI. Therefore, it can be used for estimating whole-brain intracortical myelin-related changes, which are difficult to measure directly using existing noninvasive neuroimaging tools (Iwatani et al. 2015). Dividing the T1w signal intensity by the corresponding T2w values increases the contrast of the myelin content and reduces the signal receiver-coil bias (Glasser and Van Essen 2011). Consequently, the T1w/T2w ratio image may be used to investigate age-related changes in signal intensity in both adults and infants (Grydeland et al. 2013; Lee et al. 2015). This measure has been used previously as an estimate of myelin content in adults (Glasser and Van Essen 2011; Grydeland et al. 2013; Iwatani et al. 2015), children (Grydeland et al. 2013), and infants 40-48 wGA (Lee et al. 2015). Although other factors might probably contribute to the signal in the T1w/T2w ratio, these values can be used as a structural maturation index, mainly representative of myelination and measured by combining various sensitivities of the T1w and T2w images relative to water.

4.2 Materials and methods

4.2.1 Participants

The CAEPs recorded from 17 preterm neonates (mean recording age = 30.47 wGA, 28.4 to 32.2 wGA), recruited in our previous study (Mahmoudzadeh et al. 2017), were reanalyzed for the current study. The infants were considered to be normal for their gestational age on the basis of auditory and clinical neurological assessments and their EEG. Furthermore, they had appropriate birth weight, size, and head circumference for their term age. Clinical features of the infants are presented in Table 4.1. The infants' parents provided written informed consent and the study was approved by the Amiens University Hospital local ethics committee (CPP

Nord-Ouest II) according to the guidelines of the Declaration of Helsinki of 1975 (ref ID-RCB 2008-A00728-47).

Table 4.1: Clinical features of the participants.

Infant No.	Gender	GA at test (wGA)	Birth weight (gr)	Size at birth (cm)	Head circumference at birth (cm)
1	M	31.71	1560	42	30
2	M	29.57	1157	37	29
3	F	31.42	1260	40	29
4	M	30.57	1730	41	28
5	F	31.85	1190	41	30
6	F	32.14	1200	42	30
7	M	32.28	1550	41	31
8	F	31.14	1400	39	28
9	M	29.85	1110	40	28
10	M	28.71	1010	39	28
11	M	28.42	1100	36	28
12	F	28.57	1030	37	30
13	F	31.57	1410	43	31
14	M	30.85	1200	42	29
15	M	30.28	1160	38	29
16	F	28.42	950	36	26
17	M	30.71	1320	42	30

4.2.2 Auditory stimuli, recording and preprocessing

The auditory stimuli consisted of syllables, /ba/ and /ga/, produced by a male and a female speakers and matched for intonation, intensity, total duration (285 ms), prevoicing and voiced formant transition duration (40/45 ms). The syllables were repeated in series (trials) of four separated by 600 ms intervals between syllable onsets. Five series, with inter-series intervals of 1,600 ms of silence, constituted a block and each block lasted 20 s and was followed by 40 s of silence. In each block, the repeated syllable was randomly selected among the four possible syllables (/ba/^{male}, /ba/^{female}, /ga/^{male}, /ga/^{female}). In the standard trials, the same syllable was repeated four times, whereas in deviant trials, the last syllable differed from the first three in voice or phonetic dimension. The stimuli were presented at ≈70 dB hearing level via speakers placed at the infant's feet (Mahmoudzadeh et al. 2013, 2017).

The EEG signals were recorded using Ag/AgCl surface electrodes and a nasion reference, with a sampling rate of 2,048 Hz. They were amplified by A.N.T (Enschede, The Netherlands) and filtered between DC-50 Hz. The number of electrodes (31-61) was determined according to the infant's head circumference, with a minimum of 31 electrodes placed on the same 10–20 reference points in all infants. The recordings were band-pass filtered between 1 and 20 Hz and down-sampled to 512 Hz. They were segmented into epochs ([−0.5 +2.7 s]) time-locked to the first syllable (S1) of the trial, providing 324 standard and 216 deviant (108 deviant phoneme

and 108 deviant voice) trials from each electrode in each subject. Trials were then baseline corrected to the 200 ms preceding S1 onset. A trial was rejected if its absolute amplitude exceeded 50 µV or if a local amplitude jump between ten successive time-points exceeded 30 µV. We only considered here the response to the first syllable because it produces the largest response. There was a decrease of amplitude for the next syllables due to habituation (Mahmoudzadeh et al. 2017). We thus merged all trials together in each infant to obtain the ERPs (in average 276 standard and 186 deviant trials).

4.2.3 Global Field Power

Global field power (GFP) measures the spatial standard deviation of the instantaneous field activity by considering the data from all electrodes (Skrandies 1990). The result is a reference-independent descriptor of the potential field calculated by equation (1) as the root of the mean of the squared potential differences (u_i - u_j) between all possible electrode pairs within the field (*n* indicates the number of electrodes).

$$GFP = \sqrt{\left(\frac{1}{2n}\right) * \sum_{i=1}^{n} \sum_{j=1}^{n} \left(u_i - u_j\right)^2} \quad (4.1)$$

GFP does not rely on the wave shapes of the individual electrodes, which makes it robust against low evoked response-to-noise ratio. Because it presents a global measure of the brain activity which can be detected on the scalp and is independent of a pre-specified topography, its maxima represent a reliable method for finding ERP components, especially in preterm infants. We considered here the latency of the first peak of the GFP to be an interesting feature for the study of age and structure-related dependencies as it may represent the first robust response of the cortical auditory areas. After channel rejection due to artifact or noise, fifteen channels common among all subjects, (Fz, F1, F2, F3, F4, C1, C2, CP1, CP2, Pz, P1, P2, Oz, O1, and O2) were used to calculate the GFP signal. We defined a time window of 0-285 ms to provide a compatible estimate of the first peak location, beginning from the onset of the first syllable, and searched for the first local maxima in this time window. Mahmoudzadeh et al. (2017) reported an 84-ms latency for the occurrence of the first peak of the GFP signal of the grand averages in a similar group of preterm infants (19 preterm neonates with mean recording age of 30.8 wGA ± 1.4) in response to the same stimuli. Hence, we expected to observe the first peaks of individual signals in a range with a mean value close to this value.

4.2.4 Structural analysis

We aimed at developing conjoint models of functional and structural brain development in preterm infants. However, because we did not have MR images of our preterm infants, we used those provided by Imperial College London[1] as an alternative although more limited approach. T1w and T2w templates corresponding to each wGA were selected from the detailed spatio-temporal structural atlas (Neonatal structural atlas – Brain Development) provided for the neonatal brain with 87 labeled structures. The atlas has been constructed using T1w and T2w MR images from 204 healthy premature neonates with a mean and standard deviation of 37.3 ± 4.8 wGA (26.7-44.3 wGA) at the time of scan. The neonatal brain was parceled into multiple cortical and subcortical regions (see Makropoulos et al. 2014 for more details on the segmentation and parcellation pipeline). The segmentation method has been further extended in (Makropoulos et al. 2016) to detect cortical sulci and provide detailed delineation of the cortical ribbon.

We used T1w/T2w ratio images to increase myelin-related signal contrast and reduce receiver-coil bias (Glasser and Van Essen 2011). A ratio image was created for each wGA image. The mean values of the ratio image intensities were extracted for each region of interest as a proxy for the maturation of that region (subsequently called maturation index). We considered two regions of interest as the global measures of the structural development (the total of gray matter (GM) and the total of white matter (WM)) and two auditory regions of interest: the middle and posterior parts of the superior temporal gyrus (mSTG and pSTG) (GM and WM values were merged). We first merged the left and right values. We also examined the other regions specified in the neonatal atlas (GM + WM averaged over right and left hemispheres) to investigate the specificities of the correlation with auditory areas.

Second, we checked for asymmetries between the left and right mSTG and pSTG. Maturation indices corresponding to mSTG and pSTG in each hemisphere were divided by the sum of the values of the two hemispheres and submitted to a *t*-test. This normalized value is less influenced by inter-subject variability, corresponding to the individual structural maturation. Therefore, it provides an appropriate measure for statistical comparison between maturation indices of the left and right hemispheres.

[1] http://brain-development.org/brain-atlases/multi-structural-neonatal-brain-atlas/

4.2.5 Joint functional-structural analysis

We associated each infant with its appropriate template image to investigate the correlations between function and structure. Infants from 29.5 to 30.5 wGA were associated with the templates for 30 wGA and similarly for the other ages. Linear regressions were performed separately to investigate correlations between the GFP first-peak latency and structural maturation indices of the total WM, mSTG, and pSTG. Then, hierarchical regression analysis was conducted to examine the unique influence of age and maturation indices of the total WM, mSTG, and pSTG on the GFP first-peak latency. Furthermore, we investigated the auditory specificity of the observed relationships by performing a partial correlation between GFP first-peak latency and maturation index of each region (i.e. all the regions provided by the neonatal atlas), controlling for the infants' age. Thus, we were able to compare the correlations between the functional feature and structural indices of different brain regions after removing the effect of age. In the last step, we further investigated the specificity of the auditory areas by examining the unique influence of the STG maturation index (WM+GM, mSTG+pSTG) on the GFP first-peak latency after removing the maturational effect of all other regions presented by the global maturation index (the total WM excluding the STG).

4.3 Results

4.3.1 Longitudinal functional analysis

Box plots of the GFP signals of the 17 preterm neonates are presented in Fig. 4.1a, with the first peak marked on the median curve. Topographic map of the brain activity at the first peak latency of the grand average GFP response is illustrated in Fig. 4.1b. The first peak is detected on the grand average GFP at 86 ms. Fig. 4.1c shows the scatter plot of the individual GFP first peak latencies *versus* age. We observed a global decrease for the first-peak latency of the GFP signal with increasing age, shown by a significant negative correlation (R^2 = 0.311, p = 0.02).

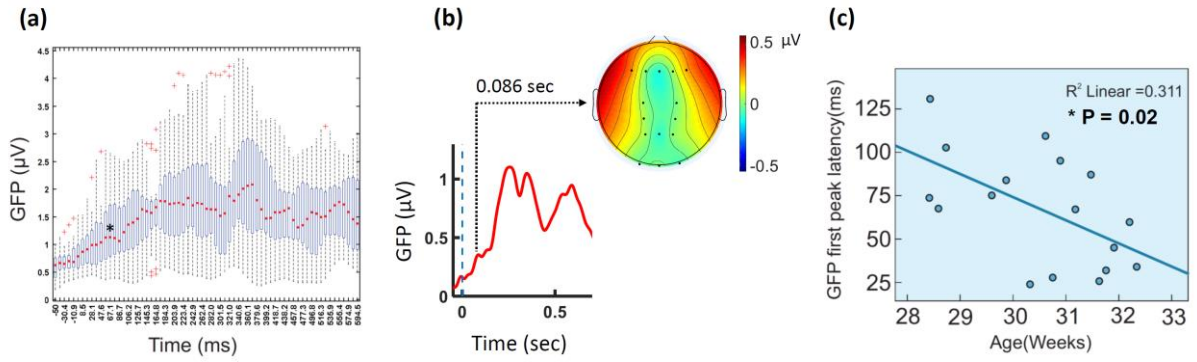

Figure 4.1: (a) Box plots of the GFP signals of 17 preterm neonates. The first peak is marked on the median curve by a star at 67.1 ms. (b) Topographic map of the brain activity at the first peak latency of the grand average GFP response. The first peak is detected on the grand average GFP at 86 ms. (c) Significant negative correlation between the first-peak latency of the individual GFP signals and age.

4.3.2 Longitudinal structural analysis

T1w and T2w templates of the neonatal brain atlas for each week of the studied age range are presented in Fig. 4.2a. T1w/T2w ratio images were created and are presented in the third row of Fig. 4.2a. For better visualization of the age-related variations, Fig. 4.2b presents the T1w/T2w intensity values on the WM surface for each weekly age interval. Developmental changes are observable in the ratio images (Fig. 4.2a), as well as the rendering on the WM surface (Fig 4.2b).

We evaluated the age-dependent changes in the maturation indices of the four regions of interest (total GM, total WM, mSTG, and pSTG) for the whole age range provided by the neonatal atlas (28-44 wGA). The maturation index of the total WM showed a large positive correlation with age ($R^2 = 0.930$, $p < 0.001$) (Fig. 4.3a). It was also the case for the maturation index of the mSTG ($R^2 = 0.929$, $p < 0.001$) (Fig. 4.3b) and of the pSTG ($R^2 = 0.915$, $p < 0.001$) (Fig. 4.3c). By contrast, there was no correlation with age for the total GM maturation index ($p > 0.1$).

Concerning hemispheric asymmetries, although an asymmetry (left > right) was observed for the normalized maturation indices of both mSTG ($p = 0.0533$, $t = 2.0860$, $df = 16$) and pSTG ($p = 0.0465$, $t = 2.1577$, $df = 16$) when the full age-range of the neonatal atlas was considered (28-44 wGA), no significant asymmetry was yet observed during the age-range of our study (28-32 wGA). It might suggest that asymmetries in the superior temporal region appear after 32 wGA. In order to investigate the effect of the hemisphere and age-range, as well as the interaction between them, we also conducted mixed ANOVA with a within-

subject factor (Left *versus* Right) and a between subject factor (T1 = 28-32 wGA *versus* T2 = 33-44 wGA). Raw values of the maturation indices were used for the mixed ANOVA analysis. For mSTG, the main effect of the hemisphere (Left *versus* Right) was non-significant ($f(1, 15) = 2.291$, $p = 0.151$) and the main effect of age-range (28-32 wGA *versus* 33-44 wGA) was significant ($f(1, 15) = 26.093$, $p < 0.001$). The interaction between hemisphere and age-range was non-significant at the 5% level ($f(1, 15) = 1.953$, $p = 0.183$). For pSTG, the main effect of the hemisphere (Left *versus* Right) was non-significant ($f(1, 15) = 1.606$, $p = 0.224$) and the main effect of age-range (28-32 wGA *versus* 33-44 wGA) was significant ($f(1, 15) = 19.435$, $p = 0.001$). The interaction between hemisphere and age-range was significant at the 5% level ($f(1, 15) = 13.997$, $p = 0.002$). To investigate the significant interaction, follow-up t-tests were conducted. There was a significant difference between Left and Right hemispheres in the age-range of 33-44 wGA ($t(11) = 4.544$, $p = 0.001$), but it was not significant for the first age range. There was a significant difference between the two age-range for the left hemisphere ($t(15) = -4.549$, $p < 0.001$) and for the right hemisphere ($t(19) = -4.179$, $p = 0.001$).

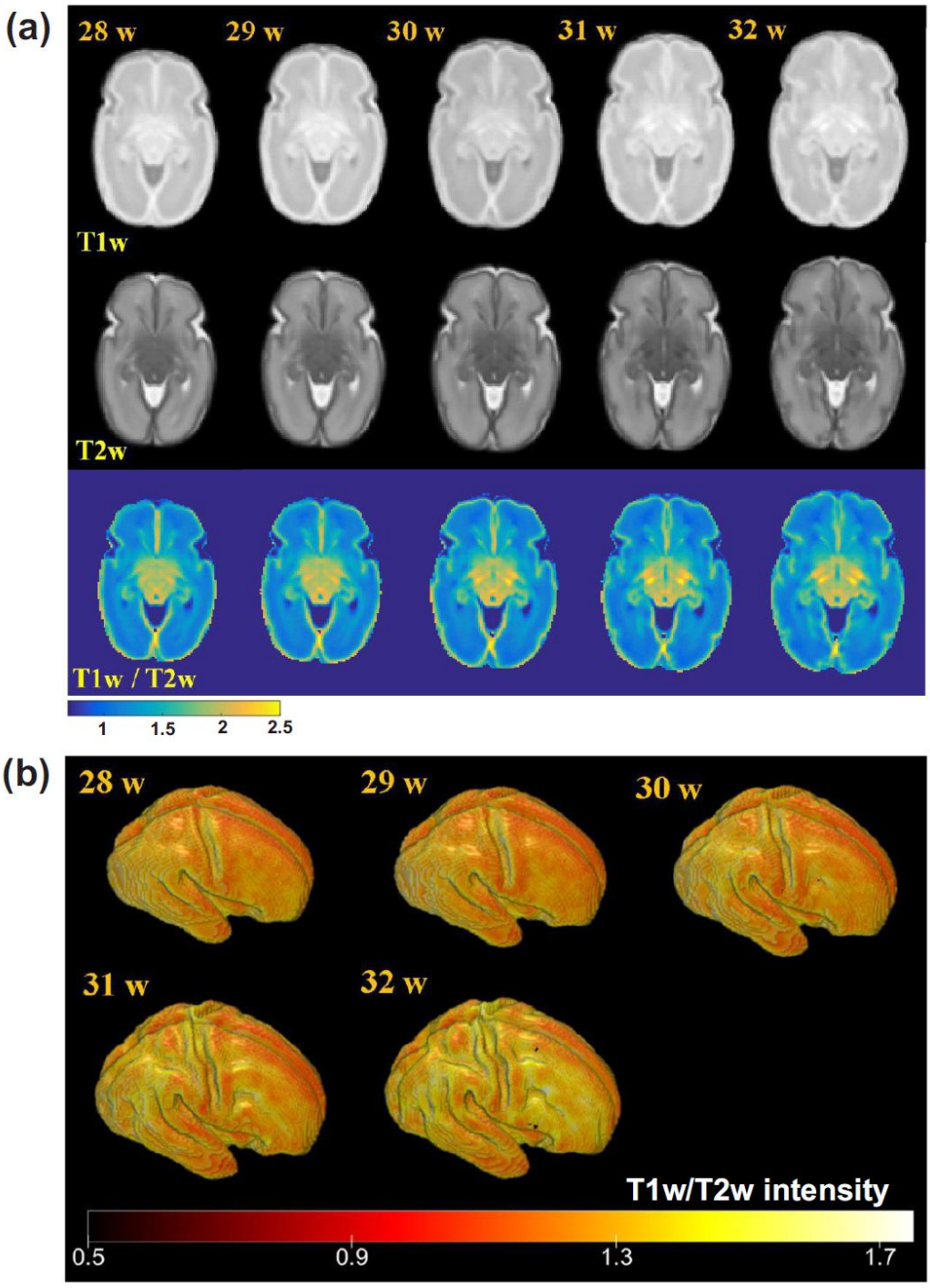

Figure 4.2: (a) T1w and T2w templates of the neonatal brain atlas and created T1w/T2w ratio images for the age range of 28 to 32 wGA. (b) Rendering of the T1w/T2w intensity values on the WM surface

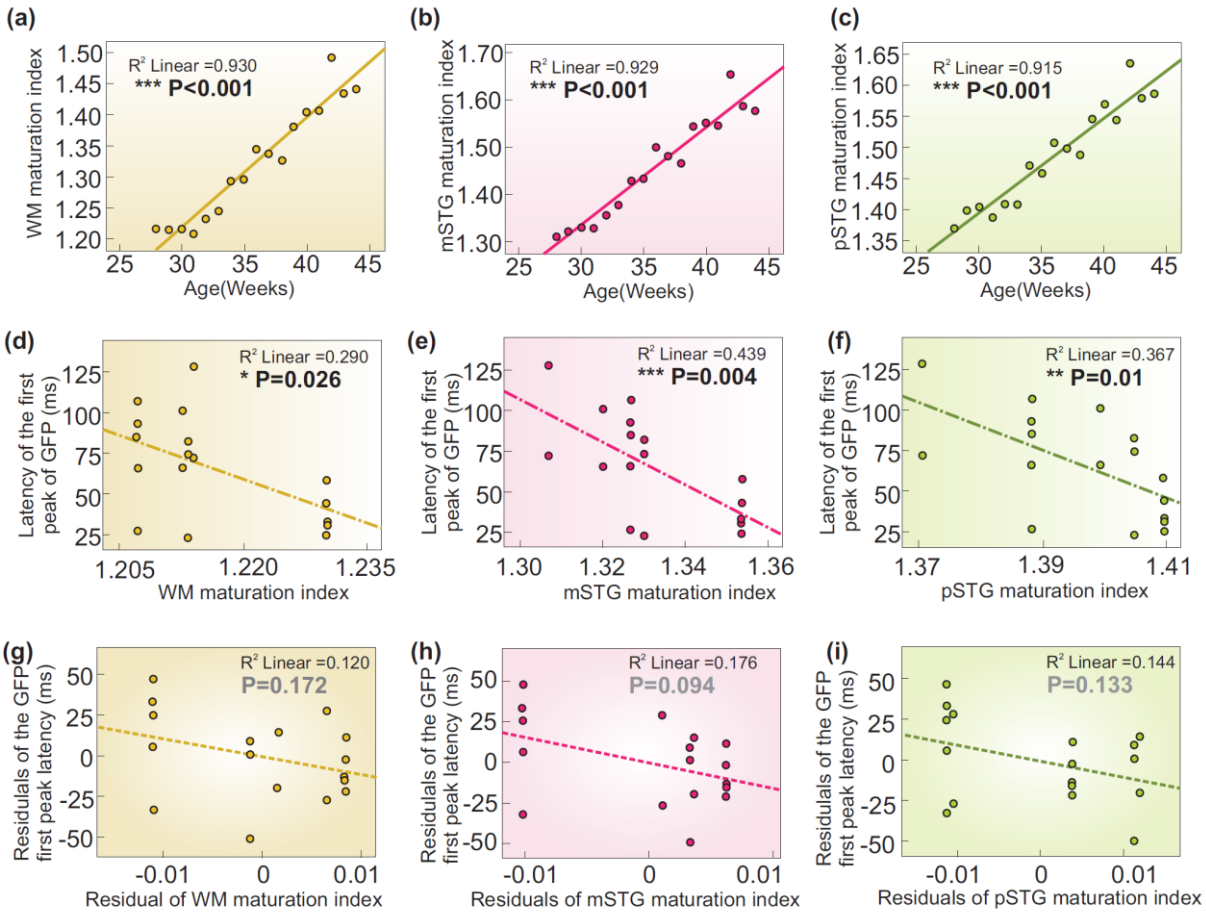

Figure 4.3: Significant positive correlation of the maturation index of the total WM (a), mSTG (b), and pSTG (c) with age. Significant negative correlation between the GFP first-peak latency and maturation index of WM (d), mSTG (e), and pSTG (f). Results of partial correlations between the GFP first-peak latency and maturation indices of WM (g), mSTG (h), and pSTG (i) after regressing out the effect of age. Significant correlations are marked with black and non-significant correlations are marked with gray P values.

4.3.3 Functional-structural analysis

A linear regression analysis was conducted separately for each of the three regions of interest (total WM, mSTG and pSTG) in relation to GFP first peak latency. Significant negative correlations were observed between the GFP first-peak latency and total WM maturation index (R^2 = 0.290, p=0.026) (Fig. 4.3d), mSTG (R^2 = 0.439, p = 0.004) (Fig. 4.3e) and pSTG maturation indices (R^2 = 0.367, p = 0.01) (Fig. 4.3f). See Table 4.2 for a summary of all significant correlations observed between measures.

We performed a hierarchical regression analysis to examine the unique influence of age and total WM maturation index on GFP first-peak latency. The full regression model (age and total WM maturation) predicted 40.5% of the variance in GFP first-peak latency (p = 0.026). Added first, age predicted 32.4% of the variance (p = 0.017). Including total WM maturation

explained a non-significant 8.1% of the additional variance in the model (p = 0.188). Added first, total WM maturation predicted 29% of the variance (p = 0.026). Including age explained a non-significant 11.6% of additional variance in the model (p = 0.121).

We applied the same statistical approach to investigate the unique effect of age and mSTG maturation on GFP first-peak latency. The full regression model (age and mSTG maturation) predicted 44.3% of the variance in GFP first-peak latency (p = 0.017). Although adding age as the first variable predicted 32.4% of the variance (p = 0.017), including mSTG maturation in the model explained a non-significant 11.9% of the additional variance (p = 0.106). Added first, mSTG maturation predicted 43.9% of the variance (p = 0.004) and including age explained a non-significant 0.4% of additional variance in the model (p = 0.767).

For pSTG maturation, the full regression model (age and pSTG maturation) predicted 42.1% of the variance in GFP first-peak latency (p = 0.022). Although adding age as the first variable predicted 32.4% of the variance (p = 0.017), including pSTG maturation in the model explained a non-significant 9.7% of the additional variance (p = 0.147). Added first, pSTG maturation predicted 36.7% of the variance (p = 0.01) and including age explained a non-significant 5.5% of additional variance in the model (p = 0.269).

In the next step, we conducted partial correlation by performing linear regression analysis between the residuals of the global functional feature and structural features of the total WM, mSTG, and pSTG after regressing out the age effect (Fig. 4.3g, h and i, respectively). Although not significant, there was still a trend towards a negative correlation between the structure and function. We further examined whether the same tendency was visible in other parcels of the brain atlas. Table 4.3 presents the correlation coefficients and P values for the partial correlations conducted between the GFP latency and structural index of each brain region (Fig. 4.4) after regressing out the effect of age. None were significant and the correlation coefficients were generally less than those for the superior temporal regions (e.g. mSTG, pSTG). We also compared the two hemispheres. We assessed the partial correlation between the extracted global functional feature and the structural maturation indices of the left and right mSTG and pSTG, separately. Absolute values of the correlation coefficients were greater for the left mSTG (0.441) and pSTG (0.443) than right mSTG (0.373) and pSTG (0.294).

In the last step, we conducted hierarchical regression to examine the unique influence of the STG maturation (WM+GM, mSTG+pSTG) on the GFP first-peak latency after removing the effect of all other regions presented as the total WM maturation. While the total WM excluding the STG defined 28.6% of the variance (p = 0.027), including the STG maturation

explained the additional 16% of the variance which is close to significance (p = 0.064). This result presents the unique influence of the STG maturation on the GFP first-peak latency after removing the maturational effect of all other regions.

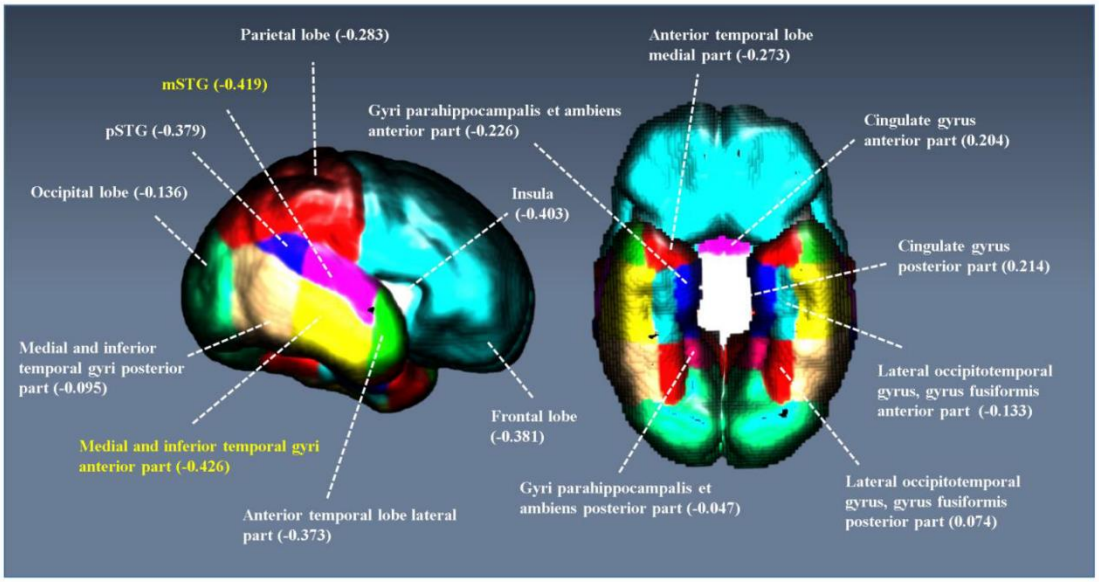

Figure 4.4: Results of the partial correlation (*r* value) between the functional feature and structural index of each ROI after regressing out the effect of age.

Table 4.2: Summary table of correlation results.

	Age (wGA)	GFP first peak latency (ms)
Age (wGA)		$R^2 = 0.311$, $p = 0.02$
Total GM maturation index	n.s.	n.s.
Total WM maturation index	$R^2 = 0.930$, $p < 0.001$	$R^2 = 0.290$, $p=0.026$
mSTG maturation index	$R^2 = 0.929$, $p < 0.001$	$R^2 = 0.439$, $p = 0.004$
pSTG maturation index	$R^2 = 0.915$, $p < 0.001$	$R^2 = 0.367$, $p = 0.01$

Table 4.3: Results of the partial correlation between the functional feature and structural index of each ROI after regressing out the effect of age.

ROIs	r	P-value *	Corrected P-value **
Medial and inferior temporal gyri anterior part	**-0.426**	**0.088**	**0.169**
Superior temporal gyrus middle part	**-0.419**	**0.094**	**0.178**
Insula	-0.403	0.108	0.200
Frontal lobe	-0.381	0.131	0.237
Superior temporal gyrus posterior part	-0.379	0.134	0.240
Anterior temporal lobe lateral part	-0.373	0.141	0.250
Parietal lobe	-0.283	0.271	0.412
Anterior temporal lobe medial part	-0.273	0.290	0.435
Gyri parahippocampalis et ambiens anterior part	-0.226	0.384	0.524
Occipital lobe	-0.136	0.603	0.698
Lateral occipitotemporal gyrus, gyrus fusiformis anterior part	-0.133	0.610	0.702
Medial and inferior temporal gyri posterior part	-0.095	0.718	0.771
Gyri parahippocampalis et ambiens posterior part	-0.047	0.859	0.839
Cingulate gyrus posterior part	0.214	n.m. ***	n.m.
Cingulate gyrus anterior part	0.204	n.m.	n.m.
Lateral occipitotemporal gyrus, gyrus fusiformis posterior part	0.074	n.m.	n.m

* Before multiple comparison correction
** After multiple comparison correction
*** Not meaningful; Since the correlation between GFP first peak latency and myelination of this region is positive, it does not suit for further analysis.

4.4 Discussion

Here, we observed a number of associations between structural maturation, electrophysiological function, and age, which support a biophysical model of developmental changes in the auditory system of preterm infants. Myelination of the human brain begins early, from the second half of pregnancy, and lasts to the end of adolescence, with a peak during the first post-natal year (Van der Knaap and Valk 1995a, b; Baumann and Pham-dinh 2001). The formation and progression of myelination vary across cerebral regions, with a progressive trend from the center to the periphery, and earlier and more rapid occurrence in sensory (somatosensory, vision, audition) than motor pathways (Yakovlev and Lecours 1967; Brody et al. 1987; Kinney et al. 1988; Baumann and Pham-dinh 2001). Myelination along the cochlear nerve and within the auditory brainstem occurs almost at the onset of hearing and the auditory cortex and associated WM tracts experience a pattern of myelination that is simultaneous with language acquisition, suggesting a significant interaction between auditory experience, auditory circuit maturation, and myelination (Long et al. 2018).

Several maturational processes occur throughout development of the preterm infant's brain, including microstructural organization of the cortical plate and subplate, evolution of the

membranes, connectivity, cortical folding, synaptic bursting, pruning, etc. All of these processes may affect neuronal conduction velocity, but the main factor that contributes to the acceleration of ERP latencies is certainly the establishment of myelination around neuronal axons. The mean value of T1w/T2w ratio images in each ROI, is considered in adults (Glasser and Van Essen 2011; Grydeland et al. 2013; Iwatani et al. 2015), children (Grydeland et al. 2013), and infants (Lee et al. 2015) to be an estimate of myelination. Although it may also be sensitive to other maturational processes in preterm infants, it can be considered as a myelination proxy during the age range of our study.

It is worth mentioning that although the myelination index is highly correlated with age in some regions (e.g. mSTG and pSTG), it is not the case for other regions (e.g. Gyri parahippocampalis et ambiens posterior part). This confirms the different myelination profiles of different brain regions in the age-range of our study. When investigating the variations in the functional feature, we should be able to distinguish between the effects of myelination index and age. Analyzing the effect of age involves implicitly all the underlying maturational processes such as the microstructural organization of the cortical plate and subplate, evolution of the membranes, connectivity, cortical folding, synaptic bursting, pruning, etc as well as myelination. However, when we investigate the effect of the proposed maturation index, we only consider the impact of myelination on the functional feature. Therefore, it is valuable to know how much of the variation in the functional feature is caused by the myelination index and how much is influenced by the age as a more comprehensive feature.

Cortical brain development can be studied in preterm infants who now survive when born after 28 wGA and even 23 wGA, as a result of intensive care (Mahmoudzadeh et al. 2017). The auditory system is already operative at this early age (Copriviza and Lima 1984) and CAEPs have been recorded from 27 wGA (Rotteveel et al. 1987), with differences in wave amplitude and latency as a function of age (Weitzman and Graziani 1968; Rotteveel et al. 1987). The progressive maturation of the peripheral nerves certainly participates in the acceleration of ERP latencies, but also cortical maturation. Hierarchical regression allowed us to examine the factors affecting the variance in the latency of the GFP first-peak. Maturation index and age, both highly inter-correlated in auditory areas, accounted for no significant additional variance in the GFP first-peak latency after one of these factor was entered in the analysis. Thus, we were not able to isolate a specific effect in typically developing preterm neonates. Adding new regions did not change the main result: age, myelination of auditory areas and the latency of the GFP first peak are related indices of auditory system maturation at this period of development.

Roberts et al. (2009) have also observed in children that the decrease in latency of the left and right STG auditory responses was correlated with the increase in fractional anisotropy (FA) in the acoustic radiations, reflecting their maturation. Applying hierarchical regression analysis, these authors observed that both age and FA predict similar amount of variance in the latency of the auditory responses. In infants, a few other studies have investigated the relations between microstructure in the superior temporal regions and language development. Aeby et al. (2013) showed that language development at two years of age correlates with brain microstructure in the left STG at the term-equivalent age. Their findings suggested that higher mean, longitudinal, and transverse diffusivities at term-equivalent age in the left STG were associated with poorer language scores in later childhood. Salvan et al. (2017) also reported associations between the linguistic performance of two-year-old preterm-born infants and arcuate fasciculi microstructure at term. For a systematic review of the relationships between language outcome and underlying brain structures in school-aged preterm-born children, the reader may refer to (Stipdonk, Franken, and Dudink 2018). Correlational measures between language scores and brain volume or FA of specific brain structures were extracted in the publications reviewed in this study. It should be noted that in these studies as in ours, the measures are only correlational and many other factors such as intra-uterine growth, gestational age at birth, socio-economic level, and parental education may affect inter-individual variability (Dubois et al. 2016). Thus, characterizing the maturation of this pathway in preterm infants, and inter-infants variability is crucial to understand the long-term effects of premature birth. Future studies controlling these factors are needed to build robust biomarkers for detecting early deviations in developmental trajectories related to perinatal disorders or diseases (Dubois et al. 2016).

Our study, in which we attempted to relate structure and function, opens the way to detecting early deviations related to perinatal disorders or diseases. Because EEG is much easier to perform in neonatal units than the transfer of neonates to an MRI, understanding how ERP latencies are related to brain areas and their maturation, or lesions, would represent tremendous progress towards the investigation and monitoring of the developing brain in daily care in neonatal units.

Limitations are here that we did not have each infant anatomical MRI and relied on an atlas with representative images of each age. It is thus already surprising that we obtained significant correlations and illustrates the fact that the brain is changing from week to week. When using the atlas, we claim that we provide the structural feature representative for each wGA to correlate with the functional feature of that specific wGA, although not extracted

from the same subjects. This might be inferred as studying general developmental changes of the preterm brain, rather than measuring the variations at the individual level. Obviously, investigating the functional and structural correlations of the developing brain within the same infant would be much more powerful and provides the opportunity to study how individual variations in the structural maturation account for individual functional differences. It is worth noting that generally using the atlas is justified if and only if between-subject variability in the maturation index is smaller than the variation due to the age. In our study, we had no access to parcellated images of individual preterm infants to check for individual variations in the maturation index. However, there are some facts which justify that the index is more affected by age than the subjects' variability. The maturation index is related to the myelination, which is affected significantly by age at early stages of development (Lee et al. 2015; Adibpour et al. 2019; Van der Knaap and Valk 1995a, b; Baumann and Pham-dinh 2001). Furthermore, the index is a relative value. If we were able to extract the feature for each individual subject, the T1 intensity of a subject would be divided by T2 intensity of the same subject, which is somehow similar to a normalization reducing the between-subject variability. Regarding the between-subject variability in the geometry, although there might be differences in defining the brain regions, the ratio intensity values would be averaged for each ROI, which reduces the effect of difference in gerometry.

4.5 Conclusion

In this study, we attempted to relate developmental changes of the latency of CAEPs to a structural maturation index, presumed to be representative of myelination. The observed associations between structural maturation, electrophysiological function, and age, support a biophysical model of developmental changes in the auditory system of preterm infants. The findings may help detect early deviations in the functional or structural development related to perinatal disorders or diseases.

Acknowledgement

This work was supported by the Picardie regional council (Hemisphere Nord), by EGIDE France and CISSC Iran under the grant number 961/93-9-2 (Jundi Shapour scientific collaboration program) and by the Co-tutelle program of the French Embassy in Tehran for Ph.D. students. It was also partially supported by COGC, Iran in the framework of the Neurobiom project under grant number 96P97.

4.6 References

Adibpour P et al (2019) Anatomo-Functional Correlates of Auditory Development in Infancy. bioRxiv.

Adibpour P, Dubois J, Dehaene-Lambertz G (2018) Right but Not Left Hemispheric Discrimination of Faces in Infancy. Nature Human Behaviour 2: 67–79. http://dx.doi.org/10.1038/s41562-017-0249-4.

Aeby A et al (2013) Language Development at 2 Years Is Correlated to Brain Microstructure in the Left Superior Temporal Gyrus at Term Equivalent Age : A Diffusion Tensor Imaging Study. NeuroImage 78: 145–51. http://dx.doi.org/10.1016/j.neuroimage.2013.03.076.

Alho K et al (1990) Event-related Brain Potential of Human Newborns to Pitch Change of an Acoustic Stimulus. Electroencephalogr Clin Neurophysiol 77: 151–55.

Baumann N, Pham-dinh D (2001) Biology of Oligodendrocyte and Myelin in the Mammalian Central Nervous System. Physiol Rev 81: 871–927.

Bisiacchi PS, Mento G, Suppiej A (2009) Cortical Auditory Processing in Preterm Newborns: An ERP Study. Biological Psychology 82: 176–85.

Brody B, Kinney H, Kloman A, Gilles F (1987) Sequence of Central Nervous System Myelination in Human Infancy . I . An Autopsy Study of Myelination. J Neuropathol Exp Neurol 46: 283–301.

Cheour M et al (2002) Electric Brain Responses Obtained from Newborn Infants to Changes in Duration in Complex Harmonic Tones. Dev Neuropsychol 22: 471–79.

Cheour-Luhtanen M et al (1996) The Ontogenetically Earliest Discriminative Response of the Human Brain. Psychophysiology 33: 478–481.

Copriviza KL, Lima CG (1984) Auditory Arousal in Preterm Infants. NSSLHA 11: 3–9.

Daneshvarfard F et al (2019) Neurodevelopment and Asymmetry of Auditory-Related Responses to Repetitive Syllabic Stimuli in Preterm Neonates Based on Frequency-Domain Analysis. Scientific Reports 9:10654.

Dockstader C, Gaetz W, Rockel C, Mabbott DJ (2012) White Matter Maturation in Visual and Motor Areas Predicts the Latency of Visual Activation in Children. Hum Brain Mapp 33: 179–91.

Draganova R et al (2007) Serial Magnetoencephalographic Study of Fetal and Newborn Auditory Discriminative Evoked Responses. Early Hum Dev 83: 199–207.

Dubois J et al (2016) MRI and M / EEG Studies of the White Matter Development in Human Fetuses and Infants : Review and Opinion. Brain Plast 2: 49–69.

Dubois J et al (2008) Microstructural Correlates of Infant Functional Development : Example of the Visual Pathways. J Neuros 28: 1943–48.

Glasser MF, Van Essen DC (2011) Mapping Human Cortical Areas In Vivo Based on Myelin Content as Revealed by T1- and T2-Weighted MRI. J Neurosci 31: 11597–616.

Graziani LJ, Katz L, Weitzman ED (1974) The Maturation and Interrelationship of EEG Patterns and Auditory Evoked Responses in Premature Infants. Electroencephalogr Clin Neurophysiol 36:367–75.

Grydeland H et al (2013) Intracortical Myelin Links with Performance Variability across the Human

Lifespan : Results from T1- and T2- Weighted MRI Myelin Mapping and Diffusion Tensor Imaging. J Neurosci 33: 18618–30.

Holst M (2005) Development of Auditory Evoked Fields in Human Fetuses and Newborns: A Longitudinal MEG Study. Clin Neurophysiol 116: 1949–1955.

Iwatani J et al (2015) Use of T1-Weighted / T2-Weighted Magnetic Resonance Ratio Images to Elucidate Changes in the Schizophrenic Brain. Brain Behav 5: 1–14.

Kinney HC, Brody BA, Kloman AS, Gilles FH (1988) Sequence of Central Nervous System Myelination in Human Infancy II . Patterns of Myelination in Autopsied Infants. J Neuropathol Exp Neurol 47: 217–34.

Van der Knaap MS, Valk J (1995a) Myelin and White Matter. In: Van der Knaap MS, Valk J (ed) Magnetic Resonance of Myelin, Myelination and Myelin Disorders. Springer- Verlag, Berlin.

Van der Knaap MS, Valk J (1995b) Myelination and Retarded Myelination. In: Van der Knaap MS, Valk J (ed) Magnetic Resonance of Myelin, Myelination and Myelin Disorders. Springer-Verlag, Berlin.

Kushnerenko E et al (2001) Central Auditory Processing of Durational Changes in Complex Speech Patterns by Newborns: An Eventrelated Brain Potential Study. Dev Neuropsychol 19: 83–97.

Lee K et al (2015) Early Postnatal Myelin Content Estimate of White Matter via T1w / T2w Ratio. Proc SPIE Int Soc Opt Eng 9417: 1–7.

Long P, Wan G, Roberts MT, Corfas G (2018) Myelin Development, Plasticity, and Pathology in the Auditory System. Dev Neurobiol 78: 80–92.

Mahmoudzadeh M et al (2013) Syllabic Discrimination in Premature Human Infants Prior to Complete Formation of Cortical Layers. PNAS 110: 4846–51.

Mahmoudzadeh M et al (2017) Functional Maps at the Onset of Auditory Inputs in Very Early Preterm Human Neonates. Cereb Cortex 27: 2500–2512.

Makropoulos A et al (2014) Automatic Whole Brain MRI Segmentation of the Developing Neonatal Brain. IEEE T MED IMAGING 33: 1818–31.

Makropoulos A et al (2016) Regional Growth and Atlasing of the Developing Human Brain. NeuroImage 125: 456–78. http://brain-development.org/brain-atlases/multi-structural-neonatal-brain-atlas/.

"Neonatal Structural Atlas – Brain Development." http://brain-development.org/brain-atlases/multi-structural-neonatal-brain-atlas/.

Novitski N et al (2007) Neonatal Frequency Discrimination in 250–4000 Hz Range: Electrophysiological Evidence. Clin Neurophysiol 118: 412–419.

Price D et al (2017) Age-Related Delay in Visual and Auditory Evoked Responses Is Mediated by White- and Grey-Matter Differences. nature communications 8:15671.

Roberts TP et al (2009) Developmental Correlation of Diffusion Anisotropy with Auditory-Evoked Response. Neuroreport 20: 1586–91.

Rotteveel JJ et al (1987) The Maturation of the Central Auditory Conduction in Preterm Infants until Three Months Post Term . V . The Auditory Cortical Response (ACR). Hear Res 27: 95–110.

Salvan P et al (2017) Language Ability in Preterm Children Is Associated with Arcuate Fasciculi

Microstructure at Term. Human Brain Mapping 38: 3836–47.

Skrandies W (1990) Global Field Power and Topographic Similarity. Brain Topogr 3: 137–41.

Stipdonk LW, Franken MJP, Dudink J (2018) Language Outcome Related to Brain Structures in School-Aged Preterm Children : A Systematic Review. PLoS ONE 13: e0203298. http://dx.doi.org/10.1371/journal.pone.0196607.

Stufflebeam SM et al (2008) A Non-Invasive Method to Relate the Timing of Neural Activity to White Matter Microstructural Integrity. Neuroimage 42: 710–16.

Weitzman WD, Graziani LJ (1968) Maturation and Topography of the Auditory Evoked Response of the Prematurely Born Infant. Psychobiol 1: 79-89.

Yakovlev PI, Lecours AR (1967) The Myelogenetic Cycles of Regional Maturation in the Brain. In: Minowski A (ed) Regional Development of the Brain in Early Life. Blackwell, Oxford, pp 3–69.

Chapter 5

Conclusion

In an attempt to investigate functional and structural development of the human brain, we employed non-invasive neuroimaging techniques, such as EEG and MRI, to study the neural correlates of speech processing, investigate lateralization of the CAEPs in response to syllabic stimuli and explore the correlations between developmental changes of the functional and structural features of the auditory system, in premature neonates. We started by presenting various studies, investigating age-related changes of the human brain at different periods of life, in both functional and structural characteristics. Functional and structural features extracted in different studies were introduced and their age-dependent variations were reported at different ages. In the next step, we presented the focus of our study which is based on the study of the preterm infants' brain. Therefore, we established some of the basics regarding the dynamics of the functional and structural development in premature neonates, as well as the functional and structural interaction in the early stages of development. Previous studies in these fields were reviewed and discussed. Specifically, we highlighted the studies which assessed both the functional and anatomical points of view, through measures that have developmental relevance (i.e. latency of the evoked responses recorded with EEG, and DTI measures sensitive to the myelination).

In Chapter 2 all the materials and methods necessary for our analyses were elaborated. Chapters 3 and 4 were dedicated to the analyses, results and discussion. Hereafter, the importance of monitoring the normal development of the preterm brain is presented. Moreover, the findings of the studies presented in Chapter 3 and 4 are summarized and discussed very briefly. Furthermore, the challenges and limitations of our studies are mentioned which may be helpful in designing future studies.

Preterm infants, even born as early as 23 wGA, may survive if taken under intensive care [88]. Many of the structural and functional capabilities of the brain, observed in later months of development, are proved to be already matured in the normal healthy preterm neonates. Monitoring the normal development of the preterm brain, is therefore, of great interest in both

functional and structural aspects. ERP can be used as an appropriate tool to non-invasively characterize the normalcy of brain activities according to age and identify early dysfunctions. On the other hand, MR imaging has become a popular modality for investigating normal structural development and pathological deviations due to its non-ionizing radiation and soft tissue differentiation. Analysis of the ERPs and MR images of the preterm infants, provides insights on the functional and structural maturation of the brain at each wGA.

In the current thesis, we analyzed both the CAEPs and MR images of the preterm infants to investigate developmental changes. Our study, could be divided into two main parts. In the first part (Chapter 3), we analyzed the CAEPs of the preterm infants (29.57 to 34.14 wGA) in response to repetitive syllabic stimuli in the frequency domain. We investigated developmental changes, as well as the asymmetry of the functional responses of the preterm brain based on the extracted frequency features. We observed significant positive correlations between the age and the amplitude and PC value at the target frequency. These observations were consistent with the structural mechanisms that occurred at this period of development, including the increase of synchronization within a larger population of neurons, resulting in more clearly defined evoked potentials relative to the background noise. Furthermore, we reported a rightward asymmetry for the amplitude at the target frequency, which is consistent with the results reported previously for other age ranges.

In the second part of our analyses, we focused on investigating the correlations between the functional and structural aspects of the preterm infants' brain development. To be more specific, we tried to relate developmental changes of the CAEPs (in the form of a decrease in the GFP first-peak latency) to the structural maturation index related to myelination. We presented the specificity of the interaction between the global functional feature and structural myelination index of auditory-involved areas extracted from MR images of the infants at the same age. Therefore, a functional-structural relationship characteristic of typically developing preterm neonate is presented by our study which is the first, as far as we know, focusing on the joint functional and structural development of the auditory-involved areas in preterm infants.

Most of the neonatal language researches concerns how the infants' brain acquires and learns different aspects of the language. Although some of the features are already present in the even early-born preterm infants, the experience is crucial to maintain them and to learn the specific properties of a language. The study of Mahmoudzadeh et al. [201] on preterm infant's (28-32 wGA) speech perception showed how the immature brain processes syllabic information. Their results demonstrated that particular regions of the cortex, critical for

language acquisition and processing, contain inherent language-specific representations in early infancy. In the current thesis, we used the same repetitive syllabic stimuli as [201], to further investigate the capability of the preterm brain to follow the rhythmicity of the external ecological stimuli. Our findings showed that the preterm brain is able to follow the syllabic-rate modulation with rightward lateralization, a functionality observed previously in adults, children and newborns.

Analyzing ERPs of preterm infants is challenging due to the inherent characteristics of the EEG at this early period of development. The origin of the ERPs in prematures is unknown and they present different shapes and different maxima compared to what is observed later during the development. This should be considered in analyzing ERPs of preterms with the main purpose of finding the amplitude and latencies of the components. In addition, the EEG background activity on which ERPs are superimposed induces a kind of background noise which necessitates increasing considerably the number of trials. This is probably one of the main problems making the studies on preterms very difficult, specifically before 35 wGA [201]. Our idea of analyzing the preterms' ERPs in the frequency domain (Chapter 3), or extracting a global feature (Chapter 4) which is less influenced by the variabilities of the individual electrodes, may help in overcoming the inherent variability of the preterm ERPs.

In our structural analysis, we focused on the myelination and correlated structural and functional features that have developmental relevance based on the common underlying biological phenomenon of myelination. However, this type of structure-function relationship is restricted regarding the fact that myelination is only one of the several aspects of brain development. Several maturational processes affect the development of the preterm infant's brain, including microstructural organization of the cortical plate and subplate, the evolution of the membranes, connectivity, cortical folding, synaptic bursting, pruning, etc. We should notice that all of these processes may influence the conduction velocity. However, the myelination plays a key role in learning and cognitive development, increasing the speed of neural information transmission and thus accelerating the ERP latencies. Therefore, studying the structural maturation related to the myelination and its functional counterpart might be helpful in clarifying some aspects of cognitive development. It is also noteworthy to mention that our estimate of myelination (i.e. the mean values of the T1w/T2w ratio image in each ROI) may also be sensitive to other maturational processes in preterm infants. Nevertheless, it may still be considered as a structural maturation index, with significant changes during the age range of our study.

In our joint structural and functional study, we observed some associations between the structural maturation, electrophysiological function, and age of the preterm infants supporting a biophysical model of developmental changes in their auditory system. However, although our study and those of others report some associations between certain structures and functions, it should be noted that it is not possible to relate a specific structure to a determined function since many structures are involved in each specific functional task. Furthermore, we should notice that we may not determine which the cause is and which the consequence is for these sorts of relationships. Specifically, in the study of prematures, several other factors may affect inter-individual variability among infants, such as intra-uterine growth and gestational age at birth. Therefore, characterizing individual differences in the anatomical and functional behavior of the infants is challenging. Further studies controlling these factors may provide robust biomarkers for detecting early deviations in developmental trajectories related to perinatal disorders or diseases. As we described in Chapter 4, we used MR templates of a neonatal atlas provided for each week of GA to correlate with our functional data. Although acquiring structural and functional data of the same preterm infant at the same time is very difficult, the comparison of anatomo-functional changes across modalities within the same subjects is recommended to characterize the development of auditory brain networks more accurately. In our joint structural and functional analysis, we focused on the relationship between the GFP first peak latency and myelination. In future, we may aim to extract some other functional and structural features form the ERPs and MRIs to investigate the presence of other types of correlation between the structure and function of the infants at this period of development. Furthermore we may apply more sophisticated correlation and regression approaches such as non-linear analysis to investigate the relation between the structure and function.

Chapter 6

French summary

6.1 Introduction

Le développement du cerveau humain, en tant que processus dynamique, débute avant la troisième semaine de la vie fœtale et se poursuit tout au long de la vie. Les changements du cerveau humain liés à l'âge peuvent être étudiés d'un point de vue structurel ou fonctionnel. Alors que la première approche concerne les modifications géométriques, dimensionnelles et anatomiques du cerveau avec l'âge, les modifications des comportements, des sorties et des réponses neurologiques à différents stimuli endogènes ou exogènes au cours du développement sont prises en compte dans l'approche fonctionnelle.

Diverses études ont examiné séparément les modifications structurelles et fonctionnelles du cerveau humain liées à l'âge. Les caractéristiques fonctionnelles extraites étudiées pour les variations dépendant de l'âge incluent l'amplitude maximale et la latence des réponses évoquées auditives, les caractéristiques dans le domaine fréquentiel et les mesures de connectivité fonctionnelle. Les caractéristiques structurelles peuvent inclure le volume cortical, la surface, l'épaisseur, la gyrification et l'indice de repliement, l'indice de myélinisation ou les mesures de connectivité structurelle. De nombreuses études ont présenté des tendances de développement pour différentes caractéristiques fonctionnelles et structurelles du cerveau humain à différentes périodes de la vie. Cependant, seules quelques études se sont intéressées aux changements conjoints structuraux et fonctionnels. Une question clé, bien que difficile, dans l'étude du neurodéveloppement est de savoir comment ces changements fonctionnels et structuraux s'affectent l'un l'autre. En d'autres termes, comment les changements structuraux dans le cerveau conduisent à l'amélioration des fonctions cognitives au cours du développement. Plusieurs études ont été consacrées aux changements cérébraux structuraux et fonctionnels à différentes périodes de la vie, y compris aux premiers stades de développement, mais il existe peu de publications sur l'analyse simultanée du développement structurel et fonctionnel chez le nouveau-né prématuré.

Les bébés prématurés peuvent survivre après 23 wGA, du fait de l'amélioration des prises en charges dans les unités de soins intensifs [88]. Il a été prouvé que de nombreux aspects structurels et fonctionnels du cerveau sont déjà matures chez les prématurés en bonne santé. La surveillance des modifications développementales du cerveau prématuré présente donc un grand intérêt, tant du point de vue fonctionnel que structurel. Les réponses de potentiels de évoqués (ERPs) constituent un outil approprié pour caractériser de manière non invasive la normalité des activités fonctionnelles du cerveau en fonction de l'âge, et l'IRM est devenue une approche populaire pour étudier le développement structurel normal du fait de ses rayonnements non ionisants.

Le système auditif humain est opérationnel dès le plus jeune âge et les potentiels évoqués auditifs corticaux (CAEP) sont enregistrés dès 27 WGA [56]. Bien que plusieurs études se concentrent sur les caractéristiques temporelles des réponses corticales des nouveau-nés prématurés, peu ont été menées sur l'analyse de ces réponses dans le domaine fréquentiel. Dans la thèse actuelle, le développement des CAEP mis en jeu par des stimuli syllabiques répétitifs est étudié chez les nouveau-nés prématurés sur la base d'une 'analyse dans le domaine fréquentiel. Pour mieux caractériser la latéralisation fonctionnelle des réponses cérébrales chez le prématuré dans le traitement des informations auditives, nous avons évalué la latéralisation des réponses à une tâche auditive répétitive spécifique.

Pour étudier les corrélats fonctionnels et structurels du cerveau du prématuré, les CAEP ont été analysés de manière à extraire le premier temps de latence maximal de la puissance du champ électrique global (Global Field Power, GFP), en tant que caractéristique fonctionnelle. Les images IRM ont été analysées pour extraire un indice de maturation lié à la myelinisation considéré comme caractéristique structurelle. Nous avons ensuite cherché à corréler les caractéristiques structurelles et fonctionnelles ayant une pertinence pour le développement, selon l'hypothèse d'unphénomène biologique sous-jacent commun que serait la myélinisation.

6.2 Neurodéveloppement et asymétrie des réponses auditives liées à des stimuli syllabiques répétitifs chez les nouveau-nés prématurés sur la base d'une analyse du domaine fréquentiel

6.2.1 Participants, stimuli et enregistrements

Les signaux EEG de 16 nouveau-nés prématurés dont l'âge moyen au moment de l'enregistrement était de 31.48 wGA (29.57 à 34.14 semaines), recrutés dans notre étude précédente [88], ont été réanalysés aux fins de la présente étude. Tous les nourrissons avaient

un poids de naissance, une taille et un tour de tête appropriés pour leur terme. L'électroencéphalogramme était considéré comme normal pour l'âge gestationnel. Les enfants étaient considérés à faible risque de lésions cérébrales sur la base d'évaluations neurologiques auditives et cliniques normales. Un consentement éclairé écrit a été fourni par les parents des nourrissons et l'étude a été approuvée par le comité d'éthique local (CPP Nord-Ouest II) de l'hôpital universitaire d'Amiens, conformément aux directives de la déclaration d'Helsinki de 1975 (réf. ID-RCB 2008-A00728- 47).

Les stimuli consistaient en quatre syllabes (/ ba / et / ga /, produites par des locuteurs masculins et féminins) présentées à un niveau d'audition confortable (70 dB) via des haut-parleurs placés aux pieds du nourrisson [88] [101]. Les syllabes ont été appariées pour l'intonation, l'intensité, la durée totale (285 ms), la prévision et la durée de transition du formant exprimé (40/45 ms). Elles ont été présentées en séries de 4, espacées chacune de 600 ms. Cinq séries séparées par 1600 ms de silence constituaient un bloc. Chaque bloc durait 20 secondes et était suivi de 40 secondes de silence. Dans chaque bloc, la syllabe répétée a été choisie au hasard parmi les 4 syllabes possibles. Cette présentation avait été appliquée dans notre précédente étude pour évaluer la discrimination syllabique chez les prématurés [88] [101]. Alors que dans les essais standards, la même syllabe était répétée quatre fois, dans les essais déviants, la dernière syllabe différait des trois premières en termes de voix ou de dimension phonétique. Bien que différente du paradigme classique ASSR, cette présentation régulière a permis d'étudier la capacité du cerveau prématuré à suivre des stimulations écologiques externes. Par conséquent, seules les réponses enregistrées correspondant aux essais standards ont été utilisées dans cette partie de l'étude pour une analyse plus poussée.

Les signaux EEG ont été enregistrés en utilisant des électrodes de surface Ag / AgCl et une référence nasion. La fréquence d'échantillonnage était de 2048 Hz et les signaux étaient amplifiés par A.N.Ts (Enschede, Pays-Bas) et filtrés à DC-50 Hz. L'impédance des électrodes a été maintenue au-dessous de 5 kΩ et le nombre des électrodes (31 à 61) a été déterminé en fonction du tour de tête du nouveau-né prématuré. Un minimum de 31 électrodes ont été placées selon le système 10-20 pour tous les nouveau-nés prématurés et des électrodes supplémentaires ont été placées sur des positions intermédiaires en fonction du tour de tête des enfants.

Les signaux enregistrés ont été filtrés par un filtre passe-bande entre 1 et 20 Hz et sous-échantillonnés à 512 Hz. Ils ont été segmentés en époques ([−0.5 + 2.7 s]) liés à la première syllabe (S1) de l'essai, fournissant 180 essais standard pour chaque électrode d'enregistrement pour chaque sujet. La ligne de base des essais a ensuite été corrigée (200 ms avant le début de

S1). Une procédure automatique de rejet d'artefacts a été appliquée comme suit. Chaque essai était rejeté si son amplitude absolue dépassait 50 µV ou lorsqu'un saut d'amplitude local entre dix instants successifs dépassait 30 µV. Il restait en moyenne 156 essais pour chaque enfant et chaque électrode après exclusion de l'artefact.

6.2.2 Analyses de fréquence, de cohérence et d'asymétrie

Les réseaux corticaux étant exposés à une syllabe toutes les 600 ms, nous nous attendions à un pic distinctif aux alentours de 1.6 Hz et à ses harmoniques. La réponse temporelle correspondant à l'intervalle de temps des essais après correction de la ligne de base ([0 + 2.7 s]) a été transformée dans le domaine fréquentiel à l'aide de la FFT. Nous avons ensuite mesuré les amplitudes maximales du spectre de la FFT à la fréquence cible et à sa première harmonique, et testé l'effet de l'âge sur cette mesure. Les amplitudes du spectre FFT à la fréquence cible et à sa première harmonique ont été extraites pour chaque sujet et chaque électrode et moyennées sur les 15 canaux (Fz, F1, F2, F3, F4, C1, C2, CP1, CP2, Pz, P1, P2, Oz, O1 et O2) pour tous les sujets.

Nous avons appliqué la cohérence de phase (PC) en tant que caractéristique fréquentielle complémentaire pour étudier la réponse des prématurés à la stimulation auditive. Le calcul de la cohérence de phase nécessite la segmentation du CAEP en plusieurs sous-moyennes. Les sous-moyennes sont ensuite transformées dans le domaine fréquentiel à l'aide de la FFT. Dans la présente étude, une moyenne de séries de 10 essais a été établie, fournissant plusieurs sous-moyennes indépendantes du total des essais disponibles pour chaque électrode de chaque sujet. Chaque forme d'onde moyennée a été soumise à une analyse spectrale FFT. La PC a été déterminée au moyen de l'équation suivante:

$$PC = [\left(\frac{1}{n}\sum cos\Phi_i\right)^2 + \left(\frac{1}{n}\sum sin\Phi_i\right)^2]^{1/2} \quad (6.1)$$

où Φi est l'angle de phase de la composante de Fourier de la ième sous-moyenne et n le nombre de sous-moyennes. PC varie entre 0 et 1, ce qui est directement proportionnel à la variabilité. Il estime le degré de dispersion ou de regroupement des phases à chaque fréquence. Plus les phases moyennes sont identiques, plus la valeur PC tend vers un. La valeur de PC à la fréquence cible de la réponse auditive a été testée pour sa dépendance par rapport à l'âge. Nous choisissons la valeur de PC à la fréquence cible, car elle constitue le pic

le plus significatif pour lequel la réponse est mieux adaptée aux stimuli et pour laquelle la cohérence devrait être maximale.

Un coefficient d'asymétrie fonctionnel a été défini comme un indice de latéralisation, LI = (Droite-Gauche) / (Droite + Gauche), pour la caractéristique la plus saillante, l'amplitude de la fréquence syllabique cible, à chaque site d'électrode et soumise à un test t. La valeur normalisée, Droite / (Droite + Gauche) ou Gauche / (Droite + Gauche), est moins influencée par la variabilité intersubjective liée à la maturation auditive individuelle. Par conséquent, il fournit une mesure plus sensible que les indices d'origine (gauche ou droite) pour la comparaison statistique des activités des hémisphères droit et gauche. Le nombre de mesures répétées a été corrigé avec la correction du taux de fausse découverte (FDR).

6.2.3 Résultats

Les réponses temporelles ainsi que les spectres de FFT et de cohérence de phase pour une électrode droite (F4) et pour une électrode gauche (F3) sont illustrés à la Fig. 6.1 pour un nouveau-né (30 semaines et 4 jours d'AG). Comme prévu, des pics distincts ont été observés à la fréquence cible et à la première harmonique.

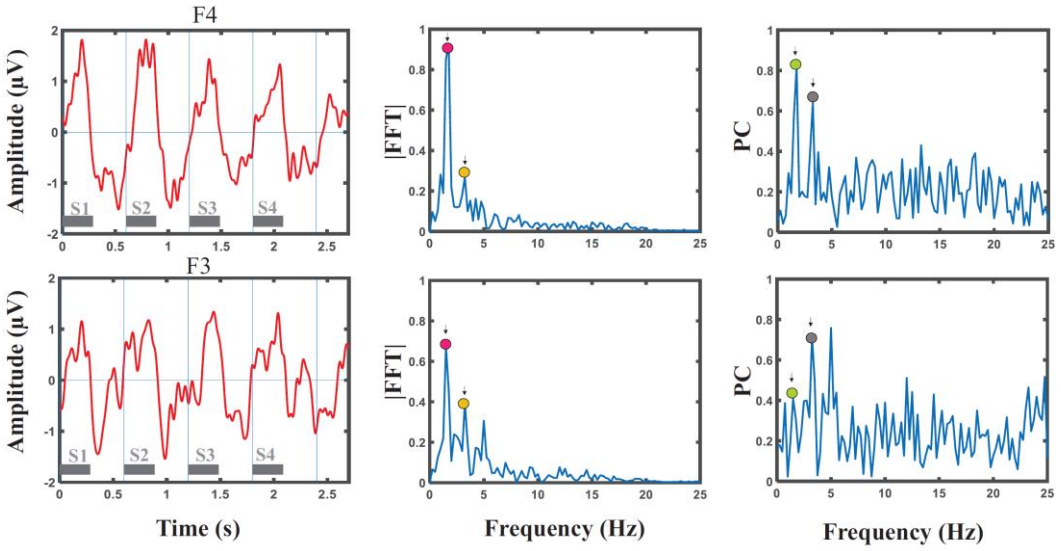

Figure 6.1: Réponses temporelles, spectres FFT et PC pour un nouveau-né (30 semaines et 4 jours d'AG) sur une électrode droite (F4, rangée supérieure) et une gauche (F3, rangée inférieure). Les amplitudes de crête correspondant à la fréquence cible et à la première harmonique sont marquées dans les spectres FFT et PC.

Une augmentation globale des amplitudes du spectre FFT à la fréquence cible et à son harmonique ont été observée avec l'âge, représentée par une corrélation positive entre amplitude et âge, significative à la fréquence cible (R^2 = 0.263, p = 0.042), mais pas à la première harmonique (R^2 = 0.156, p = 0.13). Un effet de l'âge (R^2 = 0.318, p = 0.023) a

également été observé pour la cohérence de phase moyennée sur les 15 canaux de chaque prématuré.

Des cartes topographiques de l'amplitude des pics des réponses à la fréquence cible, et à la première harmonique et du PC à la fréquence cible ont été créées pour fournir la distribution des caractéristiques extraites. Ils présentaient un motif asymétrique qui nous incitait à examiner l'asymétrie de manière plus détaillée.

Les coefficients d'asymétrie ont été calculés pour chaque paire d'électrodes disponibles en faisant la moyenne des valeurs de LI entre les sujets (figure 6.2.a). Nous avons effectué une analyse t-test unilatérale. Des cercles rouges ont été attribués aux zones auditives marquées par un fort biais vers la droite (valeurs p corrigées: P6-P5: p <0.001, C6-C5: p = 0.029, C4-C3: p = 0.045, F6-F5: p = 0.043, Fc2-Fcl: p = 0.043). La taille de l'effet des différences entre les moyennes des canaux appariés a également été calculée comme suit: d de Cohen (P6-P5: d = 2.080, C6-C5: 1.343, C4-C3: 0.779, F6-F5: 0.859, Fc2-Fc1: 0.836). De plus, nous avons vérifié la latéralité dans la direction opposée. Bien que Af4-Af3 (d = -1.012) et Cp4-Cp3 (d = -0.828) aient présenté des valeurs de p inférieures à 0,05, ils n'ont montré aucune latéralisation à gauche significative après correction du FDR. Enfin, nous n'avons pas observé de variations de l'indice de latéralisation avec l'âge dans la tranche d'âge considérée dans la présente étude.

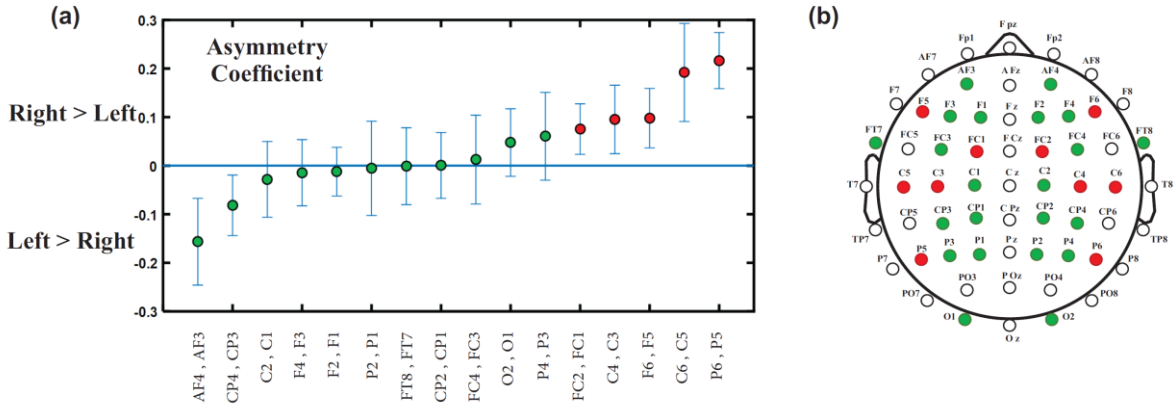

Figure 6.2: (a) Coefficients d'asymétrie calculés comme la moyenne des valeurs de LI sur les sujets pour chaque paire d'électrodes disponibles. Les barres d'erreur indiquent l'erreur standard, (b) L'emplacement des paires d'électrodes disponibles sur la tête. Les électrodes avec des biais vers la droite sont marquées par des cercles rouges dans les deux figures. Les cercles verts indiquent les paires de canaux sans biais vers la droite. Les cercles blancs correspondent aux paires de canaux non étudiés en raison de l'insuffisance des données disponibles.

6.2.4 Discussion

Des analyses de fréquence et de cohérence de phase des CAEP ont été effectuées chez les prématurés très jeunes afin d'évaluer les caractéristiques temporells des réponses neuronales du réseau auditif immature. Dans la tranche d'âge considérée dans notre étude (29.57 à 34.14 wGA), les neurones rejoignent leurs emplacements cibles et génèrent de nombreuses connexions dans la plaque corticale [162]. Cette synaptogenèse neuronale fournit la base d'une synchronisation accrue au sein d'une population plus large de neurones, ce qui participe à la possibilité d'extraire plus clairement les potentiels évoqués du bruit de fond. Ce mécanisme constitue la base structurelle des corrélations positives significatives observées entre l'âge et l'amplitude et la valeur du PC à la fréquence cible. L'augmentation de la cohérence de phase (PC) révèle que la réponse neuronale est de plus en plus conforme au stimulus, tandis que l'augmentation de l'amplitude pourrait être liée au nombre de neurones et à leurs capacités de synchronisation. Les deux caractéristiques révèlent l'amélioration fonctionnelle du traitement de l'information auditive au cours du troisième trimestre de la grossesse.

Concernant l'asymétrie, il a été émis l'hypothèse que chaque hémisphère est dominant pour l'analyse des modulations à différentes échelles de temps et que les modulations du taux de phonèmes se latéralisent vers l'hémisphère gauche, tandis que la spécialisation à droite est principalement impliquée dans les ASSR à basse fréquence et les taux de modulation plus lents tels que concernant la modulation syllabique [190]. Bien qu'une asymétrie droite pour les modulations lentes ait été rapportée auparavant chez les adultes [190], les enfants [197] et les nouveau-nés [198] [199], il n'était pas clair si une certaine latéralisation pourrait déjà être observée chez les prématurés. Nos résultats suggèrent qu'un biais vers la droite est déjà en place chez les prématurés.

Les résultats actuels, ainsi que les observations précédentes [88] [101], pourraient avoir des implications importantes pour la surveillance de l'émergence et du développement normal de fonctionnalités cérébrales spécifiques chez le nouveau-né prématuré. Plus spécifiquement, l'analyse de fréquence convient très bien aux études sur les nouveau-nés prématurés et à terme et peut fournir une approche utile pour évaluer certains aspects fonctionnels de la capacité des circuits auditifs sous-jacents au neurodéveloppement normal.

6.3 Corrélats fonctionnels et structurels du cerveau du prématuré: mise en relation des modifications développementales des réponses évoquées auditives à la maturation de la myéline

6.3.1 Participants, stimuli et enregistrements

Les CAEP enregistrés chez 17 nouveau-nés prématurés (âge d'enregistrement moyen = 30.47 WGA, 28.4 à 32.2 WGA), recrutés dans notre étude précédente [88], ont été réanalysés pour la présente étude. Les stimuli, les enregistrements et les prétraitements sont identiques à ceux de la partie 6.2.1. Sauf que nous avons utilisé à la fois des essais standard et des essais déviants pour les besoins de cette partie des analyses.

6.3.2 Puissance de champ globale

La puissance de champ globale (Global Field Power, GFP) mesure l'écart type spatial de l'activité de champ instantanée en prenant en compte les données de toutes les électrodes [214]. Le résultat est un descripteur du champ de potentiel indépendant de la référence calculé par l'équation (2) comme racine de la moyenne des différences de potentiel au carré (ui - uj) entre toutes les paires d'électrodes possibles dans le champ (n indique le nombre d'électrodes).

$$GFP = \sqrt{\left(\frac{1}{2n}\right) * \sum_{i=1}^{n} \sum_{j=1}^{n} (u_i - u_j)^2} \quad (6.2)$$

La GFP présente une mesure globale de l'activité cérébrale pouvant être détectée sur le cuir chevelu. Par conséquent, les moments où les maxima de la GFP sont atteints sont le bon choix pour les études sur les ERP chez le nouveau-né prématuré. Ici, la latence du premier pic du signal GFP est considérée comme la caractéristique fonctionnelle d'intérêt pour l'étude des dépendances liées à l'âge et à la structure. Quinze canaux communs à tous les sujets (Fz, F1, F2, F3, F4, C1, C2, CP1, CP2, Pz, P1, P2, Oz, O1 et O2) ont été utilisés pour calculer le signal GFP.

6.3.3 Analyse structurelle

Ici, nous avons cherché à développer des modèles conjoints de développement cérébral fonctionnel et structurel chez le nouveau-né prématuré. Cependant, les images IRM des nouveau-nés prématurés à l'étude pour l'extraction des caractéristiques fonctionnelles n'étaient pas disponibles. En guise d'approche alternative, nous avons considéré les images IRM du

référentiel Imperial College London, bien que cela ait limité l'étude. Les modèles T1w et T2w correspondant à chaque WGA ont été sélectionnés à partir de l'atlas structurel spatio-temporel détaillé fourni pour le cerveau néonatal avec 87 structures marquées. Nous avons utilisé des images de rapport T1w / T2w pour augmenter le contraste du signal lié à la myéline et réduire le biais de la bobine du récepteur [149]. Une image de ratio a été créée pour chaque WGA de 28 à 32, correspondant à la tranche d'âge de nos données fonctionnelles. Les valeurs moyennes du ratio intensités d'image ont été extraites pour chaque région d'intérêt en tant qu'indice de maturation pour cette région spécifique du cerveau. La spécificité a été vérifiée en mesurant l'indice de maturation à la fois pour la MG totale et la MW totale, en tant que deux mesures potentielles du développement structurel cérébral chez les nouveau-nés prématurés. De plus, cet indice a été calculé pour toutes les régions du cerveau spécifiées par l'atlas néonatal (GM + WM), y compris le gyrus temporal supérieur médian (mSTG) et sa partie postérieure (pSTG), supposées être plus impliquées dans les tâches auditives. Toutes les régions ont été considérées pour étudier les relations structurelles et fonctionnelles, en recherchant celles présentant les meilleurs coefficients de corrélation.

6.3.4 Analyse fonctionnelle et structurelle conjointe

Nous devions associer l'âge de chaque nourrisson à l'âge correspondant (en WGA) de l'ensemble de données structurelles afin d'étudier les corrélations entre la fonction et la structure. Par exemple, les nourrissons de 29.5 à 30.5 WGA ont été associés aux modèles pour 30 WGA. Une régression linéaire a été réalisée pour étudier les corrélations entre les indices fonctionnels de latence du premier pic de la GFP et structurel lié à la maturation structurelle de la MW totale, du mSTG et du pSTG. Ensuite, une analyse de régression hiérarchique a été réalisée pour examiner l'influence unique des indices d'âge et de maturation de la MW totale, du mSTG et du pSTG sur la latence du premier pic de la GFP. De plus, nous avons étudié la spécificité auditive des relations observées en effectuant une corrélation partielle entre la latence du premier pic de la GFP et l'indice de maturation de chaque ROI, en tenant compte de l'âge des nourrissons. Ainsi, nous avons pu comparer les corrélations entre les indices fonctionnels et structurels de différentes ROI après avoir éliminé l'effet de l'âge.

6.3.5 Résultats

Nous avons observé une diminution globale de la latence du premier pic du signal GFP avec l'âge, illustrée par une corrélation négative significative (R^2 = 0.311, p = 0.02). Nous

avons évalué les changements dépendant de l'âge dans les indices de maturation des quatre régions d'intérêt (GM total, MW totale, mSTG et pSTG) pour la plage d'âge complète fournie par l'atlas néonatal utilisé (28-44 wGA). L'indice de maturation de la MW totale a montré une corrélation positive significative avec l'âge (R^2 = 0.930, p <0.001), alors qu'il n'y avait pas de corrélation significative pour les variations de l'indice de maturation GM total dépendant de l'âge. Il y avait des corrélations positives significatives entre l'indice de maturation du mSTG et l'âge (R^2 = 0.929, p < 0.001) et l'indice de maturation du pSTG et l'âge (R^2 = 0.915, p < 0.001).

Concernant les corrélations fonction-structure, nous avons observé une corrélation négative significative entre la latence du premier pic de la GFP et l'indice de maturation de la MW totale (R^2 = 0.290, p = 0.026), ainsi qu'une corrélation négative significative entre la latence du premier pic de la GFP et l'indice de maturation du mSTG (R^2 = 0.439, p = 0.004) et une corrélation négative significative entre le premier pic de latence de la GFP et l'indice de maturation du pSTG (R^2 = 0.367, p = 0.01). Dans les modèles hiérarchiques, ni l'indice de maturation structurel ni l'âge n'ont contribué à une variance supplémentaire significative de la latence du premier pic de GFP après prise en compte de la variance associée à l'autre paramètre.

Nous avons effectué une analyse de régression linéaire entre les résidus de la fonction fonctionnelle globale et l'indice de maturation structurelle de chaque région d'intérêt après régression de l'effet de l'âge (figure 6.3). Les valeurs absolues des coefficients de corrélation étaient supérieures pour certaines zones impliquées dans l'audition (par exemple, mSTG, pSTG, insula et lobes frontaux et pariétaux) que pour les zones non auditives (par exemple, le lobe occipital et le gyrus occipito-temporal latéral, qui sont plus impliqués dans les tâches visuelles d'ordre supérieur).

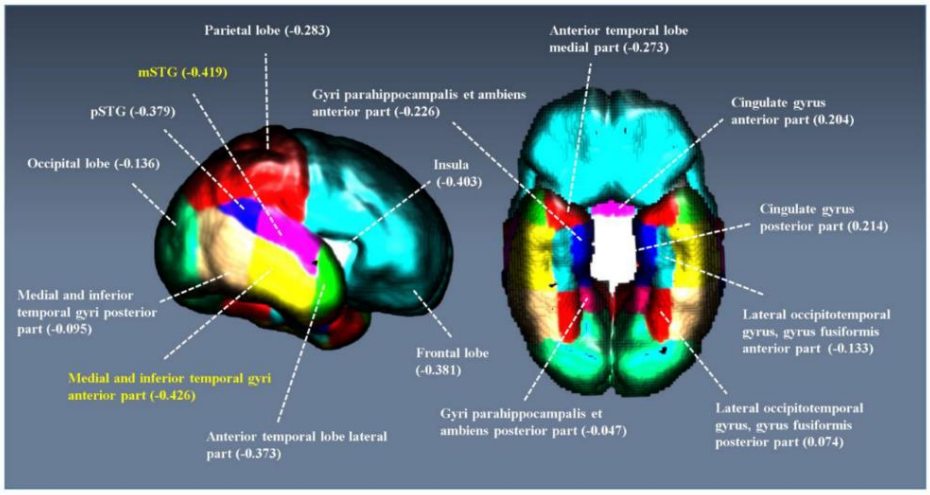

Figure 6.3: Résultats de la corrélation partielle (valeur r) entre la caractéristique fonctionnelle et l'indice structurel de chaque région d'intérêt après régression de l'effet de l'âge.

6.3.6 Discussion

Ici, nous avons observé un certain nombre d'associations entre les indices de maturation structurels et fonctionnels, et l'âge, qui soutiennent un modèle biophysique lié à des changements développementaux du système auditif chez les nouveau-nés prématurés. Differents processus de maturation vont s'enchaîner tout au long du développement cérébral chez le prématuré, notamment l'organisation microstructurale de la plaque et de la sous-plaque corticales, l'évolution des membranes, la connectivité, le repliement cortical, l'éclatement synaptique, l'élagage, etc. Bien que tous ces processus puissent affecter la vitesse de conduction neuronale, L'établissement de la myélinisation autour des axones neuronaux est le principal facteur contribuant à l'accélération des latences ERP. La valeur moyenne des images du rapport T1w / T2w dans chaque ROI, qui est considérée comme une estimation de la myélinisation, peut également être sensible à d'autres processus de maturation chez les nouveau-nés prématurés. Néanmoins, il peut encore être considéré comme un indice de maturation structurel, qui se développe au cours de la tranche d'âge de notre étude. En ce qui concerne l'émergence de la myélinisation et l'enregistrement précoce des CAEP, nous avions l'intention de mesurer le développement fonctionnel et structurel correspondant pour la tranche d'âge de 28 à 32 ans. Les résultats ont confirmé les modifications attendues des caractéristiques fonctionnelles et structurelles extraites en fonction de l'âge. La régression hiérarchique a montré que l'indice de maturation lié à l'âge ne représentait pas de variance supplémentaire significative dans la latence du premier pic de la GFP, après prise en compte de la variance associée à l'autre paramètre. Une analyse de régression a montré que l'âge et

l'indice de maturation prédisent presque la même variance de la latence du premier pic de la GFP. Étant donné la corrélation étroite qui existe entre la myélinisation et l'âge au cours de cette période de développement, nos résultats suggèrent que la prédiction de la latence du premier pic de la GFP peut s'appuyer sur la myélinisation ou l'âge des nouveau-nés prématurés dans le cas d'un développement typique.

Ici, nous avons utilisé les modèles d'imagerie fournies par un atlas néonatal réalisé pour chaque semaine d'âge gestationnel afin d'établir une corrélation avec nos données fonctionnelles. Malgré les difficultés d'acquisition simultanée de données structurelles et fonctionnelles du même prématuré, il est recommandé de comparer les modifications anatomo-fonctionnelles d'une modalité à l'autre chez un même sujet afin de caractériser le développement de réseaux auditifs cérébraux et d'établir des spécifications et des déductions précises. Ceci est éthiquement difficile à mettre en œuvre pratiquement et n'a pas été réalisé dans cette étude rétrospective.

6.4 Conclusion

Pour tenter d'étudier le développement fonctionnel et structurel du cerveau humain, nous avons utilisé des techniques de neuroimagerie non invasives, telles que l'EEG et l'IRM, pour étudier chez les nouveau-nés prématurés: les corrélats neuronaux du traitement de la parole, la latéralisation des CAEP en réponse à des stimuli syllabiques et, les corrélations entre les modifications développementales des caractéristiques fonctionnelles et structurelles du système auditif.

À notre connaissance, il s'agit de la première étude portant sur le développement fonctionnel et structurel du réseau auditif chez le nouveau-né prématuré. Dans la présente étude, certaines associations sont présentées entre les indices de maturation structurelle, fonctionnelle et l'âge qui soutiennent un modèle biophysique des modifications développementales du système auditif chez le prématuré. Ce travail constitue une nouvelle approche intéressante permettant à terme de détecter des déviations précoces de la relation structure fonction liées aux troubles perinataux. Étant donné que l'enregistrement EEG est beaucoup plus facile que l'IRM dans les unités néonatales, comprendre le lien entre les latences ERP et les structures cérébrales au cours du développement normal ou pathologique constituerait un progrès considérable pour la recherche et le suivi des soins quotidiens dans les unités néonatales.

References

[1] J. Stiles and T. L. Jernigan, “The basics of brain development,” vol. 20, pp. 327–348, 2010.

[2] M. H. Johnson and M. de Haan, “Building a brain,” in *developmental cognitive neuroscience*, 4th ed., Wiley Blackwell, 2015, p. 52.

[3] P. R. Huttenlocher, “Morphometric study of human cerebral cortex development.,” *Neuropsychologia*, vol. 28, no. 6, pp. 517–527, 1990.

[4] P. R. Huttenlocher, C. de Courten, L. G. Garey, and H. Van der Loos, “Synaptogenesis in human visual cortex–evidence for synapse elimination during normal development,” *Neurosci. Lett.*, vol. 33, pp. 247–252, 1982.

[5] C. A. Simpkins and A. M. Simpkins, “Brain development through the lifespan,” in *Neuroscience for clinicians*, springer, 2013, pp. 158–161.

[6] L. Spear, *The behavioral neuroscience of adolescence*. New York: NY: Norton, 2010.

[7] H. Haug, “Are neurons of the human cerebral cortex really lost during aging? A morphometric examination,” in *Senile dementia of Alzheimer type*, vol. 12, no. 4, J. Tarber and W. H. Gispen, Eds. Berlin: Springer- Verlag, 1985, pp. 150–163.

[8] H. Berger, “Über das Elektrenkephalogramm des Menschen,” *Arch. Psychiatr. Nervenkr.*, vol. 87, pp. 527–570, 1929.

[9] F. Daneshvarfard, N. Maarefi, H. Abrishami Moghaddam, and F. Wallois, “A survey on stimuli for visual cortical function assessment in infants,” *Brain Dev.*, vol. 40, pp. 2–15, 2018.

[10] T. Farroni and E. Menon, “Visual perception and early brain development,” *Early Child. Dev.*, vol. 5, pp. 1–6, 2008.

[11] E. Ahtola, S. Stjerna, N. Stevenson, and S. Vanhatalo, “Use of eye tracking improves the detection of evoked responses to complex visual stimuli during EEG in infants,” *Clin. Neurophysiol. Pract.*, vol. 2, pp. 81–90, 2017.

[12] B. MacDonald and R. J. Barry, “Significance and novelty effects in single-trial ERP components and autonomic responses.,” *Int. J. Psychophysiol.*, vol. 117, pp. 48–64, 2017.

[13] S. Jee Eun and J. Eun Ha, “Age-related differences in ERP components associated with processing homonyms depending on the context type of adnominal and verb phrases,” *Commun. Sci. Disord.*, vol. 23, no. 2, pp. 360–377, 2018.

[14] K. Kompatsiari, G. Candrian, and A. Mueller, “Test-retest reliability of ERP components: A short-term replication of a visual Go/NoGo task in ADHD subjects.,” *Neurosci. Lett.*, vol. 617, pp. 166–172, 2016.

[15] J. Péron *et al.*, “Vocal emotion decoding in the subthalamic nucleus : An intracranial ERP study in Parkinson ’ s disease,” *Brain Lang.*, vol. 168, pp. 1–11, 2017.

[16] X. Li *et al.*, “Attentional bias in MDD: ERP components analysis and classification using a dot-probe task,” *Comput. Methods Programs Biomed.*, vol. 164, pp. 169–179, 2018.

[17] J. V. Odom *et al.*, “ISCEV STANDARDS ISCEV standard for clinical visual evoked potentials : (2016 update),” *Doc. Ophthalmol.*, vol. 133, no. 1, pp. 1–9, 2016.

[18] J. V. Odom *et al.*, “Visual evoked potentials standard,” *Doc. Ophthalmol.*, vol. 108, pp. 115–123, 2004.

[19] R. Sharma, S. Joshi, K. D. Singh, and A. Kumar, “Visual evoked potentials: Normative values and gender differences,” *J. Clin. Diagnostic Res.*, vol. 9, pp. 12–15, 2015.

[20] F. Di Russo, A. Martinez, M. I. Sereno, S. Pitzalis, and S. A. Hillyard, “Cortical sources of the early components of the visual evoked potential,” *Hum. Brain Mapp.*,

vol. 15, no. 2, pp. 95–111, 2002.
[21] E. Reuter *et al.*, “A non-linear relationship between selective attention and associated ERP markers across the lifespan,” *Front. Psychol.*, vol. 10, no. 30, pp. 1–15, 2019.
[22] D. Tome, F. Barbosa, K. Nowak, and J. Marques-Teixeira, “The development of the N1 and N2 components in auditory oddball paradigms : a systematic review with narrative analysis and suggested normative values,” *J. Neural Transm.*, vol. 122, no. 3, pp. 375–391, 2015.
[23] M. Valdes-sosa, M. A. Bobes, V. Rodriguez, and T. Pinilla, “Switching attention without shifting the spotlight : Object-based attentional modulation of brain potentials,” *J. Cogn. Neurosci.*, vol. 10, no. 1, pp. 137–151, 1998.
[24] C. Colombatto and G. Mccarthy, “The effects of face inversion and face race on the P100 ERP,” *J. Cogn. Neurosci.*, vol. 29, no. 4, pp. 664–676, 2017.
[25] P. Walsh, N. Kane, and S. Butler, “The clinical role of evoked potentials,” *J Neurol Neurosurg Psychiatry*, vol. 76, pp. 16–22, 2005.
[26] R. Van Dinteren, M. Arns, M. L. A. Jongsma, and R. P. C. Kessels, “P300 development across the lifespan : A systematic review and meta-analysis,” vol. 9, no. 2, p. e87347john, 2014.
[27] R. J. Johnson, “On the neural generators of the P300 component of the event-related potential.,” *Psychophysiology*, vol. 30, pp. 90–97, 1993.
[28] C. C. Duncan-Johnson and E. Donchin, “On quantifying surprise: The variation of event-related potentials with subjective probability,” *Psychophysiology*, vol. 14, pp. 456–467, 1977.
[29] J. B. Isreal, C. D. Wickens, and E. Donchin, “The dynamics of P300 during dual-task performance,” *Prog. Brain Res.*, vol. 54, pp. 416–421, 1980.
[30] A. F. Kramer and D. L. Strayer, “Assessing the development of automatic processing: An application of dual-task and event-related brain potential methodologies,” *Biol. Psychol.*, vol. 26, pp. 231–267, 1988.
[31] J. Polich, “Normal variation of P300 from auditory stimuli,” *Electroencephalogr. Clin. Neurophysiol.*, vol. 65, pp. 236–240, 1986.
[32] S. Finnigan, M. S. Humphreys, S. Dennis, and G. Geffen, “ERP ‘old/new’ effects: Memory strength and decisional factor(s),” *Neuropsychologia*, vol. 40, pp. 2288–2304, 2002.
[33] T. C. Gunter, A. D. Friederici, and H. Schriefers, “Syntactic gender and semantic expectancy: ERPs reveal early autonomy and late interaction,” *J. Cogn. Neurosci.*, vol. 12, pp. 556–568, 2000.
[34] S. C. Steffensen, A. J. Ohran, D. N. Shipp, K. Hales, S. H. Stobbs, and D. E. Fleming, “Gender-selective effects of the P300 and N400 components of the visual evoked potential,” *Vision Res.*, vol. 48, pp. 917–925, 2008.
[35] M. J. Taylor and D. L.McCulloch, “Visual Evoked Potentials in infants and children,” *J Clin. Neurophysiol.*, vol. 9, no. 3, pp. 357–372, 1992.
[36] I. Benavente, P. Tamargo, N. Tajada, V. Yuste, and M. J. Olivan, “Flash visually evoked potentials in the newborn and their maturation during the first six months of life,” *Doc Ophthalmol*, vol. 110, pp. 255–263, 2005.
[37] E. Schwindt *et al.*, “The impact of extrauterine life on visual maturation in extremely preterm born infants,” *Pediatr. Res.*, vol. 84, pp. 403–410, 2018.
[38] J. Polich, “EEG and ERP assessment of normal aging,” *Electroencephalogr. Clin. Neurophysiol.*, vol. 104, no. 3, pp. 244–256, 1997.
[39] Y. M. Cycowicz, “Memory development and event-related brain potentials in children,” vol. 54, pp. 145–174, 2000.
[40] D. E. Linden, “The p300: where in the brain is it produced and what does it tell us?,”

Neurosci., vol. 11, no. 6, pp. 563–576, 2005.
[41] R. Van Dinteren, R. J. Huster, M. L. A. Jongsma, R. P. C. Kessels, and M. Arns, "Differences in cortical sources of the event-related P3 potential between young and old participants indicate frontal fompensation," *Brain Topogr.*, vol. 31, no. 1, pp. 35–46, 2018.
[42] I. Pavarini *et al.*, "On the use of the P300 as a tool for cognitive processing assessment in healthy aging A review," *Dement Neuropsychol.*, vol. 12, no. 1, pp. 1–11, 2018.
[43] K. Cassady *et al.*, "Sensorimotor network segregation declines with age and is linked to GABA and to sensorimotor performance," *Neuroimage*, vol. 186, pp. 234–244, 2019.
[44] C. Cheng, M. Lin, and S. Yang, "Age effect on automatic inhibitory function of the somatosensory and motor cortex : An MEG study," *Front. Aging Neurosci.*, vol. 10, p. 53, 2018.
[45] S. Heuninckx, N. Wenderoth, and S. P. Swinnen, "Systems neuroplasticity in the aging brain : Recruiting additional neural resources for successful motor performance in elderly persons," *J. Neurosci.*, vol. 28, no. 1, pp. 91–99, 2008.
[46] E. Verdú, D. Ceballos, J. J. Vilches, and X. Navarro, "Influence of aging on peripheral nerve function and regeneration," *J Peripher Nerv Syst*, vol. 5, no. 4, pp. 191–208, 2000.
[47] J. R. Isler *et al.*, "Frequency domain analyses of neonatal flash VEP," *Pediatr. Res.*, vol. 62, no. 5, pp. 581–585, 2007.
[48] A. Prochazka, J. Kukal, and O. Vysata, "Wavelet transform use for feature extraction and EEG signal segments classification," in *3rd international symposium on communication,control and signal processing*, 2008, pp. 12–14.
[49] J. Steffener, C. G. Habeck, and Y. Stern, "Age-related changes in task related functional network connectivity," *PLoS One*, vol. 7, no. e44421, 2012.
[50] R. Litovsky, "Development of the auditory system," *Handb. Clin. Neurol.*, vol. 129, pp. 55–72, 2015.
[51] L. W. Olsho, E. G. Koch, N. B. Spetner, E. A. Carter, and C. F. Halpin, "Pure-tone sensitivity of human infants," *J. Acoust. Soc. Am.*, vol. 84, pp. 1316–1324, 1988.
[52] S. E. Trehub, B. A. Schneider, B. A. Morrongiello, and L. A. Thorpe, "Auditory sensitivity in school-age children," *J. Exp. Child Psychol.*, vol. 46, pp. 273–285, 1988.
[53] A. M. Tharpe and D. H. Ashmead, "A longitudinal investigation of infant auditory sensitivity," *Am J Audiol*, vol. 10, pp. 104–112, 2001.
[54] L. W. Olsho, E. G. Koch, and C. F. Halpin, "Level and age effects in infant frequency discrimination," *J. Acoust. Soc. Am.*, vol. 82, pp. 454–464, 1987.
[55] J. M. Sinnott and R. N. Aslin, "Frequency and intensity discrimination in human infants and adultsa," *J. Acoust. Soc. Am.*, vol. 78, pp. 1986–1992, 1985.
[56] J. I. Rotteveel, R. de Graaf, D. F. Stegeman, E. J. Colon, and Y. M. Visco, "The maturation of the central auditory conduction in preterm infants until three months post term . V . The auditory cortical response (ACR)," *Hear Res*, vol. 27, pp. 95–110, 1987.
[57] B. Cone and R. Whitaker, "Dynamics of infant cortical auditory evoked potentials (CAEPs) for tone and speech tokens," *Int J Pediatr Otorhinolaryngol*, vol. 77, pp. 1162–1173, 2013.
[58] J. L. Wunderlich and B. K. Cone-Wesson, "Maturation of CAEP in infants and children: A review," *Hear. Res.*, vol. 212, pp. 212–223, 2006.
[59] V. M. Little, D. G. Thomas, and M. R. Letterman, "Single-trial analyses of developmental trends in infant auditory event-related potentials," *Dev. Neuropsychol.*, vol. 16, pp. 455–478, 1999.
[60] E. D. Weitzman and L. J. Graziani, "Maturation and topography of the auditory evoked

response of the prematurely born infant," *Dev. Psychobiol.*, vol. 1, pp. 79–89, 1968.
[61] E. S. Ohlrich and A. B. Barnet, "Auditory evoked responses during the first year of life," *Electroencephalog Clin Neurophysiol*, vol. 32, pp. 161–169, 1972.
[62] E. Kushnerenko, R. Cepomiene, P. Balan, V. Fellman, M. Huotilainen, and R. Nììtìnen, "Maturation of the auditory event-related potentials during the first year of life," *Neuroreport*, vol. 13, pp. 47–51, 2002.
[63] S. Lippe, N. Kovacevic, and A. R. McIntosh, "Differential maturation of brain signal complexity in the human auditory and visual system," *Front. Hum. Neurosci.*, vol. 3, pp. 1–9, 2009.
[64] M. Huotilainen *et al.*, "Auditory magnetic responses of healthy newborns," *Neuroreport*, vol. 14, pp. 1871–1875, 2003.
[65] A. Barnet, E. Ohlrich, I. Weiss, and B. Shanks, "Auditory evoked potentials during sleep in normal children from ten days to three years of age," *Electroencephalog Clin Neurophysiol*, vol. 39, pp. 29–41, 1975.
[66] D. G. Thomas *et al.*, "Event-Related Potential Variability as a Measure of Information Storage in Infant Development," *Dev. Neuropsychol.*, vol. 13, pp. 205–232, 1997.
[67] J. L. Wunderlich, B. K. Cone-wesson, and R. Shepherd, "Maturation of the cortical auditory evoked potential in infants and young children," *Hear. Res.*, vol. 212, pp. 185–202, 2006.
[68] K. L. Tremblay, C. Billings, and N. Rohila, "Speech evoked cortical potentials: Effects of age and stimulus presentation rate," *J Am Acad Audiol*, vol. 15, pp. 226–237, 2004.
[69] R. C. Knickmeyer *et al.*, "A structural MRI study of human brain development from birth to 2 years," *J Neurosci*, vol. 28, pp. 12176–12182, 2008.
[70] J. H. Gilmore *et al.*, "Longitudinal development of cortical and subcortical gray matter from birth to 2 years," *Cereb Cortex*, vol. 22, pp. 2478–2485, 2011.
[71] M. Kuklisova-murgasova *et al.*, "A dynamic 4D probabilistic atlas of the developing brain," *Neuroimage*, vol. 54, pp. 2750–2763, 2011.
[72] J. N. Giedd, J. Blumenthal, N. O. Jeffries, F. X. Castellanos, H. Liu, and A. Zijdenbos, "Brain development during childhood and adolescence : a longitudinal MRI study," *Nat. Neurosci.*, vol. 2, pp. 861–863, 1999.
[73] J. Dubois, D. Germanaud, H. Angleys, F. Leroy, and C. Fischer, "Exploring the successive waves of cortical folding in the developing brain using MRI and spectral analysis of gyrification," in *IEEE 13th International Symposium on Biomedical Imaging (ISBI)*, 2016, pp. 261–264.
[74] H. Xue *et al.*, "Automatic segmentation and reconstruction of the cortex from neonatal MRI," *Neuroimage*, vol. 38, pp. 461–477, 2007.
[75] E. R. Sowell, P. M. Thompson, C. M. Leonard, S. E. Welcome, E. Kan, and A. W. Toga, "Longitudinal mapping of cortical thickness and brain growth in normal children," *J Neurosci*, vol. 24, pp. 8223–8231, 2004.
[76] L. M. Wierenga, M. Langen, B. Oranje, and S. Durston, "Unique developmental trajectories of cortical thickness and surface area," *Neuroimage*, vol. 87, pp. 120–126, 2014.
[77] A. B. Storsve *et al.*, "Differential longitudinal changes in cortical thickness , surface area and volume across the adult life span: Regions of accelerating and decelerating change," *J Neurosci*, vol. 34, pp. 8488–8498, 2014.
[78] J. Dubois and G. Dehaene-Lambertz, "Fetal and postnatal development of the cortex : MRI and genetics," in *Brain Mapping: An Encyclopedic Reference*, A. Toga, Ed. Elsevier Inc., 2015, pp. 11–19.
[79] T. White and C. C. Hilgetag, "Gyrification and neural connectivity in schizophrenia," *Dev. Psychopathol.*, vol. 23, pp. 339–352, 2011.

[80] V. Rajagopalan *et al.*, "Local tissue growth patterns underlying normal fetal human brain gyrification quantified in utero," *J Neurosci*, vol. 31, pp. 2878–2887, 2011.
[81] E. Armstrong *et al.*, "The ontogeny of human gyrification," *Cereb. Cortex*, vol. 5, pp. 56–63, 1995.
[82] K. Zilles, N. Palomero-gallagher, and K. Amunts, "Development of cortical folding during evolution and ontogeny," *Trends Neurosci.*, vol. 36, pp. 275–284, 2013.
[83] W. Gaetz, T. P. L. Roberts, K. D. Singh, and S. D. Muthukumaraswamy, "Functional and structural correlates of the aging brain: Relating visual cortex (V1) gamma band responses to age-related structural change," *Hum Brain Mapp*, vol. 33, pp. 2035–2046, 2012.
[84] T. J. Whitford, C. J. Rennie, S. M. Grieve, C. R. Clark, E. Gordon, and L. M. Williams, "Brain maturation in adolescence : Concurrent changes in neuroanatomy and neurophysiology," *Hum. Brain Mapp.*, vol. 28, pp. 228–237, 2007.
[85] A. Horowitz, D. Barazany, I. Tavor, M. Bernstein, G. Yovel, and Y. Assaf, "In vivo correlation between axon diameter and conduction velocity in the human brain," *Brain Struct. Funct.*, vol. 220, pp. 1777–1788, 2015.
[86] T. P. L. Roberts *et al.*, "Developmental correlation of diffusion anisotropy with auditory-evoked response," *Neuroreport*, vol. 20, pp. 1586–1591, 2009.
[87] D. Price *et al.*, "Age-related delay in visual and auditory evoked responses is mediated by white-and grey-matter differences," *Nat. Commun.*, vol. 8, 2017.
[88] M. Mahmoudzadeh *et al.*, "Functional maps at the onset of auditory inputs in very early preterm human neonates," *Cereb Cortex*, vol. 27, pp. 2500–2512, 2017.
[89] R. J. Wagener, M. Witte, J. Guy, N. Mingo-Moreno, S. Kügler, and J. F. Staiger, "Thalamocortical connections drive intracortical activation of functional columns in the mislaminated reeler somatosensory cortex," *Cereb. Cortex*, vol. 26, pp. 820–837, 2016.
[90] M. André *et al.*, "Electroencephalography in premature and full-term infants. Developmental features and glossary," *Neurophysiol. Clin.*, vol. 40, pp. 59–124, 2010.
[91] M. Tolonen, J. M. Palva, S. Andersson, and S. Vanhatalo, "Development of the spontaneous activity transients and ongoing cortical activity in human preterm babies," *Neuroscience*, vol. 145, pp. 997–1006, 2007.
[92] N. J. Stevenson *et al.*, "Functional maturation in preterm infants measured by serial recording of cortical activity," *Sci. Rep.*, vol. 7, pp. 1–7, 2017.
[93] L. S. De Vries and L. Hellström-Westas, "Role of cerebral function monitoring in the newborn," *Arch. Dis. Child. Fetal Neonatal Ed.*, vol. 90, pp. 201–208, 2005.
[94] P. M. Iyer *et al.*, "Functional connectivity changes in resting-state EEG as potential biomarker for Amyotrophic Lateral Sclerosis," *PLoS One*, vol. 10, pp. 1–14, 2015.
[95] N. Japaridze *et al.*, "Neuronal networks during burst suppression as revealed by source analysis," *PLoS One*, vol. 10, pp. 1–18, 2015.
[96] F. Wallois, "Synopsis of maturation of specific features in EEG of premature neonates," *Neurophysiol. Clin.*, vol. 40, pp. 125–126, 2010.
[97] M. D. I. Lamblin *et al.*, "Electroencephalography of the premature and term newborn. Maturational aspects and glossary," *Neurophysiol. Clin.*, vol. 29, pp. 123–219, 1999.
[98] L. J. Graziani, L. Katz, and E. D. Weitzman, "The maturation and interrelationship of EEG patterns and auditory evoked responses in premature infants," *Electroencephalogr. Clin. Neurophysiol.*, vol. 36, pp. 367–375, 1974.
[99] M. T. Colonnese *et al.*, "A conserved switch in sensory processing prepares developing neocortex for vision," *Neuron*, vol. 67, pp. 480–498, 2010.
[100] P. S. Bisiacchi, G. Mento, and A. Suppiej, "Cortical auditory processing in preterm newborns: An ERP study," *Biol. Psychol.*, vol. 82, pp. 176–185, 2009.

[101] M. Mahmoudzadeh, G. Dehaene-lambertz, M. Fournier, G. Kongolo, and S. Goudjil, “Syllabic discrimination in premature human infants prior to complete formation of cortical layers,” *Proc. Natl. Acad. Sci.*, vol. 110, pp. 4846–4851, 2013.
[102] G. Dehaene-Lambertz and S. Dehaene, “Speed and cerebral correlates of syllable discrimination in infants,” *Nature*, vol. 370, pp. 292–295, 1994.
[103] T. Bekinschtein, S. Dehaene, B. Rohaut, l F. Tade, L. Cohen, and L. Naccache, “Neural signature of the conscious processing of auditory regularities,” *Proc Natl Acad Sci U S A*, vol. 106, pp. 1672–1677, 2009.
[104] A. Basirat, S. Dehaene, and G. Dehaene-Lambertz, “A hierarchy of cortical responses to sequence violations in three-month-old infants,” *Cognition*, vol. 132, pp. 137–150, 2014.
[105] K. Snyder, S. J. Webb, and C. A. Nelson, “Theoretical and methodological implications of variability in infant brain response during a recognition memory paradigm,” *Infant Behav. Dev.*, vol. 25, pp. 466–494, 2002.
[106] T. W. Picton, M. S. John, A. Dimitrijevic, and D. Purcell, “Human auditory steady-state responses,” *Int J Audiol*, vol. 42, pp. 177–219, 2003.
[107] P. Adibpour, “Anatomo-functional correlates of visual and auditory development : insights on the ontogeny of face and speech processing lateralization,” de l’université Pierre et Marie Curie, 2017.
[108] I. Kostović and M. Judaš, “Embryonic and fetal development of the human cerebral cortex,” *Brain Mapp. An Encycl. Ref.*, vol. 2, pp. 167–175, 2015.
[109] P. Rakic, “Mode of cell migration to the superficial layers of fetal monkey neocortex,” *J. Comp. Neurol.*, vol. 145, pp. 61–83, 1972.
[110] I. Kostović and M. Judaš, “The development of the subplate and thalamocortical connections in the human foetal brain,” *Acta Paediatr. Int. J. Paediatr.*, vol. 99, pp. 1119–1127, 2010.
[111] D. D. M. O’Leary, S. J. Chou, and S. Sahara, “Area patterning of the mammalian cortex.,” *Neuron*, vol. 56, pp. 252–269, 2007.
[112] P. Rakic, “A small step for the cell, a giant leap for mankind: a hypothesis of neocortical expansion during evolution,” *Trends Neurosci.*, vol. 18, pp. 383–388, 1995.
[113] N. Bayatti *et al.*, “Progressive loss of PAX6, TBR2, NEUROD and TBR1 mRNA gradients correlates with translocation of EMX2 to the cortical plate during human cortical development,” *Eur. J. Neurosci.*, vol. 28, pp. 1449–1456, 2008.
[114] W. Z. Wang *et al.*, “Subplate in the developing cortex of mouse and human,” *J. Anat.*, vol. 217, pp. 368–380, 2010.
[115] I. Kostovic and P. Rakic, “Developmental history of the transient subplate zone in the visual and somatosensory cortex of the macaque monkey and human brain,” *J. Comp. Neurol.*, vol. 297, pp. 441–470, 1990.
[116] I. Kostovic and P. Goldman-Rakic, “Transient cholinesterase staining in the mediodorsal nucleus of the thalamus and its connections in the developing human and monkey brain,” *J. Comp. Neurol.*, vol. 219, pp. 431–447, 1983.
[117] I. Kostoví and M. Judaš, “Correlation between the sequential ingrowth of afferents and transient patterns of cortical lamination in preterm infants,” *Anat. Rec.*, vol. 267, pp. 1–6, 2002.
[118] J. Krmpotic´-Nemanic´, I. Kostovic´, Z. Kelovic´, D. Nemanic´, and L. Mrzljak, “Development of the human fetal auditory cortex: growth of afferent fibers,” *Acta Anat*, vol. 116, pp. 69–73, 1983.
[119] I. Kostović and M. Judaš, “Transient patterns of cortical lamination during prenatal life: Do they have implications for treatment?,” *Neurosci. Biobehav. Rev.*, vol. 31, pp. 1157–1168, 2007.

[120] S. Vanhatalo and K. Kaila, “Development of neonatal EEG activity: From phenomenology to physiology,” *Semin. Fetal Neonatal Med.*, vol. 11, pp. 471–478, 2006.
[121] S. Vanhatalo and L. Lauronen, “Neonatal SEP - Back to bedside with basic science,” *Semin. Fetal Neonatal Med.*, vol. 11, pp. 464–470, 2006.
[122] H. Lagercrantz and J. Changeux, “The emergence of human consciousness: From fetal to neonatal life,” *Pediatr. Res.*, vol. 65, pp. 255–260, 2009.
[123] I. Kostović, “Structural and histochemical reorganization of the human prefrontal cortex during perinatal and postnatal life,” *Prog Brain Res*, vol. 85, pp. 223–240, 1990.
[124] M. Marin-Padilla, “Structural organization of the human cerebral cortex prior to the appearance of the cortical plate,” *Anat. Embryol. (Berl).*, vol. 168, pp. 21–40, 1983.
[125] I. Bystron, C. Blakemore, and P. Rakic, “Development of the human cerebral cortex: Boulder Committee revisited,” *Nat. Rev. Neurosci.*, vol. 9, pp. 110–122, 2008.
[126] P. R. Huttenlocher and C. Bonnier, “Effects of changes in the periphery on development of the corticospinal motor system in the rat,” *Dev. Brain Res.*, vol. 60, pp. 253–260, 1991.
[127] G. M. Innocenti and D. J. Price, “Exuberance in the development of cortical networks,” *Nat. Rev. Neurosci.*, vol. 6, pp. 955–965, 2005.
[128] Z. Petanjek *et al.*, “Extraordinary neoteny of synaptic spines in the human prefrontal cortex,” *Proc. Natl. Acad. Sci.*, vol. 108, pp. 13281–13286, 2011.
[129] J. L. Thomas, N. Spassky, E. Perez Villegas, C. Olivier, and E. Al., “Spatiotemporal development of oligodendrocytes in the embryonic brain,” *J. Neurosci. Res.*, vol. 59, pp. 471–476, 2000.
[130] N. Baumann and D. Pham-dinh, “Biology of Oligodendrocyte and Myelin in the Mammalian Central Nervous System,” *Physiol Rev*, vol. 81, pp. 871–927, 2001.
[131] A. Barkovich, B. Kjos, D. Jackson Jr., and D. Norman, “Normal maturation of the neonatal and infant brain: MR imaging at 1.5 T.,” *Radiology*, vol. 166, pp. 173–180, 1988.
[132] S. E. Poduslo and Y. Jang, “Myelin development in infant brain,” *Neurochem. Res.*, vol. 9, pp. 1615–1626, 1984.
[133] I. Kostović, M. Judaš, M. Radoš, and P. Hrabač, “Laminar organization of the human fetal cerebrum revealed by histochemical markers and magnetic resonance imaging,” *Cereb. Cortex*, vol. 12, pp. 536–544, 2002.
[134] J. Dubois, I. Kostovic, and M. Judas, “Development of Structural and Functional Connectivity,” *Brain Mapp. An Encycl. Ref.*, vol. 2, pp. 423–437, 2015.
[135] E. Takahashi, R. D. Folkerth, A. M. Galaburda, and P. E. Grant, “Emerging cerebral connectivity in the human fetal Brain: An MR tractography study,” *Cereb. Cortex*, vol. 22, pp. 455–464, 2012.
[136] I. Kostović *et al.*, “Perinatal and early postnatal reorganization of the subplate and related cellular compartments in the human cerebral wall as revealed by histological and MRI approaches,” *Brain Struct. Funct.*, vol. 219, pp. 231–253, 2014.
[137] B. A. Brody, H. C. Kinney, A. S. Kloman, and F. H. Gilles, “Sequence of central nervous system myelination in human infancy,” *J. Neuropathol. Exp. Neurol.*, vol. 46, pp. 283–301, 1987.
[138] J. A. Scott *et al.*, “Growth trajectories of the human fetal brain tissues estimated from 3D reconstructed in utero MRI,” *Int. J. Dev. Neurosci.*, vol. 29, pp. 529–536, 2011.
[139] S. Groeschel, B. Vollmer, M. D. King, and A. Connelly, “Developmental changes in cerebral grey and white matter volume from infancy to adulthood,” *Int. J. Dev. Neurosci.*, vol. 28, pp. 481–489, 2010.
[140] P. Shaw *et al.*, “Neurodevelopmental trajectories of the human cerebral cortex,” *J.*

Neurosci., vol. 28, pp. 3586–3594, 2008.
[141] J. G. Chi, E. C. Dooling, and F. H. Gilles, "Gyral development of the human brain," *Ann. Neurol.*, vol. 1, pp. 86–93, 1977.
[142] J. Dubois, L. Hertz-Pannier, A. Cachia, J. F. Mangin, D. Le Bihan, and G. Dehaene-Lambertz, "Structural asymmetries in the infant language and sensori-motor networks," *Cereb. Cortex*, vol. 19, pp. 414–423, 2009.
[143] M. Momeni, H. A. Moghaddam, R. Grebe, C. Gondry-Jouet, and F. Wallois, "Temporal resolvability analysis of macroscopic morphological development in neonatal cerebral magnetic resonance images," *Neuropediatrics*, vol. 45, pp. 217–225, 2014.
[144] M. Momeni, H. Moghaddam, R. Grebe, C. Gondry-Jouet, and F. Wallois, "Neonatal atlas templates for the study of brain development using magnetic resonance images," *Curr. Med. Imaging Rev.*, vol. 11, pp. 38–48, 2015.
[145] J. Dubois, M. Benders, A. Cachia, and F. Lazeyras, "Mapping the early cortical folding process in the preterm newborn brain," *Cereb Cortex*, vol. 18, pp. 1444–1454, 2008.
[146] F. Leroy, J. Mangin, F. Rousseau, and H. Glasel, "Atlas-free surface reconstruction of the cortical grey- white interface in infants," *PLoS One*, vol. 6, p. e27128, 2011.
[147] J. Dubois, G. Dehaene-lambertz, C. Soares, Y. Cointepas, D. Le Bihan, and L. Hertz-pannier, "Microstructural Correlates of Infant Functional Development : Example of the Visual Pathways," *J Neuros*, vol. 28, pp. 1943–1948, 2008.
[148] P. Adibpour, J. Lebenberg, C. Kabdebon, G. Dehaene-lambertz, and J. Dubois, "Anatomo-functional correlates of auditory development in infancy," *bioRxiv*, 2019.
[149] M. F. Glasser and D. C. Van Essen, "Mapping Human Cortical Areas In Vivo Based on Myelin Content as Revealed by T1- and T2-Weighted MRI," *J Neurosci*, vol. 31, pp. 11597–11616, 2011.
[150] J. Iwatani *et al.*, "Use of T1-weighted / T2-weighted magnetic resonance ratio images to elucidate changes in the schizophrenic brain," *Brain Behav*, vol. 5, pp. 1–14, 2015.
[151] H. Grydeland, K. B. Walhovd, C. K. Tamnes, L. T. Westlye, and A. M. Fjell, "Intracortical myelin links with performance variability across the human lifespan : Results from T1- and T2- weighted MRI myelin mapping and diffusion tensor imaging," *J Neurosci*, vol. 33, pp. 18618–18630, 2013.
[152] K. Lee *et al.*, "Early Postnatal Myelin Content Estimate of White Matter via T1w / T2w Ratio," *Proc SPIE Int Soc Opt Eng*, vol. 9417, pp. 1–7, 2015.
[153] J. Dubois, P. Adibpour, C. Poupon, L. Hertz-Pannier, and G. Dehaene-Lambertz, "MRI and M / EEG studies of the White Matter Development in Human Fetuses and Infants : Review and Opinion," vol. 2, pp. 49–69, 2016.
[154] J. Dubois, G. Dehaene-Lambertz, S. Kulikova, C. Poupon, P. S. Hüppi, and L. Hertz-Pannier, "The early development of brain white matter: A review of imaging studies in fetuses, newborns and infants," *Neuroscience*, vol. 276, pp. 48–71, 2014.
[155] J. Dubois, L. Hertz-Pannier, G. Dehaene-Lambertz, Y. Cointepas, and D. Le Bihan, "Assessment of the early organization and maturation of infants' cerebral white matter fiber bundles: A feasibility study using quantitative diffusion tensor imaging and tractography," *Neuroimage*, vol. 30, pp. 1121–1132, 2006.
[156] D. L. McCulloch, H. Orbach, and B. Skarf, "Maturation of the pattern-reversal VEP in human infants: A theoretical framework," *Vision Res.*, vol. 39, pp. 3673–3680, 1999.
[157] R. D. Fields, "White matter in learning, cognition and psychiatric disorders," *Trends Neurosci.*, vol. 31, pp. 361–370, 2008.
[158] A. D. Friederici and S. M. E. Gierhan, "The language network," *Curr. Opin. Neurobiol.*, vol. 23, pp. 250–254, 2013.
[159] B. M. Mazoyer, N. Tzourio, V. Frak, A. Syrota, and E. Al., "The cortical representation

of speech," *J. Cogn. Neurosci.*, vol. 5, pp. 467–479, 1993.
[160] C. Pallier *et al.*, "Brain imaging of language plasticity in adopted adults: Can a second language replace the first?," *Cereb. Cortex*, vol. 13, pp. 155–161, 2003.
[161] A. Boemio, S. Fromm, A. Braun, and D. Poeppel, "Hierarchical and asymmetric temporal sensitivity in human auditory cortices," *Nat. Neurosci.*, vol. 8, pp. 389–395, 2005.
[162] R. J. Zatorre and P. Belin, "Spectral and temporal processing in human auditory cortex," *Cereb. Cortex*, vol. 11, pp. 946–953, 2001.
[163] N. Geschwind and W. Levitsky, "Human Brain : Left-right asymmetries in temporal speech region eye tracking of observer-generated target movements," *Science (80-.).*, vol. 161, pp. 186–187, 1968.
[164] V. B. Penhune, R. J. Zatorre, and J. D. Macdonald, "Interhemispheric anatomical differences in human primary auditory cortex : Probabilistic mapping and volume measurement from magnetic resonance scans," *Cereb. cortex*, vol. 6, pp. 661–672, 1996.
[165] J. J. Hutsler, "The specialized structure of human language cortex : Pyramidal cell size asymmetries within auditory and language-associated regions of the temporal lobes," *Brain Lang.*, vol. 86, pp. 226–242, 2003.
[166] B. Anderson, B. D. Southern, and R. E. Powers, "Anatomic asymmetries of the posterior superior temporal lobes : A postmortem study," *Neuropsychiatry Neuropsychol Behav Neurol*, pp. 247–254, 1999.
[167] H. L. Seldon, "Structure of human auditory cortex. I. Cytoarchitectonics and dendritic distributions," *Brain Res.*, vol. 229, pp. 277–294, 1981.
[168] K. Zilles, M. Bacha-trams, N. Palomero-gallagher, K. Amunts, and A. D. Friederici, "Common molecular basis of the sentence comprehension network revealed by neurotransmitter receptor fingerprints," *Cortex*, vol. 63, pp. 79–89, 2015.
[169] J. Colombo and R. S. Bundy, "A method for the measurement of infant auditory selectivity *," *Infant Behav. Dev.*, vol. 4, pp. 219–223, 1981.
[170] A. Vouloumanos and J. F. Werker, "Listening to language at birth : evidence for a bias for speech in neonates," *Dev. Sci.*, vol. 10, pp. 159–171, 2007.
[171] J. Mehler, P. Jusczyk, G. Lamsertz, and F. French, "A precursor of language acquisition in young infants," *Cognition*, vol. 29, pp. 143–178, 1988.
[172] J. Bertoncini, R. Bijeljac-Babic, S. E. Blumstein, and J. Mehler, "Discrimination in neonates of very short CVs.," *J Acoust Soc Am*, vol. 82, pp. 31–37, 1987.
[173] P. D. Eimas, E. R. Siqueland, P. Jusczyk, and J. Vigorito, "Speech perception in infants," *Science (80-.).*, vol. 171(3968), pp. 303–306, 1971.
[174] P. K. Kuhl, E. Stevens, A. Hayashi, T. Deguchi, S. Kiritani, and P. Iverson, "Infants show a facilitation effect for native language phonetic perception between 6 and 12 months," *Dev. Sci.*, vol. 9, pp. F13–F21, 2006.
[175] J. F. Werker and R. C. Tees, "Cross-language speech perception : Evidence for perceptual reorganization during the first year of life," *Infant Behav. Dev.*, vol. 7, pp. 49–63, 1984.
[176] A. J. DeCasper and M. J. Spence, "Prenatal maternal speech influences newborns ' perception of speech sounds," *Infant Behav. Dev.*, vol. 9, pp. 133–150, 1986.
[177] G. Dehaene-Lambertz and S. Baillet, "A phonological representation in the infant brain," *Neuroreport*, vol. 9, pp. 1885–1888, 1998.
[178] E. W. Pang, G. E. Edmonds, R. Desjardins, S. C. Khan, L. J. Trainor, and M. J. Taylor, "Mismatch negativity to speech stimuli in 8-month-old infants and adults," *Int. J. Psychophysiol.*, vol. 29, pp. 227–236, 1998.
[179] J. Dubois *et al.*, "Primary cortical folding in the human newborn: An early marker of

later functional development," *Brain*, vol. 131, pp. 2028–2041, 2008.
[180] F. Leroy *et al.*, "Early maturation of the linguistic dorsal pathway in human infants," *J. Neurosci.*, vol. 31, pp. 1500–1506, 2011.
[181] J. Brauer, A. Anwander, D. Perani, and A. D. Friederici, "Dorsal and ventral pathways in language development," *Brain Lang.*, vol. 127, pp. 289–295, 2013.
[182] J. Dubois *et al.*, "Exploring the early organization and maturation of linguistic pathways in the human infant brain," *Cereb. Cortex*, vol. 26, pp. 2283–2298, 2016.
[183] G. Kasprian *et al.*, "The prenatal origin of hemispheric asymmetry: An in utero neuroimaging study," *Cereb. Cortex*, vol. 21, pp. 1076–1083, 2011.
[184] J. Hill *et al.*, "A surface-based analysis of hemispheric asymmetries and folding of cerebral cortex in term-born human infants," *J. Neurosci.*, vol. 30, pp. 2268–2276, 2010.
[185] H. Glasel, F. Leroy, J. Dubois, L. Hertz-Pannier, J. F. Mangin, and G. Dehaene-Lambertz, "A robust cerebral asymmetry in the infant brain: The rightward superior temporal sulcus," *Neuroimage*, vol. 58, pp. 716–723, 2011.
[186] G. Li, W. Lin, J. H. Gilmore, and D. Shen, "Spatial patterns, longitudinal development, and hemispheric asymmetries of cortical thickness in infants from birth to 2 years of age," *J. Neurosci.*, vol. 35, pp. 9150–9162, 2015.
[187] D. Bristow *et al.*, "Hearing faces: How the infant brain matches the face it sees with the speech it hears," *J. Cogn. Neurosci.*, vol. 21, pp. 905–921, 2009.
[188] M. Pena, J. F. Werker, and G. Dehaene-Lambertz, "Earlier speech exposure does not accelerate speech acquisition," *J. Neurosci.*, vol. 32, pp. 11159–11163, 2012.
[189] G. Dehaene-Lambertz *et al.*, "Language or music, mother or Mozart? Structural and environmental influences on infants' language networks," *Brain Lang.*, vol. 114, pp. 53–65, 2010.
[190] H. Poelmans, H. Luts, M. Vandermosten, P. Ghesquière, and J. Wouters, "Hemispheric asymmetry of auditory steady-state responses to monaural and diotic stimulation," *JARO - J. Assoc. Res. Otolaryngol.*, vol. 13, pp. 867–876, 2012.
[191] S. Vanvooren, H. Poelmans, M. Hofmann, P. Ghesquiere, and J. Wouters, "Hemispheric asymmetry in auditory processing of speech envelope modulations in prereading children," *J. Neurosci.*, vol. 34, pp. 1523–1529, 2014.
[192] D. A. Abrams, T. Nicol, S. Zecker, and N. Kraus, "Right-hemisphere auditory cortex is dominant for coding syllable patterns in speech," *J. Neurosci.*, vol. 28, pp. 3958–3965, 2008.
[193] J. A. Hämäläinen, A. Rupp, F. Soltész, D. Szücs, and U. Goswami, "Reduced phase locking to slow amplitude modulation in adults with dyslexia: An MEG study," *Neuroimage*, vol. 59, pp. 2952–2961, 2012.
[194] M. Schonwiesner, R. Rübsamen, and D. Y. Von Cramon, "Hemispheric asymmetry for spectral and temporal processing in the human antero-lateral auditory belt cortex," *Eur. J. Neurosci.*, vol. 22, pp. 1521–1528, 2005.
[195] M. Tervaniemi and K. Hugdahl, "Lateralization of auditory-cortex functions," *Brain Res. Rev.*, vol. 43, pp. 231–246, 2003.
[196] R. J. Zatorre, P. Belin, and V. B. Penhune, "Structure and function of auditory cortex: Music and speech," *Trends Cogn. Sci.*, vol. 6, pp. 37–46, 2002.
[197] D. A. . Abrams, T. Nicol, S. Zecker, and N. Kraus, "Abnormal cortical processing of the syllable rate of speech in poor readers," *J. Neurosci.*, vol. 29, pp. 7686–7693, 2009.
[198] S. Telkemeyer *et al.*, "Sensitivity of newborn auditory cortex to the temporal structure of sounds," *J. Neurosci.*, vol. 29, pp. 14726–14733, 2009.
[199] S. Telkemeyer, S. Rossi, T. Nierhaus, J. Steinbrink, H. Obrig, and I. Wartenburger, "Acoustic processing of temporally modulated sounds in infants: Evidence from a

combined near-infrared spectroscopy and EEG study," *Front. Psychol.*, vol. 2, pp. 1–14, 2011.
[200] E. S. Kappenman and S. J. Luck, "The effects of electrode impedance on data quality and statistical significance in ERP recordings," *Psychophysiology*, vol. 47, pp. 888–904, 2010.
[201] M. Mahmoudzadeh, "Évaluation de la mise en place des réseaux du langage chez le nouveau-né prématuré: Ét de électro-hémodynamique par enregistrements électroencéphalographique (EEG) et de spectroscopie proche de l'infrarouge fonctionnelle (fSPIR)," L'Université de Picardie Jules Verne, 2011.
[202] C. S. Herrmann, S. Rach, J. Vosskuhl, and D. Strüber, "Time-frequency analysis of event-related potentials: A brief tutorial," *Brain Topogr.*, vol. 27, pp. 438–450, 2014.
[203] J. Alaerts, H. Luts, M. Hofmann, and J. Wouters, "Cortical auditory steady-state responses to low modulation rates," *Int. J. Audiol.*, vol. 48, pp. 582–593, 2009.
[204] G. M. Bidelman and S. P. Bhagat, "Objective detection of auditory steady-state evoked potentials based on mutual information," *Int. J. Audiol.*, vol. 55, pp. 313–319, 2016.
[205] R. A. Dobie and M. J. Wilson, "Objective detection of 40 Hz auditory evoked potentials: phase coherence vs. magnitude-squared coherence," *Electroencephalogr. Clin. Neurophysiol.*, vol. 92, pp. 405–413, 1994.
[206] B. Sayers, H. Beagley, and J. Riha, "Pattern analysis of auditory-evoked EEG potentials," *Audiology*, vol. 18, pp. 1–16, 1979.
[207] J. Fridman, R. Zappulla, and et al, "Application of phase spectral analysis for brain stem auditory evoked potential detection in normal subjects and patients with posterior fossa tumors," *Audiology*, vol. 23, pp. 99–113, 1984.
[208] J. Jerger, R. Chmiel, J. D. Frost, and N. Coker, "Effect of sleep on the auditory steady state evoked potential," *Ear Hear.*, no. 4, pp. 240–245, 1986.
[209] D. R. Stapells, S. Makeig, and R. Galambos, "Auditory steady-state responses : threshold prediction using phase coherence," *Electroencephalogr. Clin. Neurophysiol.*, vol. 67, pp. 260–270, 1987.
[210] T. W. Picton, J. Vajsar, R. Rodriguez, and K. B. Campbell, "Reliability estimates for steady-state evoked potentials," *Electroencephalogr. Clin. Neurophysiol.*, vol. 68, pp. 119–131, 1987.
[211] R. W. Thatcher, "Coherence, phase differences, phase shift, and phase lock in EEG/ERP analyses," *Dev. Neuropsychol.*, vol. 37, pp. 476–496, 2012.
[212] X. Hung Ta and et al, "Phase analysis of hand movement-related EEG activity," 2014. [Online]. Available: https://www.slideserve.com/keala/phase-analysis-of-hand-movement-related-eeg-activity.
[213] D. Lehmann and W. Skrandies, "Reference-free identification of components of checkerboard-evoked multichannel potential fields," *Electroencephalogr. Clin. Neurophysiol.*, vol. 48, pp. 609–621, 1980.
[214] W. Skrandies, "Global Field Power and Topographic Similarity," *Brain Topogr*, vol. 3, pp. 137–141, 1990.
[215] H. Y. Zheng, J. W. Minett, G. Peng, and W. S. Y. Wang, "The impact of tone systems on the categorical perception of lexical tones: An event-related potentials study," *Lang. Cogn. Process.*, vol. 27, pp. 184–209, 2012.
[216] "Neonatal Structural Atlas – Brain Development." [Online]. Available: http://brain-development.org/brain-atlases/multi-structural-neonatal-brain-atlas/.
[217] A. Makropoulos *et al.*, "Regional growth and atlasing of the developing human brain," *Neuroimage*, vol. 125, pp. 456–478, 2016.
[218] A. Serag *et al.*, "Construction of a consistent high-definition spatio-temporal atlas of the developing brain using adaptive kernel regression," *Neuroimage*, vol. 59, pp. 2255–

2265, 2012.
[219] A. Makropoulos *et al.*, “Automatic Whole Brain MRI Segmentation of the Developing Neonatal Brain,” *IEEE T MED IMAGING*, vol. 33, pp. 1818–1831, 2014.
[220] K. Van Leemput, F. Maes, D. Vandermeulen, and P. Suetens, “Automated model-based tissue classification of MR images of the brain,” *IEEE T MED IMAGING*, vol. 18, pp. 897–908, 1999.
[221] I. S. Gousias *et al.*, “Magnetic resonance imaging of the newborn brain: Manual segmentation of labelled atlases in term-born and preterm infants,” *Neuroimage*, vol. 62, pp. 1499–1509, 2012.
[222] K. P. Whittall, A. L. MacKay, D. A. Graeb, R. A. Nugent, D. K. B. Li, and D. W. Paty, “In vivo measurement of T2 distributions and water contents in normal human brain,” *Magn. Reson. Med.*, vol. 37, pp. 34–43, 1997.
[223] C. Laule, E. Leung, D. K. B. Li, A. L. MacKay, and G. R. W. Moore, “Myelin water imaging in multiple sclerosis: quantitative correlations with histopathology.,” *Mult Scler*, vol. 12, pp. 747–753, 2006.
[224] P. Flom, “How to interpret hierarchical regression,” *Sciencing*, 2017. [Online]. Available: https://sciencing.com/interpret-hierarchical-regression-8554087.html.
[225] B. Kim, “Hierarchical Linear Regression,” *Statistical Consulting Associate, University of Virginia Library*, 2016. [Online]. Available: https://data.library.virginia.edu/hierarchical-linear-regression/.
[226] Y. Benjamini and Y. Hochberg, “Controlling the False Discovery Rate: A practical and powerful approach to multiple testing,” *J. R. Stat. Soc. Ser. B*, vol. 57, pp. 289–300, 1995.
[227] J. D. Storey, “A direct approach to false discovery rates,” *J. R. Stat. Soc. Ser. B Stat. Methodol.*, vol. 64, pp. 479–498, 2002.

Appendix I

A survey on stimuli for visual cortical function assessment in infants

Brain & Development 40 (2018) 2–15

BRAIN & DEVELOPMENT
Official Journal of the Japanese Society of Child Neurology

www.elsevier.com/locate/braindev

Review article

A survey on stimuli for visual cortical function assessment in infants

Farveh Daneshvarfard[a,b], Nasrin Maarefi[c], Hamid Abrishami Moghaddam[a,b,*], Fabrice Wallois [b,d]

[a] *Faculty of Electrical Engineering, K.N. Toosi University of Technology, Tehran, Iran*
[b] *Inserm UMR 1105, Faculté de Médecine, Université de Picardie Jules Verne, Amiens, France*
[c] *Faculty of Computer Engineering, K.N. Toosi University of Technology, Tehran, Iran*
[d] *Inserm UMR 1105, Centre Hospitalier Universitaire d'Amiens, Amiens, France*

Received 10 May 2017; received in revised form 19 July 2017; accepted 21 July 2017

Abstract

Visual processing, as a significant and complex functionality of the human brain, changes during the life span with the most developmental changes in the infancy. Different types of visual stimuli are needed for evaluating different functionalities of the infants' visual system. Selecting appropriate visual stimuli is an important issue in evaluating visual cortical functions in infants. Properties of stimulation influence responses of visual system and must be adjusted according to the age and specific function which is going to be investigated. In this review, the most commonly used stimuli to elicit visual evoked potentials (VEPs) are evaluated and characteristics of VEPs extracted by these stimulations are studied. Furthermore, various studies investigating different functionalities such as selectivity for orientation and directional motion are presented. Valuable results regarding emerging and maturation times of different functions and normative data for clinical diagnosis are provided by these studies.
© 2017 The Japanese Society of Child Neurology. Published by Elsevier B.V. All rights reserved.

Keywords: Visual stimuli; Visual functionality; Infants; Visual evoked potentials

1. Introduction

Visual processing, as a significant functionality of the human brain, is not a fixed ability at birth and develops during the infancy. Different types of visual stimuli are needed for evaluating these developmental changes in infants' visual system.

Appropriate stimuli are selected based on the infant's age and his/her perception of the environment. Newborns are poor in fixation and discrimination of color and orientation. Therefore, they are mostly investigated by black and white stimuli, especially different types of checkerboards and designs with angles. By 3 months, they are attracted to colored objects and are capable of glancing at smaller objects as small as 2.5 cm. Furthermore, visual attention and visual searching begin in this period of time. The infant can fixate at 1 m at 5–6 months and his/her acuity improves rapidly to near maturity by 6–9 months of age. Between 9 months and 1 year, the infant is alert to unfamiliar people and objects. Visual acuity is

*Corresponding author at: Department of Biomedical Engineering, Faculty of Electrical Engineering, K.N. Toosi University of Technology, Seyedkhandan, Dr. Shariati Ave, P.O. Box 16315-1355, Tehran, Iran.
E-mail addresses: f.daneshvarfard@ee.kntu.ac.ir (F. Daneshvarfard), n.maarefi@email.kntu.ac.ir (N. Maarefi), hamid.abrishami@u- picardie.fr (H. Abrishami Moghaddam), fabrice.wallois@u-picardie.fr (F. Wallois).

http://dx.doi.org/10.1016/j.braindev.2017.07.010
0387-7604/© 2017 The Japanese Society of Child Neurology. Published by Elsevier B.V. All rights reserved.

between 20/20[1] and 20/30 at 2 years and the child's brain functions are near to adult basic sensory processing abilities at 2–5 years of age [1].

Development of visual acuity and functionality is evaluated using a preferential looking (PL) test or the visual evoked potential (VEP) recordings. In a PL experiment, the subject is presented with two stimulus fields, including the target and non-target regions (e.g. black and white stripes as the target and homogeneous gray area as the background). The location of the target is randomly alternated. Typically, infants will look at the target rather than the background, in the case of target detection. Beside this behavioral method of vision evaluation, visual evoked potentials are also used to assess the integrity and maturity of the visual system in infants. VEPs refer to electrical potentials, initiated by brief visual stimuli. VEP waveforms are extracted from the electro-encephalogram (EEG) by signal averaging. They are used for measuring functional integrity of the visual pathways from retina via the optic nerves to the visual cortex of the brain [2].

This paper covers an evaluation of different types of visual stimuli and the most commonly used stimulations to initiate visual evoked potentials. It also tends to provide some information about designing proper visual stimuli for investigating different functionalities of the infants' brain. Contrast and orientation sensitivity and direction of motion recognition, as well as color vision, are examples of different functionalities which can be studied separately through specific kinds of stimuli.

2. Patterned and flashed stimuli

Flash, pattern reversal (PR) and pattern onset/offset are three common types of stimuli used in evaluating visual functionality. A photo-stimulator, as a flash stimulus, requires minimal cooperation of the patient and is well suited for the case of poor optical quality or poor vision. The PR stimulus consists of black and white checks or gratings which reverse their light and dark regions, alternatively. Overall luminance of the pattern must be constant during the reversal. The most significant parameters for defining this stimulus include visual angle of each check or the spatial frequency of bars or gratings. PR is the most preferred stimuli in clinical purposes because of its low variability in waveform and timing. For pattern onset/offset, the pattern is abruptly exchanged with a gray background of the same overall luminance. This stimulus is best suited for detection of malingering and for use in patients with nystagmus [3]. VEPs may be elicited by either patterned or flashed visual stimuli. Stimulation at low rates (up to 4/s) will lead to ''transient" VEPs and that of higher rates (10/s or higher) will produce responses that relatively oscillate at the frequency of stimulation and are called ''steady- state" VEPs. One of the advantages of steady-state evoked potentials over transient evoked potentials is that they are not much affected by psychological variables such as attention and consequently, they are less variable [4]. Characteristics of steady-state evoked potentials and their advantages as well as details of analysis in frequency domain have been summarized by Regan [4]. Responses elicited by patterned stimuli are ''pattern" VEPs or PVEPs and those elicited by flashed stimuli are ''flash" VEPs or FVEPs. PVEPs are less variant to intra- and inter individual variability and detect minor visual pathway abnormality more accurately than FVEPs. Checkerboard PR and sinusoidal grating are the most widely used pattern stimuli because of their relative simplicity and reliability. Furthermore, flashed stimuli are more convenient for patients who are unable to fixate or attend to the stimulus [5].

VEP characteristics are affected by check size and visual field span of the patterned stimuli. Changing these parameters allows selective testing of specific regions of the visual pathway. In most clinical experiments, patients are screened using a video display with field subtending 10–40 arc deg and check size of about 1 arc deg. For most of clinical applications, a single check size of about 1 arc deg, or a little smaller, such as about 50′, is sufficient. There is no need to use larger checks for children; since they can fixate properly to the stimuli and also their visual systems are mature enough to use the same size stimuli as adults [2].

3. ISCEV standard stimuli for clinical visual evoked potentials

International society for clinical electrophysiology of vision (ISCEV) has proposed a subset of stimulus and recording conditions which provide useful clinical information and can be implemented in most clinical laboratories. This subset of stimulus consists of: 1. PR-VEPs elicited by checkerboard stimuli with large 1° (i.e., 60 arc min) and small 0.25° (15 arc min) checks. 2. Pattern onset/offset VEPs elicited by checkerboard stimuli with large 1° (60 arc min) and small 0.25° (15 arc min) checks. 3. FVEP elicited by a brief luminance increment, which subtends a visual field of at least 20° and is presented in a dimly illuminated room [3].

Mean luminance required for the patterned stimuli is 50 cd/m^2 and the contrast between black and white regions should be more than 80% according to Michelson contrast. Michelson contrast is defined as

[1] In the expression 20/x vision, the numerator (20) is the distance in feet between the subject and presented chart and the denominator (x) represents the distance at which a person with 20/20 acuity would discern the same optotype. Thus, 20/40 means that a person with 20/20 vision would discern the same optotype from 40 feet away. In other words, the person possesses half the spatial resolution and needs twice the size to discern the optotype.

the difference between the highest and lowest luminance of the pattern divided by sum of the two values. Reversal rate of the PR stimuli is proposed to be 2.0 ± 0.2 reversals per second. Onset duration of the pattern onset/offset stimuli should be 200 ms separated by 400 ms of background presentation. The ISCEV standard is based on the onset portion of the VEP elicited by onset/offset stimulation. Duration of the flash stimuli should be less than 5 ms and its luminance should be about 3 cd/m^2. Furthermore, the flash rate is required to be in the range of 0.9–1.1 flash per second [3].

A single recording channel with a midline occipital active electrode is used for the ISCEV proposed VEP tasks. Responses descripted as follows reflect the typical waveforms of adults 18–60 years of age. As illustrated in Fig. 1a, the PR-VEP waveform consists of N75, P100, and N135 peaks. It is recommended to measure the amplitude of P100 from the preceding N75 peak. The P100 is usually a prominent peak with relatively little variation between subjects and between repeated measurements over time. However, it can be affected by parameters such as pattern size, contrast, mean luminance, signal filtering, patient age and poor fixation [3]. The P100 peak time is very stable in the age range from 5 until 60 years old with slowing about one millisecond per decade. In testing young infants, VEP should be recorded for 300 ms or longer as VEP components may have long peak times during early maturation. Latency of the P100 decreases as the infant matures and by about age 4–5 years, peak time shortens to about 100 ms [2].

VEP to standard onset/offset stimuli typically consists of a positive peak (C1) at approximately 75 ms, a negative peak (C2) at approximately 125 ms and a positive peak (C3) around 150 ms (Fig. 1b). VEP to flash stimuli consists of several negative and positive waves (Fig. 1c). Peak time of the first detectable component is approximately 30 ms and components are recordable with peak latencies of up to 300 ms. The most robust components of FVEP are the N2 peak at around 90 ms and P2 peak at around 120 ms [3].

4. Study of VEP characteristics using flashed and patterned stimuli

VEP characteristics depend on various parameters including infants' age and properties of the stimuli. Latency and amplitude of P100 in transient VEPs are largely affected by pattern properties such as luminance, contrast, spatial frequency (or check size) and stimulus field size [6–8]. An increase is observed in the latency of P100 as pattern luminance decreases and the reason may be the reduction of retinal illuminance [9]. Decreasing the contrast leads to amplitude reduction and latency prolongation [7, 10] and P100 latency shows a U-shaped function versus check size [10, 11].

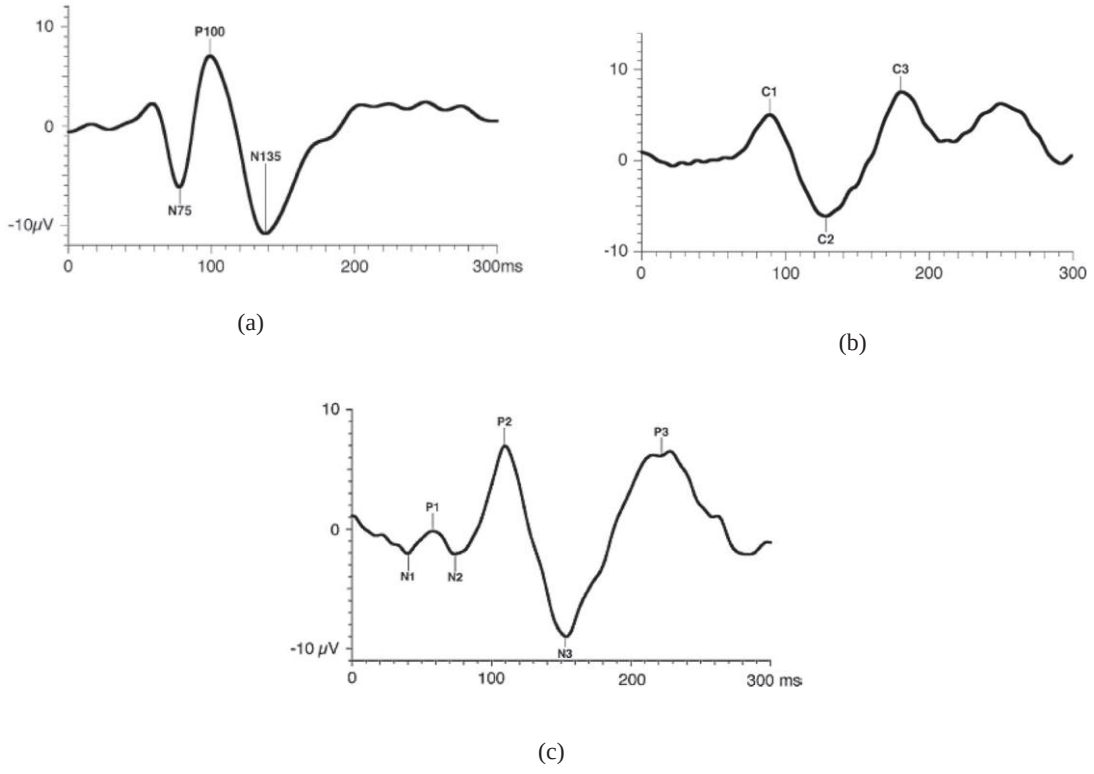

Fig. 1. a. A normal pattern reversal VEP, b. A normal pattern onset/offset VEP, c. A normal FVEP. Responses reflect the typical waveforms for adults of 18–60 years old [3].

Amplitude and latency of VEPs are also affected by age, sex and pupil size [6, 9, 12, 13]. Presence of a curvilinear relationship between the P100 latency and age was reported [10, 14] and females demonstrated shorter P100 latency and larger P100 amplitude than males [10, 14]. Furthermore, latency of P100 increases by 2–3 ms/mm of decreased pupillary diameter while the amplitude has a decreasing trend as the pupil size becomes smaller [9].

Fig. 2a shows an example of equipment needed for recording PVEPs in infants and Fig. 2b illustrates samples of VEPs obtained from one infant at different ages in response to pattern stimulation with 30′ check size [15]. As it can be seen from the waveforms, latency of the first major positive peak (P100) decreases rapidly in the first weeks of life. Several studies evaluated maturation of the visual system of infants using VEPs and investigated the effect of developmental changes and visual stimuli's properties on the VEPs components. Different forms of flashed and patterned stimuli have been used in these assessments. Benavente et al. [16] evaluated flash visually evoked potentials in newborns and their maturation during the first six months of life. The aim of their study was to obtain normative data based on components of FVEPs in the newborn. One hundred and nine normal newborn children, aged from 12 h to 5 days with a mean of 2.5 days, were studied. The distance between stimulating lamp and the subject was 50 cm and the rate of flashing was 1 flash per second. They reported a great morphological variability in the FVEPs and concluded that this variability and the presence of early components in some cases are because of differences in maturity of the visual system at birth. Despite morphological variability observed in the FVEPs, the latency of P2 in the newborn has low variability and can be used as an appropriate parameter to extract normative data.

Kraemer et al. [17] investigated the potential development of FVEP in normal neonates and tried to find indicators for relating the development to visual behavior. They included twenty healthy infants, born at term (38–41 weeks), in their study. The infants were placed in their mother's lap and a binocular stimulus was delivered with a Grass PS 22 flash stimulator to them. The distance between the infants and the stimuli was approximately 0.75 m. VEPs were recorded longitudinally from the day of birth to the following weeks and months. The result suggested great variability in VEPs and so in visual function on the day of birth. In the early development, a potential of long latency and duration was reported and was replaced later by a more compound and mature potential of shorter latency. To be more specific, there were no potentials with latency shorter than 100 ms during the first four weeks of life and then the responses, consisting of a negative potential (N1) with a latency of less than 100 ms and a succeeding positive peak (P1) were developed. The important process which leads to functional maturation and latencies decrement is the myelination. Conduction velocity is

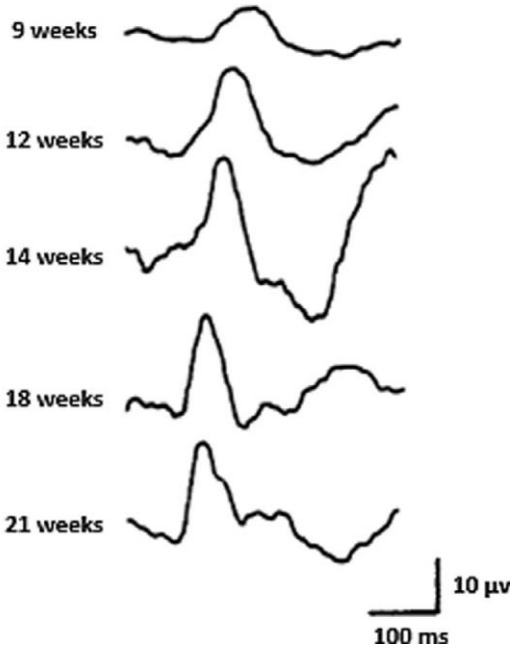

(a) (b)

Fig. 2. a. An example of equipment needed for recording pattern VEPs in infants, b. Pattern VEPs of one infant at different ages in response to checkerboard stimulation with 30′ check size [15].

low in neonates because of unmyelinated fibers and increases with the progress in myelination process. Results also suggested that VEP variations at approximately five weeks were simultaneous with the development of responsive smiling and enhanced visual interest of the infants.

Prager et al. [18] used patterned transient VEPs as a method for assessing visual function of infants. Visual field of the pattern stimuli covered the central 20°×26° of the retina and the stimulations were presented at 3.9 reversals per second. Visual acuity can be estimated using transient VEPs. If an evoked potential is observed after the pattern stimuli, the spatial resolution threshold of the pattern can be determined. Furthermore, peak response time and amplitude of the VEP vary by check size. Three different check sizes were presented (60′, 30′, and 15′) in this experiment. VEP latencies and amplitudes were measured for a cohort of 118 subjects at both 4 and 8 months. Results were used to evaluate the effect of age on sensitivity to check size. Applying statistical tests on the gathered data showed that both latency and amplitude differ significantly as a function of both check size and age. However, latency variations were much more marked between 4 and 8 months of age in comparison to amplitude variations. Latency decreases with both check size increment and age. Amplitude was significantly larger for larger checks and decreased between 4 and 8 months of age at all check sizes. Amplitude decrease with age is most likely resulted from the insulating effect of the skull and skin thickening which strengthens as the infant get older.

Isler et al. [19] analyzed FVEP of neonates in frequency domain. Subjects were 12 normal term infants within 2 days of birth. The stimuli consisted of multiple blocks of thirty 100 ms white light flashes which were delivered to the neonates at a rate of one flash per second. A Grass PS33 flash unit was used as the flash stimulus and was held approximately 20 cm from the infants' eyes. FVEP has been used widely as a method for evaluating developmental changes and visual maturation. However, its clinical utility in the cortical function assessment has been debated [18, 20–25]. The inadequacy of time domain VEP analysis motivated this study and so frequency domain parameters of VEP data were presented as alternative and complementary measures of the neural dynamics generating the evoked response. Isler et al. provided a set of frequency-dependent measures from a 128-electrode electroencephalographic recording. For the frequency domain analysis each trial of the recorded VEP was divided into eight non-overlapping, one pre-stimuli and seven post-stimuli, segments. Fast Fourier transforms (FFTs) were taken for each segment after removal of the segment mean and applying a Hann window. Several frequency parameters including power spectra, cross spectra between channels, phase synchrony between pairs of electrodes, local coherence and phase locking at each electrode were calculated. A nonrandom phase is present in the EEG at the time of a prominent ERP peak occurrence, and so a frequency domain measure of phase locking provides an alternative way to detect ERP components. Parameters such as band power, cross spectrum and phase locking showed significant variations occurring in the same time window as VEP. This fact demonstrated the sensitivity of these measures to the neural dynamics underlying VEP. The mentioned sensitivity was generally greater at lower frequency bands. The most power changes occurred over posterior regions in the 16Hz band. Smaller significant band power changes occurred in frontal and central regions and at lower frequencies. Totally, frequency dependent measures may be used for characterizing aspects of the cortical response that are difficult or impossible to assess with the time domain of VEP alone.

5. Stimuli for measuring visual acuity of infants

Visual abilities of infants and visual information detected by them are so poor compared with those of adults. Visual acuity, the ability to detect fine details, is measured by showing specific stimuli to the subject. Several pairs of stimuli are shown to the infants. Each pair consists of a black and white stripes pattern paired side-by-side with a gray patch. This visual preference or PL method is based on the fact that if the infant can discriminate the stripes, he/she will look at them for longer time in comparison to the gray patch. The stripe width is varied in different steps and the smallest stripe width that is detectable by the infant gives an estimate of his/her acuity. Another method for measuring acuity is to record VEPs from the visual areas of the brain while the infant is shown stripes and gray stimuli. The acuity is then estimated as the smallest stripe width that has provided a VEP different from that of the gray stimuli. Final value of the acuity for infants can be estimated by combining these two measures. Acuity estimation of the infants is generally between 10 and 30 times poorer than that of the adults [26].

6. Investigating selective cortical responses using specific types of stimuli

Primary visual cortex of infants' brain shows sensitive responses to particular values of orientation, direction of motion, grating sensitivity and spatial frequency variations. Development of these selective cortical responses is an important indicator of visual processing during the early months of life. However, the emerging time of these responses occurs at different ranges of age. Specific types of stimuli are applied for studying onset and maturity of selective cortical responses and comparing the results related to each selectivity. Mentioned aspects of

visual development are interested fields of study and were assessed in several works.

6.1. Perception of orientation, motion and spatial frequency

Braddick et al. [27] evaluated VEP responses of infants that are signatures of cortical orientation-selectivity and directional motion selectivity. They concluded that human cortical direction selectivity emerges at a later age than cortical orientation selectivity. In fact, they compared the responses directly in the same group of infants to investigate whether the later appearance of direction selectivity was intrinsic, or a function of the spatiotemporal characteristics of the stimuli used. For this purpose, they elicited orientation-reversal (OR) VEPs and direction-reversal (DR) VEPs in different experiments by two stimuli. Random pixel and grating patterns were used for direction and orientation analysis respectively, in infants aged 4–18 weeks.

The OR stimulus consisted of sine wave gratings, of spatial frequency 0.3 c/deg, which change in both orientation and phase. The orientation changes between 45 and 135 at a rate of 4 reversals/s and phase change occurs at a rate of 24 changes per second. In each orientation, reversal dark region in the 45 grating pattern is replaced by a light region in the 135 grating, or vice versa. The average local luminance variation, resulted from both pattern orientation changes and phase shifts, affects the responses generated by orientation-sensitive mechanisms. In order to eliminate the phase shift effect, orientation-sensitive responses are separated by frequency analysis. The DR stimuli consisted of a random checkerboard pattern moving horizontally at a velocity of 5.5 deg/s. The direction of the motion was reversed 4 times per second and the random pattern was replaced with a new one at the midway and end of each reversal. As mentioned for the orientation stimuli, direction-sensitive responses are also separated by frequency analysis. Using the mentioned two stimuli and changing some of the parameters (type, velocity and reversal frequency) they concluded that the youngest infants (aged 5–7 weeks) are more sensitive to orientation changes and direction sensitivity is not observed before 8 weeks even with the stimuli parameters variations.

As mentioned earlier, directional selectivity is one of the most important aspects of cortical visual processing investigated in several studies. Directional selectivity does not emerge in infants in the first weeks of life [28]. However, many studies confirmed its development in later weeks using behavioral methods and evoked potentials. Wattam-Bell [29] found that first responses to DR emerged at around 10 weeks of age. Emerging time of these responses depends on velocity of the stim- uli. For instance, responses to motion at 20 deg/s emerged several weeks later than the responses corresponding to the motion at 5 deg/s [29]. On the other hand, the results of behavioral studies reported that directional motion discrimination occurred earlier, at around 7 weeks of age [28, 30–33].

Lee et al. [34] used transient P1 latency and phase-based calculated latency for evaluating the motion processing maturation in infancy in comparison to adults. Previous studies confirmed the latency of VEP as a proper feature as compared to amplitude in both within and between subjects' analysis [35–37]. In this experiment, the DR visual evoked potentials were recorded from 61 adults (median age 21.4 years, range 17– 43 years) at 1–16 reversals per second (r/s) and 76 infants (age 7.7–79.0 weeks) at 2–8 r/s. The stimuli consisted of random array with pixel-size of 0.44 displaced horizontally at 5.5 deg/s. The direction of motion periodically reversed (the DR frequency) and pattern of pixels changed randomly at the rate twice that of DR frequency as "random jumps" (i.e., the jump occurred every 125 ms for a 4 r/s DR). The DRs were accompanied by local contrast events that could be detected by non-directional neurons. Hence, the jumps without DRs were used to isolate the directional component of responses by subtracting from jump plus DR component. The sequence of pattern was displayed on the monitor at 40 cm from the participants.

The results showed that the calculated latency were longer than P1 latency in both adults and infants. In contrast to transient latency, which is related to the time of initial directional response, the calculated latency reflects the whole time of processing in the complete waveform. The transient latency in infants was not significantly different from adults at 10 weeks but the calculated latency was not similar to adults until 30 weeks of age. As a result, the development of calculated latency for DR was much more prolonged compared to transient P1 latency.

Banton et al. [38] evaluated the ability of infants to discriminate direction of motion. Last studies of infant direction discrimination were limited to 180° of direction differences and showed that infants begin to distinguish opposing direction of motion when they are in the range 6–10 weeks of age [33,34]. But in this study, the stimuli differed in direction by various degrees between 8 and 180°. Six-, 12-, and 18-week-old infants participated in the experiment. The stimuli were random-dot kinematograms consisting of a field of moving dots divided into a background and a small circular sub-region (i.e. the 'target'). The direction of motion was controlled independently in the background and target regions and the directional difference was varied in order to measure direction discrimination thresholds. Direction of motion was fixed for the background dots (vertical drift) and differed from vertical by 0, 8, 16, 23, 34, 45, 90 or 180° for the target dots. Each dot had a luminance of 13.8 cd/m^2 and they were randomly distributed on a

0.012 cd/m^2 background with a density of 10%. Dots were moved with speed of 11°/s and their lifetime was unlimited. Furthermore, the target itself was placed in apparent motion. It appeared like a moving circle on either the left or right side of the display. The target was displaced every 500 ms, through five pseudo-random positions (Fig. 4). This sequence was repeated indefinitely to produce continuous motion. This motion attracted infants' attention more and enhanced their preference for the target side of the display. An observer watched the infant, as he/she viewed the display, and decided if the infant preferred to look at the left or the right side of the display. Direction discrimination threshold was reported as 22° for 12- and 17° for 18-week-old infants and it was indeterminate at 6 weeks of age.

The aim of the paper published by Blumenthal et al. [39] was evaluating the fast development of global motion processing in human infants using directional eye movement (DEM) technique. This technique is based on the fact that the subject makes directionally eye movement in response to moving stimuli. Infants with 3, 4, 5, and 7 months of age were tested in the study and the results were used for motion processing assessment. The applied stimulus was a stochastic motion display which subtended 63.20°× 55.40° and included 600 dots (1°× 1°; dot density = 1 dot per deg^2) in a gray background (5.51 cd/m^2). Some of these dots, named signal dots, moved to left or right by 42° during 13.33 ms in every vertical refresh which created coherent rightward or leftward motion. The lifetime of signal dots was 267 ms which equals to 20 vertical refreshes. Ninety-five percent of the coherent dots were presented in a new location after the lifetime and the remaining (5%), called noise dots, were replaced every vertical refresh and their movement was in a random fashion.

At first, a contrast sensitivity task was performed for each subject. The contrast of the dots was varied during this task in order to find a contrast threshold for each subject. The contrast of the dots was varied from 5.62 cd/m^2 to 31.22 cd/m^2 for the infants and from 5.52 cd/m^2 to 8.27 cd/m^2 for the adults). Then a coherence sensitivity task was performed based on the results of the first task. In the second task, the initial contrast of the dots was 2.5 the subject's contrast threshold and the proportion of the signal dots was varied from 9.5% to 95% for the infants and from 9% to 90% for the adults to determine the coherence threshold. Results of the experiments showed that in spite of contrast sensitivity which increased with age, global motion sensitivity was stable between 3 and 7 months of age as well as between infancy and adulthood. This fact suggests that the global motion processing develops quickly before 3 months of age.

Shahani et al. [40] evaluated maturation of spatial frequency and orientation selectivity of primary visual cortex of infants and compared the result with those of adults. In order to do this, they measured the effects of an adapting grating on the VEPs recorded in response to a test grating stimulus. This effect was measured as a function of the difference between the spatial frequency and orientation of both adapting and test grating stimuli. Each stimulus cycle consisted of an adaptation period of 400 ms, an inter-stimulus interval varied randomly between 100 and 200 ms, a pre-stimulus interval of 30 ms, a test-stimulus presentation of 50 ms and a blank interval of 350 ms. The test stimulus was a horizontal grating having a spatial frequency of 0.4 c/deg and contrast of 0.45 and the adapting stimulus was a high-contrast grating (0.9), which varied in spatial frequency (0.1–1.12 c/deg) and orientation (0°–45°). Four adults and two infants with corrected ages of three to eleven weeks were tested in multiple sessions and their VEPs were recorded from Oz, O1 and O2. Laplacian derivations were calculated online as 2 times the potential of the middle electrode (Oz) minus the sum of the potentials of the surrounding electrodes (O1 and O2). The amplitude of the first prominent component of the Laplacian derivations was measured from the averaged baseline value 30 ms before the stimulus onset to the corresponding peak. The Laplacian derivation of the VEPs usually consists of a positive component (P1), which is not always recognizable in the monopolar derivations. In the absence of the adapting pattern, the peak latency of the positive Laplacian component P1 was about 240 ms at three weeks of age and approached adult values of about 120 ms at 11 weeks. When both the adapting and test stimuli were presented, spatial frequency and orientation of the adapting grating changed the P1 amplitude of the test stimuli VEPs. The maximum change of the P1 amplitude was observed when both stimuli had the same spatial frequency and orientation. Relative changes in P1 amplitude of the test stimuli VEPs produced by adapting gratings of variable spatial frequency had almost the same characteristic for all the subjects with age ranged between three weeks and 22 years. Characteristic of relative changes in P1 amplitude produced by adapting gratings of variable orientation was almost the same for infants older than six weeks and adults. Therefore, they suggest that the receptive fields of neurons in infant striate cortex are narrowly tuned in spatial frequency at three weeks of age but orientation tuning is less mature. The reason may be that receptive fields elongate substantially as the infant's age increases from three to six weeks.

6.2. Visual acuity and preferences

Brown and Yamamoto [41] measured visual acuity in newborn and preterm infants with grating acuity cards. Three groups of infants were included in their study. The first group consisted of 24 preterm infants with

33–42 weeks of gestational age (GA) and the second group were 37 full-term infant patients with non-neuronal diseases and GA ranged up to 48 weeks. The third group consisted of 30 normal full-term infants of less than 1 week old. Fig. 3 shows two types of card used in this experiment. Cards of the first type (Fig. 3a) were gray and covered 35×56 cm^2 with a 12×14 cm^2 central rectangular window which showed the black and white stripes with contrast of 0.87. The second type of card (Fig. 3b) was similar to the first one, but it was taller (39 cm) and had longer stripes (23 cm). The infants were held by a nurse and observed the cards. Another person, called the observer, displaced the grating stimulus and decided whether the infants could resolve the stripes. The distance between the cards and the infants was 36 cm. When the stripes were wide the infant turned his or her gaze toward them and when they were narrow, the infants was distracted and looked somewhere else. Visual acuity of each infant was estimated as the width of the narrowest stripes the observer judged the infant could see. The average visual acuity was reported 20/815 for the normal newborn infants at 39 or 40 weeks of GA and was reported 20/872 and 20/951 for the pre-term and full-term infant patients in the same age range, respectively. They also reported visual acuity improvement by the rate of 0.46 octave/month between 34 and 44 weeks of GA.

Visual acuity development was also investigated by Mayer et al. [42]. Fifty infants and children between 5 months and 5 years of age were included in the study and a PL procedure was designed for obtaining estimations of visual acuity. The stimuli consisted of a large gray cardboard screen with two 9° apertures, located 18° to the left and right of a 4 mm peephole at the center of the screen. On each trial a square-wave target grating was presented from one aperture and a very high spatial frequency grating was placed behind the other aperture as the blank stimulus. The target grating's spatial frequency was variable from 1.05 to 81.1 c/deg. A gray cardboard shutter concealed the stimulations from the subject between trials. The shutter contained a central hole to allow the observer to view the subject's face and a small red light flashed by the observer for attracting the subject's gaze at the beginning of each trial. Children were seated at a measured distance of 54 ± 3 cm from the screen and the infants sat on their parents' lap in front of the screen. The results showed that the visual acuity developed systematically from 5 c/deg at 5 months to 40 c/deg at 5 years of age and was close to the value corresponding to adult acuity in 5 years old children.

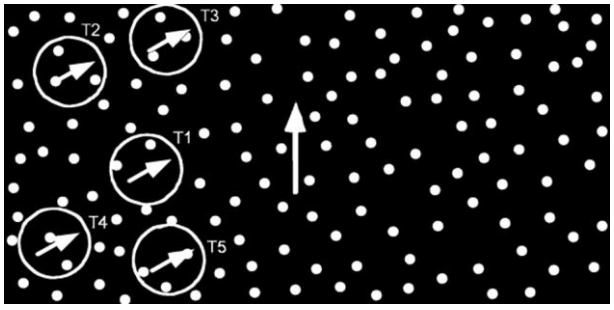

Fig. 3. The moving stimuli. Motion of the dots is represented by arrows. The displacement of the circular target over time is represented as T1–T5. The target was defined by direction of motion and circular outlines were not present in the actual stimuli [38].

Skoczenski and Norcia [43] studied the development of vernier acuity and grating acuity in subjects ranged from early infancy to adolescence (40 infants, aged from 1.5 to 18 months; 34 children, aged 2–14 years; and 5 adults, aged from 18 to 37 years). VEPs were applied for studying these two components of pattern vision. The vernier acuity stimulus consisted of two gratings including vertical square-wave grating with 80% contrast and 114 cd/m^2 mean luminance and another similar grating with five offsets. Offsets appeared as displacement in alternate rows of the latter grating. These two grating were replaced with temporal frequency of 5 Hz. The spatial frequency of both gratings was 1 c/deg for infants and 2 c/deg for children and adults. They examined different offsets in logarithmic steps, from large to small, to determine thresholds of vernier acuity at different ages. The offset was varied from 20 to 1 arc min for the youngest infants, and from 15 to 0.5 arc min for 8- to 18-months-old infants, and from 10 to 0.2 arc min for 2-years-olds. The grating acuity stimulus was the simple grating without offset as mentioned above but it appeared and was replaced with mean-luminance matched blank field at the rate of 5 Hz. The spatial frequency of the grating stimuli changed from 1 to 12 c/deg for the youngest infants, from 2 to 22 c/deg for older infants, and from 3 to 33 c/deg for 2 years old and all older subjects. In both experiments, the distance between the subject and the stimuli was 100 cm for infants up to 8 months, 150 cm for 8- to 18-month-olds, and 200 cm for 2-year-olds and above.

Results of this study showed that values of Vernier and grating acuity were similar from early infancy to 6 years but lower vernier acuity, by a factor of 2, was observed in infants at 6–10 weeks. Also both acuities were 20–40 times lower than adult level in this range. As mentioned in previous study [44] grating acuity improves completely by the age of 6 years but the vernier acuity improvement continues until 8 years of age and reaches to full maturity at 14 years old (0.2–0.4 arc min).

Sireteanu et al. [45] showed that infants, in the first months of life, prefer to look at repetitive visual patterns, rather than uniquely deviating targets. A forced-choice PL procedure was used to determine the infantile preference. The infant subjects were between 2 and

12 months of age and toddlers and young children were between 12 and 60 months of age. The stimuli applied in the experiment, were white cards with the size of 25×56 cm^2. There was a target on one side of the card among 15 randomly similar shapes as distractors. Both target and distractors were black (12 cd/m^2) and the luminance of background was 106 cd/m^2. As illustrated in Fig. 5a, a circle with a gap of 90° was presented on the right side of the card as a target between 15 complete circles. In a similar stimulus, shown in Fig. 5b, a complete circle is presented as a target between 15 circles with gaps in random directions. Results of the experiments show that the pattern of preferences in first months of infancy differs from adults and infants' preference is more toward background pattern rather than target pattern. After the end of first year, their preference starts to become to adult-like preference and at 3–4 years of age, toddlers show an adult-like pattern of preferences toward deviating targets. The transition of infantile to adult-like preference might show remodeling of human brain during this time.

6.3. Stereopsis and color vision

Stereoscopic depth perception and color discrimination are two other functionalities of the infant's brain which can be assessed by using various stimuli. Several studies presented emerging time of these functionalities after conducting some visual experiments. Fox et al. [46] assessed stereoscopic depth perception in three age groups of infants (2.5-, 3.5- and 4.5- month-old infants). A dynamic random-element stereogram containing a stereoscopic form was presented to the infants. Viewers with stereopsis can perceive stereoscopic contours and those without stereopsis can only perceive a random distribution of the dots or elements. The stereogram display used in this work, consisted of a large array of red and green dots which is viewed through red and green filters and stimulates each eye separately. This procedure is the well-established anaglyph method of stereoscopic presentation. The stereoscopic form used in this stimulus was a 100° by 15° rectangle, positioned in the center of the screen at the beginning of each stereoscopic test trial. The stereoscopic form was moved horizontally, to left and right, to evaluate visual attention of the infant. An observer inferred the direction of form displacement based on the infant's eye movement. Visual tracking of the stereoscopic form would be evidence of the possession of stereopsis. Performance of the observer's judgment did not differ from chance for 2.5-month group but it was greater than chance for both 3.5- and 4.5-month groups. It was concluded that the stereopsis does not emerge earlier than 3 months of age. Takai et al. [47] used a computer-based random-dot stereo test for evaluating development of stereoscopic acuity in infants longitudinally. Stereoscopic acuity, also called stereoacuity, is the smallest detectable depth difference that can be seen in binocular vision. Seven full-term normal infants with the age of 12–23 weeks were included in the experiment. The test was repeated at 2- to 3-month intervals until the children reached 2 years of age, and then was repeated at 6- to 12-month intervals until they reached 5 years of age. TV Random Dot Stereo Test (Nippon Tenganyaku Kenkyusho, Tokyo, Japan), which is a commercially available stereoacuity test for infants, was used in this study. This test is a computer-based program that creates a random-dot stereogram on the right or left side of a monitor screen. The program used in this experiment generated a red and green random-dot pattern on a computer screen that subtended an angle of 26°. The stimulus was an 8° circle composed of red and green random dots that appeared alternately on the left or right sides of the monitor. The infant viewed the screen through red-and-green dissociation glasses, and in the case of recognizing a stereoscopic figure, his/her eye movements followed the figure's displacement. The degree of stereoscopic disparity could be changed in 16 steps from 2480 arc sec (2480″) to 155 ″. It was adjusted at 2480 ″ at the beginning of the test. The observer

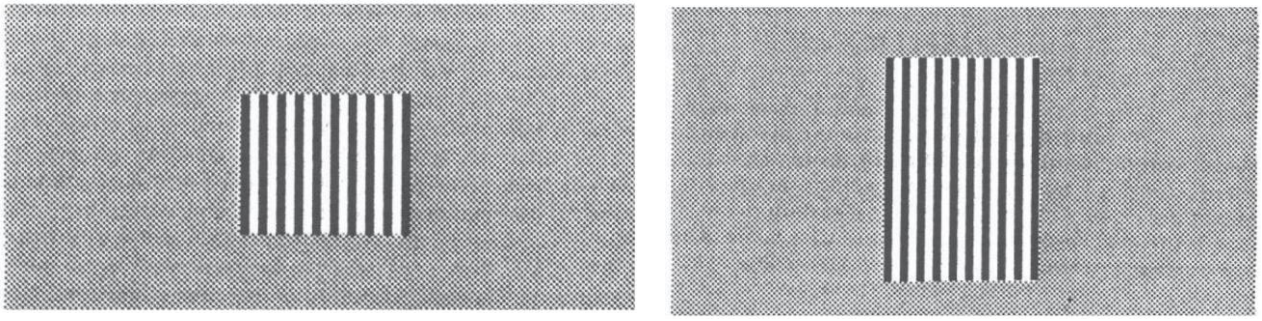

(a) (b)

Fig. 4. The grating acuity cards used in Brown and Yamamoto experiment [41], a. The cards with short stripes, b. The cards with long stripes.

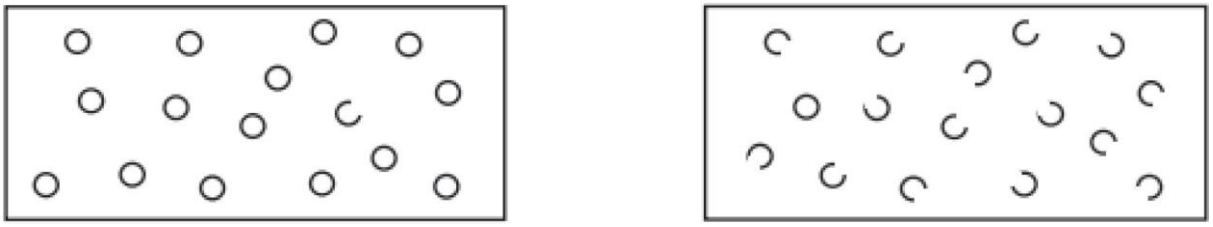

(a) (b)

Fig.5. The stimuli used for evaluating visual preferences of infants, a. Task using circle with gap as the target, b. Task using complete circle as the target [45].

watched eye movements of the subject. If the eye movements were synchronized with direction of the stimulus displacement for more than two presentations, the subject was reported as having ''passed" that disparity. The disparity was then decreased by two steps. When the eye movements did not match the direction of stimulus displacement, the infant was ''failed" that disparity and the disparity was increased one step. The test was stopped in the case of two continuous failed scores. According to the results, stereopsis was not detected in 12- or 13- week-old infants. The emergence of stereopsis was between the ages of 16 and 26 weeks (average age of 20.4 ± 3.5 weeks) with a disparity of 2480 ″ and the best stereoacuity (229 ± 184 ″) was detected at an average age of 28.9 ± 6.3 months.

Adams [48] evaluated the development of color preferences in 20 newborns, 1- and 3-months-olds and adults using a PL technique and recording their fixation time to stimulations. The infants' group consisted of newborns with mean age of 3.2 days, 1-month-olds with mean age of 5.1 weeks and 3-months-olds with mean age of 13 weeks. The stimuli were 4 colored squares (blue, green, yellow and red) and 1 gray square as a non- colored stimulus. They were produced by placing Kodak Wratten color interference filters and/or neutral density filters in the path of 3200 °k white light. Two luminance values, 3 and 30 cd/m^2, were used in each stimulus presentation and the stimuli subtended 16°×16° when viewed from 40 cm distance. The C.I.E. (1931) x and y coordinates of the chromatic stimuli were 0.19, 0.18 for blue, 0.28, 0.65 for green, 0.54, 0.43 for yellow and 0.63, 0.33 for red. The C.I.E. 1931 color spaces are the quantitative links between physical pure colors of the electromagnetic visible spectrum, corresponding to different wavelengths, and physiological perceived colors in human color vision. The results of the experiments showed that preference for chromatic stimuli over achromatic stimuli emerged at birth but there was no preference between different colors before 3 months of life. Also the preferences of adults and 3-months-olds for different colors were not the same. Three-months- olds preferred the long-wavelength colors (red and yellow) to the short-wavelength ones (blue and green), while adults preferred the short-wavelength colors (blue in particular). Furthermore, only newborns showed a brightness preference by looking longer at stimuli of lower luminance.

In another study, Adams et al. [49] conducted two experiments to examine newborns' ability to discriminate chromatic from achromatic stimuli. In the first experiment, they evaluated discrimination of gray from four chromatic stimuli (green, yellow, red and blue) using the infants' fixation time to colored-and-gray patterned stimuli and plain gray squares. Participants consisted of 240 infants, 1 to 5 days of age, at least 38 weeks' gestation and 250 g at birth. For each color, the infant was shown colored-and-gray 2×2 checker-board patterns in six different luminance contrast. Each stimulus was accompanied with a plain gray square which matched the mean luminance of the checkerboard. The stimuli subtended a region of 16°×16°, when viewed from 40 cm, and each check within the checkerboard was 8°×8°. The C.I.E. chromaticity x and y coordinates of the stimuli were 0.36, 0.53 for green, 0.50, 0.44 for yellow, 0.58, 0.32 for red and 0.29, 0.19 for blue. In the second experiment, they retested one of the discrimination (red versus gray) with a different method to eliminate brightness cues. In this experiment, 36 infants, 1–6 days of age were first habituated to a series of five gray squares of varying luminance and then tested with colored (red or blue) and gray squares. The stimuli consisted of 16°×16° gray squares of six different luminance (13.0, 8 .6, 5.5, 3.8, 2.8 and 1.9 cd/m^2), a 16°×16° red square (3.1 cd/m^2) and a 16°×16° blue square (3.2 cd/m^2). The C.I.E. chromaticity x and y coordinate values were 0.58, 0.40 for the red square and 0.22, 0.31 for blue square.

Results of the two experiments implied that newborns perceived hue and discriminated chromatic from achromatic stimuli. They showed preferences for chromatic checkerboards over gray squares of different luminance in experiment one. Also in the second experiment, they

showed preferences for red versus gray even after being habituated to other gray squares. These results explained that although infants were sensitive to changes in luminance, they also differentiated chromatic from achromatic stimulation. Another result of these tests suggested that infant color vision was not complete at birth as the newborns could not distinguish blue from gray in the two experiments.

Development of visual responses to chromatic stimuli was also examined by Rudduck and Harding [50] using transient VEPs. In order to produce a purely chromatic stimulus and to assess merely the color vision, it is necessary to eliminate luminance cues. An isoluminant chromatic stimulus may include components of different wavelengths (i.e. different colors), but perceived to be of equal brightness. However, infants are less sensitive to very small or zero brightness differences. In this study, 40 infants between the ages of 1 and 13 weeks post-term age were recruited. PR-VEPs to chromatic red and green and achromatic checks were studied. The red to green luminance ratios of the chromatic patterns were arbitrarily selected among the values 0.5, 0.8, 0.9, 1.0 (corresponding to isoluminant stimulus), 1.1, 1.2 and 1.5. PR checkerboards were produced by the Neuroscientific Venus system controlled by the application software which allowed the independent control of the colors' ratios. Previous study showed that the effect of chromatic aberration is negligible at low spatial frequencies [51] and so the checkerboard with check size of 2° (0.25 c/deg) were used for recording the VEPs.

The results showed that the waveform of the chromatic response has a simple morphology of major positive component (P1), comparable to the response of achromatic stimuli. All chromatic responses were delayed and reduced in comparison to the achromatic responses. When the chromatic luminance ratio was close to 1.0, the positive peak demonstrated an increased latency and reduced amplitude. All infants older than 7 weeks post-term demonstrated clear and repeatable responses to all chromatic stimuli including the isoluminant stimulus. One of the remarkable results of this study was about observing a change from absence to presence of an isoluminant response at the range of 6– 8 weeks. No infant younger than 7 weeks showed response to isoluminant stimulus. On the other hand, all the infants at 8 weeks and more demonstrated a clear and consistent isoluminant response. This deduction is in accordance with other studies regarding development of color vision. Infants tested behaviorally showed chromatic discrimination capability at two months [52] and few 3-week-old infants demonstrated chromatic discrimination in the experiment conducted by Clavadetscher et al. [53]. The stimuli used in this study was similar to the one applied many years earlier for evaluating chromatic vision of adults [54]. A pattern of alternate red and green sharp-edged small checks, abruptly exchanging places six times/s, was used and the amplitude of the 6-Hz component of VEP was plotted versus the ratio (green/red luminance). A clear response was reported for a color-normal subject at isoluminance, although it was smaller than the responses corresponding to the ratios adjacent to isoluminance.

As reviewed by this section, different studies explored development of various functionalities of the infants' brain as well as their emergence and maturation. Table 1 summarizes the age range, stimuli, explored functionality and main findings of each study.

7. Clinical protocol and moral considerations

The subjects should be well prepared for the experiment before presenting the stimuli and recording the VEPs. Extreme pupil sizes and anisocoria should be checked for the subjects and intact subjects will be chosen for experiment [3]. Parents of the infant subjects must be explained about details of stimuli type, condition of recording and other related information, clearly. Stimuli condition must be comfortable and well-suited for the infants. The infants can be placed in their mothers' lap comfortably during the set up and recording procedure and they should view and concentrate on the stimuli with minimal disruption. In recording VEPs, care must be taken to have the infant in a convenient position to minimize muscle and other artifact. The distance between the infants and the stimuli must be adjusted in a standard range as the infants are only capable of focusing a short distance from their farce. Furthermore, it should be guaranteed that the experiment has no harmful consequence for subjects and the parents should be aware of their infants' personal information which will be used in future reports.

While recording VEPs of infants, fixation should be monitored continuously and the recording needs to be interrupted during fixation losses. Useful strategies, including dangling and tapping the fixation screen with small objects, can be used to improve fixation. Although these strategies may degrade the stimulus procedure, the attention and fixation obtained are great advantages. Finally, experiments in young infants may be more effective if the infants is allowed to adopt his/her preferred position (sitting, reclining or over a shoulder) and there are appropriate breaks for feeding, changing, or rest [55].

Monocular stimulation is a common and standard stimulus to assess visual pathway function from one eye. However, this may not be practical in infants and binocular stimulation may be used in the case of infant visual assessment. When we use a stimulus for one eye, the other one should be covered by a patch or lid. It ensures that no light enters the unstimulated eye during the test [3].

Table 1
Summary of the age range, stimuli, explored functionality and main findings of each study.

Functionality	Age range	Stimuli	Main results	Author
Orientation and directional motion	Infants with 4–18 weeks of age	OR grating patterns and DR random checkerboards moving horizontally	Youngest infants (aged 5–7 weeks) were more sensitive to orientation changes. Direction sensitivity was not observed before 8 weeks.	Braddick [27]
Direction of motion	Adults with 17–43 years of age and infants with 7.7–79.0 weeks of age	Random array which was displaced horizontally	Transient latency in infants was not significantly different from adults at 10 weeks. Phase-based latency was not similar to adults until 30 weeks.	Lee [34]
Direction of motion	6-, 12-, and 18-week-old infants	Random-dot kinematograms	Direction discrimination threshold was 22° for 12- and 17° for 18-week-old infants and indeterminate at 6 weeks.	Banton [38]
Global motion	Infants with 3, 4, 5 and 7 months of age	Moving dots in a gray background	Global motion sensitivity was stable between 3 and 7 months and between infancy and adulthood suggesting quick development before 3 months.	Blumenthal [39]
Spatial-frequency and orientation	Adults and infants with corrected ages of 3–11 weeks	Grating patterns	Neurons were tuned in spatial frequency at 3 weeks but orientation tuning was observed in 6 weeks.	Shahani [40]
Visual acuity	Preterm infants with 33–42 weeks of GA, term infant patients with GA up to 48 weeks, normal term infants less than 1 week	Grating acuity cards	Average visual acuity was 20/815 for normal infants at 39 or 40 weeks of GA and was 20/872 and 20/951 for pre- and full-term infant patients of the same age. It improved by 0.46 octave/month between 34–44 weeks.	Brown [41]
Visual acuity	Infants and children between 5 months and 5 years of age	Square-wave target grating	Visual acuity developed from 5 c/deg at 5 months to 40 c/deg at 5 years and was close to value of adult acuity in 5 years old children.	Mayer [42]
Vernier acuity and grating acuity	Infants aged 1.5–18 months, children aged 2–14 years and 5 adults aged 18–37 years	Two gratings including vertical square-wave grating and another similar grating with five offsets	Both acuities were 20 to 40 times lower than adult level in infants. As mentioned in [44] grating acuity improved completely by the age of 6 but vernier acuity improvement continued until 8 years and reached to full maturity at 14 years old.	Skoczenski [43]
Stereoscopic depth	2.5-, 3.5- and 4.5- month-old infants	Dynamic random-element stereogram	Stereopsis did not emerge earlier than 3 months of age.	Fox [46]
Stereoscopic acuity	Infants of 12–23 weeks, test was repeated at 2- to 3-month intervals till 2 years and at 6- to 12- month intervals till 5 years	A computer-based random-dot stereo test	Stereopsis was not detected in 13-week-old infants. The emergence was between 16–26 weeks and the best stereoacuity was detected at average age of 28.9 ± 6.3 months.	Takai [47]
Color preferences	Newborns with mean age of 3.2 days, 1- and 3-months-olds and adults	4 different colored squares and 1 gray square as a non-colored stimulus	Preference for chromatic stimuli emerged at birth but there was no preference between different colors before 3 months of life.	Adams [48]
Color discrimination	Infants with 1–5 days of age	Colored-and-gray checkerboards	The newborns could not distinguish blue from gray in the experiments.	Adams [49]
Color vision	Infants between the ages of 1 and 13 weeks post-term age	Chromatic and achromatic checkerboards	Infants older than 7 weeks post term had clear responses to isoluminant chromatic stimuli.	Rudduck [50]

8. Discussion

In the current study, different types of visual stimuli to initiate visual evoked potentials were presented. Further- more, normal development of vision in infants and specific stimulations for evaluating different functionalities of visual system were studied. Human visual system features many functionalities including detection of light and perception of color, form, motion, orientation, direction, contrast and depth. Some of the functionalities more involved in infancy were studied in this review. Regan [56] described some early uses of evoked brain responses as a tool for investigation of human visual functions. These attempts include studies on distinguishing between true pattern-specific VEPs and responses affected by changes in luminance, evaluating VEPs elicited by equiluminant chromatic patterns and investigating VEPs specific to motion and stereo depth. Physiological and

anatomical findings, as well as clinical evidence of the human visual system, suggest that different components of visual processing are segregated into largely independent parallel pathways. Information regarding anatomical, physiological and perceptional segregation of color, form, movement and depth can be found in Livingstone and Hubel's experiments [57, 58]. In these studies, different aspects of visual perception are correlated with different subdivisions of the human visual system.

Assessment of visual cortical function in infants accompanies more challenges in comparison to adults. Visual ability of the infants is not fixed at birth and alters gradually during the infancy. Indeed, all functions of the visual system do not emerge at the same time and their maturity occurs in different ages. Therefore, following considerations must be cared in choosing appropriate stimuli to investigate these functionalities. Which stimuli elicit the correct response related to each functionality and what is the proper age in human infant for evaluating this functionality? As explained in this paper, different studies investigated various functionalities with the aid of exclusive stimuli which extract proper response related to the same specific functionality. In addition, these studies reported some thresholds for observing different functions in visual system of human. Orientation selectivity and direction selectivity emerge in approximately 6 weeks and 8 weeks, respectively. Direction of motion processing develops quickly before 3 months of age. Furthermore, sensitivity to spatial frequency appears in 3 weeks-old infants.

Some functions of the visual system, such as grating acuity and vernier acuity, emerge in early infancy and mature later in childhood and adolescence. Maturity of grating acuity and vernier acuity occur at 6 years and 14 years of age, respectively. As another visual function, preference in infants younger than one year is more toward background pattern rather than target pattern and become similar to adult preference at 3–4 years of age. Finally, as mentioned earlier, stereopsis does not emerge earlier than 3 months of age and average age of stereopsis emergence with a disparity of 2480″ is 20.4 ± 3.5 weeks. Furthermore, preference for chromatic stimuli over achromatic stimuli emerges at birth but there is no preference between different colors before 3 months of life.

Valuable results regarding emerging and maturation times of different functions and reported normative data for clinical diagnosis have been presented in the literature. However, some issues can be considered in future works to get more reliable results. Reported thresholds for each visual sensitivity, presented in current study, are based on the age of subjects which participated in the experiments. More accurate thresholds can be determined by testing more subjects in extended ranges of age. Furthermore, it is useful to apply more than one stimuli for investigating the same functionalities of the visual system and present final result based on merging the results of each stimulation. Another approach, which may guarantee the findings, is to use PL and VEP methods simultaneously for evaluating visual system with the same stimuli.

Acknowledgements

This work was partially supported by EGIDE France and CISSC Iran under the grant number 961/93-9-2 (Jundi Shapour scientific collaboration program). Figs. 3–5 and part b of Fig. 2 are reprinted from referenced publications with permission from Elsevier.

References

[1] Farroni T, Menon E. Visual perception and early brain development. In: Tremblay RE, Boivin M, Peters RDeV, editors. Encyclopedia on Early Childhood Development [Online]. Montreal, Quebec: Centre of Excellence for Early Childhood Development and Strategic Knowledge Cluster on Early Child Development; 2008. p. 1–6. Available at: http://www.child-encyclopedia.com/documents/FarroniMenonANGxp.pdf.

[2] Creel DJ. Webvision [Online]. Available at: http://webvision.med.utah.edu/book/electrophysiology/visually- evoked-potentials/.

[3] Odom JV, Bach M, Brigell M, Holder GE, McCulloch DL, Mizota A, et al. ISCEV standard for clinical visual evoked potentials: (2016 update). Doc Ophthalmol 2016; 133:1–9.

[4] Regan D. Steady-state evoked potentials. J Opt Soc Am 1977; 67:1475–89.

[5] Recommended Standards for Visual Evoked Potentials. In: Guideline 9B: guidelines on visual evoked potentials. American Clinical Neurophysiology Society [Online]. 2008. Available at: https://www.acns.org/pdf/guidelines/Guideline-9B.pdf.

[6] Celesia GG. Evoked potential techniques in the evaluation of visual function. J Clin Neurophysiol 1984; 1:55–76.

[7] Chiappa KH. Evoked potentials in clinical medicine. Philadelphia, PA/New York: Lippincott/Raven; 1997. p. 31–94.

[8] Tobimatsu S, Celesia GG. Studies of human visual pathophysiology with visual evoked potentials. Clin Neurophysiol 2006; 117:1414–33.

[9] Tobimatsu S, Celesia GG, Cone SB. Effects of pupil diameter and luminance changes on pattern electroretinograms and visual evoked potentials. Clin Vision Sci1988; 2:293–302.

[10] Tobimatsu S, Kurita-Tashima S, Nakayama-Hiromatsu M, Akazawa K, Kato M. Age-related changes in pattern visual evoked potentials: differential effects of luminance, contrast and check size. Electroencephalogr Clin Neurophysiol 1993; 88:12–9.

[11] Kurita-Tashima S, Tobimatsu S, Nakayama-Hiromatsu M, Kato M. Effect of check size on the pattern reversal visual evoked potential. Electroencephalogr Clin Neurophysiol 1991; 80:161–6.

[12] Bodis-Wollner I, Ghilardi MF, Mylin LH. The importance of stimulus selection in VEP practice: the clinical relevance of visual physiology. In: Cracco RQ, Bodis-Wollner I, editors. Evoked potentials. New York: Alan R Liss; 1986. p. 15–27.

[13] Tobimatsu S. Aging and pattern visual evoked potentials. Optom Vis Sci 1995; 72:192–7.

[14] Celesia GG, Kaufman D, Cone S. Effects of age and sex on pattern electroretinograms and visual evoked potentials. Electroencephalogr Clin Neurophysiol 1987; 68:161–71.

[15] Sokol S, Jones K. Implicit time of pattern evoked potentials in infants: an index of maturation of spatial vision. Vis Res 1979; 19:747–55.

[16] Benavente I, Tamargo P, Tajada N, Yuste V, Olivan MJ. Flash visually evoked potentials in the newborn and their maturation during the first six months of life. Doc Ophthalmol 2005; 110:255–63.

[17] Kraemer M, Abrahamssson M, Sjostrom A. The neonatal development of the light flash visual evoked potential. Doc Ophthalmol 1999; 99:21–39.

[18] Prager TC, Zou YL, Jensen CL, Fraley JK, Anderson RE, Heird WC. Evaluation of methods for assessing visual function of infants. J AAPOS 1999; 3:275–82.

[19] Isler JR, Grose-Fifer J, Fifer WP, Housman S, Stark RI, Grieve PG. Frequency domain analyses of neonatal flash VEP. Pediatr Res 2007; 62:581–5.

[20] Taylor MJ, McCulloch DL. Visual evoked potentials in infants and children. J Clin Neurophysiol 1992; 9:357–72.

[21] Shepherd AJ, Saunders KJ, McCulloch DL, Dutton GN. Prognostic value of flash visual evoked potentials in preterm infants. Dev Med Child Neurol 1999; 41:9–15.

[22] Hughes JR, Rechitsky I. Follow-up studies on the usefulness of the flash visual evoked potential. Clin Electroencephalogr 1996; 27:187–90.

[23] Iinuma K, Lombroso CT, Matsumiya Y. Prognostic value of visual evoked potentials (VEP) in infants with visual inattentive- ness. Electroencephalogr Clin Neurophysiol1997; 104:165–70.

[24] Hartmann EE. Infant visual development: an overview of studies using visual evoked potential measures from Harter to the present. Int J Neurosci 1995; 80:203–35.

[25] Kurtzberg D, Vaughan Jr HG. Electrophysiologic assessment of auditory and visual function in the newborn. Clin Perinatol 1985; 12:277–99.

[26] Slater A. Visual perception in the newborn infant: issues and debates. Intellectica 2002; 34:57–76.

[27] Braddick O, Birtles D, Wattam-Bell J, Atkinson J. Motion- and orientation-specific cortical responses in infancy. Vis Res 2005; 45:3169–79.

[28] Braddick O, Atkinson J, Wattam-Bell J. Normal and anomalous development of visual motion processing: motion coherence and 'dorsal-stream vulnerability'. Neuropsychologia 2003; 2003 ():1769–84.
[29] Wattam-Bell J. Development of motion-specific cortical responses in infancy. Vis Res 1991; 31:287–97.
[30] Wattam-Bell J. Visual motion processing in one-month-old infants: preferentiallookingexperiments. VisRes1996; 36:1671–7.
[31] Wattam-Bell J. Visual motion processing in one-month-old infants: habituation experiments. Vis Res 1996; 36:1679–85.
[32] Wattam-Bell J. The development of maximum displacement limits for discrimination of motion direction in infancy. Vis Res 1992; 32:621–30.
[33] Wattam-Bell J. Coherence thresholds for discrimination of motion direction in infants. Vis Res 1994; 34:877–83.
[34] Lee J, Wattam-Bell J, Atkinson J, Braddick O. Development of visual motion processing: phase and peak latencies of direction- specific visual evoked potential. J Vis 2013; 13:4.
[35] Strasburger H, Scheidler W, Rentschler I. Amplitude and phase characteristics of the steady-state visual evoked potential. Appl Opt 1988; 27:1069–88.
[36] Tomoda Y, Tobimatsu S, Mitsudome A. Visual evoked potentials in school children: a comparative study of transient and steady- state methods with pattern reversal and flash stimulation. Clin Neurophysiol 1999; 110:97–102.
[37] Sarnthein J, Andersson M, Zimmermann MB, Zumsteg D. High test-retestreliability of checkerboard reversal visual evoked potentials (VEP) over 8 months. Clin Neurophysiol 2009; 120: 1835-40.
[38] Banton T, Dobkins K, Bertenthal BI. Infant direction discrim- ination thresholds. Vis Res 2001; 41:1049–56.
[39] Blumenthal EJ, Bosworth RG, Dobkins KR. Fast development of global motion processing in human infants. J Vis 2013; 13:8.
[40] Shahani U, Manahilov V, McCulloch DL. Maturation of spatial frequency and orientation selectivity of primary visual cortex. In: Nenonen J, Ilmoniemi RJ, Katila T, (eds) Biomag 2000: Proceedings of the 12th International Conference on Biomagnetism. Amsterdam: Elsevier; 2001. p. 153–156.
[41] Brown AM, Yamamoto M. Visual acuity in newborn and preterm infants measured with grating acuity cards. Am JOphthalmol 1986; 102:245–53.
[42] Mayer DL, Dobson V. Visual acuity development in infants and young children, as assessed by operant preferential looking. Vis Res 1982; 22:1141–51.
[43] Skoczenski AM, Norcia AM. Late maturation of visual hyper- acuity. Psychol Sci 2002; 13:537–41.
[44] Skoczenski AM, Norcia AM. Development of VEP vernier acuity and grating acuity in human infants. Invest Ophthalmol Vis Sci 1999; 40:2411–7.
[45] Sireteanu R, Rettenbach R, Wagner M. Transient preferences for repetitive visual stimuli in human infancy. Vis Res 2009; 49:2344–52.
[46] Fox R, Aslin RL, Shea SL, Dumais ST. Stereopsis in human infants. Science 1980; 207:323–4.
[47] Takai Y, Sato M, Tan R, Hirai T. Development of stereoscopic acuity: longitudinal study using a computer-based random-dot stereo test. Jpn J Ophthalmol 2005; 49:1–5.
[48] Adams RJ. An evaluation of color preference in early infancy. Infant Behav Dev 1987; 10:143–50.
[49] Adams RJ, Maurer D, Davis M. Newborns' discrimination of chromatic from achromatic stimuli. J Exp Child Psychol 1986; 41:267–81.
[50] Rudduck GA, Harding GFA. Visual electrophysiology to achromatic and chromatic stimuli in premature and full term infants. Int J Psychophysiol 1994; 16:209–18.
[51] Flitcroft DI. The interactions between chromatic aberration, defocus and stimulus chromaticity: implications for visual physiology and calorimetry. Vis Res 1989; 29:349–60.
[52] Peeples DR, Teller DY. Colour vision and brightness discrimination in 2 month old human infants. Science 1975; 189:1102–3.
[53] Clavadetscher JE, Brown AM, Ankrum C, Teller DY. Spectral sensitivity and chromatic discriminations in 3- and 7-week-old human infants. J Opt Soc Am A 1988; 5:2093–105.
[54] Regan D. Evoked potentials specific to spatial patterns of luminance and colour. Vis Res 1973; 13:2381–402.
[55] McCulloch DL. Visual evoked potentials in infants. In: Introduction to infant EEG and event-related potentials. [Online]. Available at: http://www.psych.ufl.edu/bcd/wpcontent/uploads/sites/9/2016/05/LScott_2007_ERPChap_0.pdf.
[56] Regan D. Some early uses of evoked brain responses in investigations of human visual function. Vis Res 2009; 49:882–97.
[57] Livingstone MS, Hubel DH. Segregation of form, color, movement, and depth: anatomy, physiology, and perception. Science 1988; 240:740–9.
[58] Livingstone MS, Hubel DH. Psychophysical evidence for separate channels for the perception of form, color, movement, and depth. J Neurosci 1987; 7:3416–68.

Modélisation conjointe fonctionnelle et structurelle des modifications du cerveau humain liées à l'âge à l'aide de données EEG et d'images IRM

Les nouveau-nés prématurés en bonne santé présentent de nombreuses capacités structurelles et fonctionnelles. La surveillance de la dynamique neurodéveloppementale du prématuré présente donc un grand intérêt. Nous avons effectué une analyse des réponses corticales, auditives, des nouveau-nés prématurés à des stimuli syllabiques répétitifs. Les amplitudes maximales de la réponse fréquentielle à la fréquence cible et à la première harmonique, ainsi que la cohérence de phase (PC) à la fréquence cible ont été extraites. Des corrélations positives significatives ont été observées entre l'âge, l'amplitude et la valeur de la PC à la fréquence cible. En outre, une latéralisation vers l'hémisphère droit sur de nombreux canaux a généralement été observée.

Dans la partie suivante de la thèse, nous avons cherché à établir un lien entre les changements développementaux des réponses auditives corticales, caractérisés par la diminution de la latence du premier pic de la puissance de champ globale (GFP) des potentiels évoqués, et l'indice de myélinisation structurelle des zones impliquées dans l'audition, extraits à partir des images IRM d'enfants appariés pour l'âge. Les indices de maturation structurelle ont été calculés en tant que valeurs moyennes des intensités d'image T1w / T2w MR. Nous avons observé des corrélations significatives entre les indices de maturation des zones auditives impliquées et la latence du premier pic de GFP, ainsi qu'avec l'âge. Toutefois, ni l'indice de maturité structurel ni l'âge n'ont contribué à une variance supplémentaire significative de la latence du premier pic de GFP après prise en compte de la variance associée à l'autre paramètre.

Mots-clés: Nouveau-nés prématurés, développement fonctionnel, réponses évoquées auditives, stimuli syllabiques répétitifs, analyse du domaine fréquentie, cohérence de phase, asymétrie, puissance de champ globale (GFP), maturation structurelle, indice de myélinisation.

Functional and structural joint modeling of age-related changes in the human brain using EEG data and MR images

Normal healthy preterm neonates present many of the structural and functional capabilities of the human brain. Monitoring of developmental changes of the preterm brain, is therefore, of great interest in both functional and structural aspects. In the current thesis, we analyzed the preterm infants' auditory responses to repetitive syllabic stimuli. Peak amplitudes of the frequency response at the target frequency and the first harmonic, as well as phase coherence (PC) at the target frequency, were extracted. Significant positive correlations were observed between the age and the amplitude and PC value at the target frequency. Furthermore, right hemisphere lateralization over many channels was generally observed.

In the next part of our analyses, we aimed to relate developmental changes of cortical auditory responses, characterized as the decrease of the first-peak latency of the global field power (GFP), to the structural myelination index of auditory-involved areas extracted from MR images of the infants at the same age. Structural maturation indices were calculated as the mean values of T1w/T2w MR image intensities. We observed significant correlations between the maturation indices of the auditory-involved areas and GFP first-peak latency, as well as age. However, neither the structural maturation index nor age contributed to significant additional variance in the GFP first-peak latency after accounting for the variance associated with the other parameter.

Keywords: Preterm infants, functional development, aditory evoked responses, repetitive syllabic stimuli, frequency-domain analysis, phase coherence, asymmetry, global filed power, structural maturation, myelination index.